(12) INTERNATIONAL APPLICATION PUBLISHED UNDER THE PATENT COOPERATION TREATY (PCT)

(19) World Intellectual Property Organization
International Bureau

(43) International Publication Date
8 January 2009 (08.01.2009)

PCT

(10) International Publication Number
WO 2009/005546 A1

(51) International Patent Classification:
A61M 13/00 (2006.01)

(21) International Application Number:
PCT/US2008/002989

(22) International Filing Date: 5 March 2008 (05.03.2008)

(25) Filing Language: English

(26) Publication Language: English

(30) Priority Data:
60/892,952 5 March 2007 (05.03.2007) US

(71) Applicant *(for all designated States except US)*: **BOARD OF GOVERNORS FOR HIGHER EDUCATION, STATE OF RHODE ISLAND AND THE PROVIDENCE PLANTATIONS** [US/US]; 301 Promenade Street, Providence, RI 02908 (US).

(72) Inventors; and

(75) Inventors/Applicants *(for US only)*: **ZHANG, Zongqin** [US/US]; 33 Cinnamon Lane, Wakefield, RI 02892 (US). **WANG, Jinbo** [CN/CN]; 1037 Luoyu Road, Apartment 601, Building 13-21, East Campus, Wuhan, Hubei, 430074 (CN). **FADL, Ahmed** [—/US]; 360 Brown Street, Apartment 2, East Providence, RI 02914 (US).

(74) Agents: **POWERS, Arlene, J.** et al.; Gauthier & Connors LLP, 225 Franklin Street, Suite 2300, Boston, MA 02110 (US).

(81) Designated States *(unless otherwise indicated, for every kind of national protection available)*: AE, AG, AL, AM, AO, AT, AU, AZ, BA, BB, BG, BH, BR, BW, BY, BZ, CA, CH, CN, CO, CR, CU, CZ, DE, DK, DM, DO, DZ, EC, EE, EG, ES, FI, GB, GD, GE, GH, GM, GT, HN, HR, HU, ID, IL, IN, IS, JP, KE, KG, KM, KN, KP, KR, KZ, LA, LC, LK, LR, LS, LT, LU, LY, MA, MD, ME, MG, MK, MN, MW, MX, MY, MZ, NA, NG, NI, NO, NZ, OM, PG, PH, PL, PT, RO, RS, RU, SC, SD, SE, SG, SK, SL, SM, SV, SY, TJ, TM, TN, TR, TT, TZ, UA, UG, US, UZ, VC, VN, ZA, ZM, ZW.

(84) Designated States *(unless otherwise indicated, for every kind of regional protection available)*: ARIPO (BW, GH, GM, KE, LS, MW, MZ, NA, SD, SL, SZ, TZ, UG, ZM, ZW), Eurasian (AM, AZ, BY, KG, KZ, MD, RU, TJ, TM), European (AT, BE, BG, CH, CY, CZ, DE, DK, EE, ES, FI, FR, GB, GR, HR, HU, IE, IS, IT, LT, LU, LV, MC, MT, NL, NO, PL, PT, RO, SE, SI, SK, TR), OAPI (BF, BJ, CF, CG, CI, CM, GA, GN, GQ, GW, ML, MR, NE, SN, TD, TG).

Published:
— *with international search report*
— *before the expiration of the time limit for amending the claims and to be republished in the event of receipt of amendments*

WO 2009/005546 A1

(54) Title: HIGH EFFICIENCY MOUTHPIECE/ADAPTOR FOR INHALERS

(57) Abstract: An inhaler adapter configured to deliver a medication to a mouth cavity of a user. The inhaler adapter alters the flow rate of medication to the mouth cavity of the user. The inhaler adapter includes an inner cavity with several alternate designs.

HIGH EFFICIENCY MOUTHPIECE/ADAPTOR FOR INHALERS

PRIORITY INFORMATION

The present application claims priority to U.S. Provisional Patent Application 60/892,952 filed with the United States Patent and Trademark Office on March 5, 2007 all of which is incorporated herein in its entirety.

BACKGROUND OF THE INVENTION

The American Lung Association (www.lungusa.org) estimated that 26 million Americans have been diagnosed with asthma in their lifetime. Of these 26 million Americans, 10.6 million have had an asthma episode in the past 12 months. Additional 4.9% of the US populations (about 13.9 million) have Chronic Obstructive Pulmonary Disease (COPD) in their lifetime. The metered-dose inhaler (MIDI) and dry-powder inhaler (DPI) are popular devices used in the treatment of these lung diseases. However, the problems associated with inhalers are well documented. Typically, only about 10% of aerosol medicine can be delivered to the lung region. To minimize the problem and to delivery the aerosol drug in a more respirable form, spaces and chambers that are of various designs are developed. While reducing the aerosol deposition at the back of throat, the current designs used for existing spacers often contribute to the great drug loss within the delivery system. Most of these spacers are expensive and not easy to clean up.

Effective delivery to a patient is a critical aspect of any successful drug therapy. Various routes of delivery exist. Oral drug delivery of pills, capsules and elixirs is perhaps the most convenient method, but many drugs are degraded in the digestive tract before they can be absorbed. Subcutaneous injection is frequently an effective route for systemic drug delivery, but enjoys a low patient acceptance. Aerosol therapy constitutes a major part of the therapeutic

treatment for patients with lung disease such as asthma and bronchitis, and has potential for the system delivery of insulin, peptides and proteins as well (Patton and Platz, 1992). The metered-dose inhaler (MDI) and dry-powder inhaler (DPI) are popular devices used in aerosol therapies. It is also intention of many institutions to adopt and adapt inhalers for use in counter terrorism and military settings (www.dres.dnd.ca). The ability to delivery immediate therapy is crucial in saving lives where the response time or window for administering therapy or prophylaxis may be very short following biological exposure. The portable aerosol inhaler would allow easy self-administration in the field, thereby mitigating the requirement for injections or access to hospitals.

Although these inhalers are safe, portable, multi-dose, and cost-effective ways to deliver inhaled medications, the problems which patients experience with MDI and DPI are also well documented. A survey conducted by a nationally recognized asthma research center indicated that only about 50% of the people who are now using MDI are using them "correctly". The rest may actually be getting as little as 1% of the prescribed medication delivered to their lungs. In fact, there is no clear defined "correct" inhalation procedure. A lot of doctors believe that the best way for patients to inhale medication is to use what's called the "open-mouth" method, which is very different from the "close-mouth" method that is prescribed by directions that come with the medication. Most of the directions were written 20 years ago when many asthma treatment medications were first introduced. However, not all doctors are persuaded that the open-mouth method is better for every patient. Meanwhile, new types of inhalers are being developed to replace the Freon-12 (the propellant in the old inhalers). Many of these inhalers are breath-activated, so they may be easier to use than old inhalers. Nevertheless, there are still a lot of unknown factors that need to be investigated before an "improved" inhaler procedure can be

recommended. These factors include: close vs. open-mouth method, distance and angle between the inhaler and the mouth, the optimum structure of the inhaler and spacer, natural vs. controlled breath patterns, duration of breathing pause, patient health status, targeted disease site, characteristic of aerosol medication, and others. In additional to all these variables, effects of ages and genders are important.

Numerous studies on aerosol medicine delivery have been published in the past few decades. It would be a great challenge to name all these studies. Examples of these works were published in journals such as J. of Aerosol medicine, Am. Ind. Hyg. Asso. J., Thorax J., American Review of Respiratory Disease, Chest and others. Many investigators have examined the effects of aerosol diameter and flow rate on deposition of particles in the oral-pharyngeal-laryngeal airways including: Newman and Clarke, 1983; Yu and Diu, 1983; Newman, 1985; Swift, 1989; Kim and Garcia, 1993, Cheng et al, 1999, Lin et al, 2001, Dehaan and Finlay, 2001; to name a few. Deposition of monodisperse aerosol particles (2 - 12 microns) in the oral airway of healthy adult human volunteers has been reported (Lippmann and Albert 1969, Foord et al. 1978; Chan and Lippmann 1980; Stahlhofen et al. 1980, 1983; Emmett et al. 1982; Bowes and Swift 1989, to name a few.). It is suggested that impaction is the dominant deposition mechanism for these cases. Cheng et al, (1990, 1993, 1997a) studied the deposition mechanism of ultrafine particles (<0.1 microns) in human oral airway replicas. Their studies show that turbulent diffusional deposition is the dominant mechanism. A lot of aerosol experiments were designed for industrial hygiene applications.

A systematic review of the literature and detailed comparison of different inhaler devices are conducted by Brocklebank et al. (2001). Clinical effectiveness, aerosol medicine characterizations, and comparative performances of various aerosol inhaler/spacer/nebulizer are

main themes of the literature. The major problem associated with the inhaler therapy is the massive aerosol deposition within oral cavity and on oropharyngeal airways. Typically, only about 10% of aerosol medicine can reach to the lung region (Newman, et al., 1991, Davis, et al. 1992).. To minimize the problem and to deliver the aerosol drug in a more respirable form, spaces and chambers that are of various physical shapes and designs were developed. Some were as simple and straightforward as extension tubes placing the mouth at a greater distance from the inhaler. Others decelerate the aerosol by means of tortuous flow path routes or bluff body impact areas. While reducing the aerosol deposition at the back of throat, the designs used for existing spacers often contribute to the great drug loss within the delivery system. One study showed that while a spacer effectively reduced the oropharynx deposition from 75% to 32%, the drug losses in the delivery system increased from 14% to 46% (Davis, et al. 1992).

Computer simulations using the realistic human 3-D head airway geometry have not been possible due to the limitations of computer capacity as well as computation techniques until last 10 years. Elad et al. (1993) conducted the flow simulation using a simplified nose-like model. Martonen et al. (1993) and Katz & Martonen (1996) reported the numerical simulation in an idealized laryngeal/trachelbronchiel airway system using commercial software PHOENICS (a control volume scheme) and FIDAP (a finite element scheme), respectively. Kimbell et al. (1993) used the commercial software FIDAP to compute the flow and gas transport in a rat's nasal airway. Keyhani et al. (1995) conducted a similar numerical study (using FIDAP), but within the human nasal airways, of steady flow at quiet breathing condition. The airway model was truncated anterior to the nasopharynx and one side of the nasal model was used. Subramanian et al. (1998) extended this work using a computer reconstruction of both sides of the human nasal passage. The airflow in an integrated airway system including nasal, nasopharyngeal, laryngeal

and two generations of the upper tracheobronchial airway system was reported by Yu et al. (1998). Martonen et al. (2001) further extended this work using the commercial software CFX4X (a control volume numerical scheme, licensed by AEA technology, Inc). Sarangapani and Wexler (2000) also reported detail simulation results using a different nasal-nasopharyngeal airway model.

Technically speaking, the level of challenges encountered in conducting nasal and oral flow simulations was about the same, with the former involving more grid construction work while the latter requiring more numerical-converge skills due to higher inspiratory flow rate. However, it is worth noting that although many studies were published on nasal simulations as discussed above, only one work of computer simulation on airflow and particle transport in human ora/oropharyngeal airways during our extensive literature search. The medical and engineering information databases used in the search include MEDLINE (contains more than 70 databases and provides access to over 9000 journals), International Pharmaceutical Abstract (covers 800 journals in the field of pharmacy), ScienceDirect (covers 1200 journals), and Web search engines Yahoo.com and Google.com. It was found using Google.com) that a 3-D oral airway computational model was reported by Perzl in his Ph.D. thesis work in German (Perzl, 1997). The focus of the work was on the development of the numerical model. No flow-up of this work (in a form of searchable journal or web publications) and any other work of oral airways computer simulations was found.

Particle deposition in the human respiratory tract is a complicated process involving effects of fluid dynamic and particle dynamics, and complications of anatomy. It is generally agreed that the relatively high velocity and the abrupt changes in flow direction in the oral airway are the primarily responsible for the inertia deposition of particles larger than 1 μm in diameter.

There are many parameters that affect the aerosol deposition in the human oral air ways, some of theses are very well studied and documented, such as a particle size, particle density, and the respiratory flow rate.

Inertial impaction is primarily responsible for the deposition in the oral cavity. Many parameters can influence the particle impaction such as particle size, air flow rate, plume characterization (Barry and O'Callaghan, 1997), mouth piece diameter (Lin, et al., 2001) and the type of the propellant used in the pressurized Metered Dose Inhaler (pMDI) (Cheng, Fu, Yazzie and Thou, 2001).

The Chlorofluorocarbon (CFC) pressurized Metered Dose Inhaler (pMDI) has a quite different deposition patterns than Hydrofluorocarbon (HFA) pMDI. HFA inhalers have lower deposition in the oral region than the CFC inhalers at all respiratory flow rates, and correspondingly improve the lung deposition.

Considerable amount of work has been published in the general area of aerosol inhaler design and performance. However, it is noted that many of the previous studies was aimed at the inhalation toxicology studies. This includes the applications of aerosol inhalation in nuclear, biological and chemical warfare during the Cold War and inhalation exposure to aerosolized environmental pollutants. In these studies, the human subjects were natural breathing without the interference of the mouthpiece. Effects of mouthpiece design were not well studied.

It was concluded from the above brief review that a considerable amount of research work has been done in the past, which has greatly advanced the technology of aerosol therapies and knowledge of particle depositions in human extrathoracic airways. However, it is worth noting that the efficiencies of current inhalers (with and without spacers) were excessively low. The database related to the aerosol therapy applications was especially inconclusive. Accordingly, more relevant R&D work is needed. They are itemized as follows:

1. There is a great need for the development of an inhaler ancillary device that can

significantly improve delivery efficiency by minimizing massive aerosol deposition at the back of throat, reducing the drug loses in the delivery system, and meanwhile cost less. It is noted that most medical insurance companies don't cover the cost of the spacer, since it is considered as a "medical device". This cost may be acceptable to patients having chronic conditions that require frequent use of inhaler medication for a long period of time, provided the patients are willing to frequently clean the devices. However, many patients need inhaler medications for only a short period of time, in which case the high cost of the spacer is very unsatisfactory. In addition, most spacers are too big to be put in a vest pocket and far too expensive to be considered disposable. There is a great need to develop a high efficiency, portable, light, reliable, inexpensive, disposable, adaptable and easy-to-use ancillary devices for use with various inhalers.

2. Studies on the effects of particle initial conditions at the mouth entrance are needed. Aerosol initial conditions vary by different inhaler designs. At present, the major problem associated with aerosol drug inhalers is the massive deposition of aerosol drugs on the back of throat. Since it is generally known that the inertial impaction is a dominant mechanism for aerosol deposition in oropharyngeal airways, the reduction of the impaction parameter (i.e., a function of size and velocity only) for inhaled aerosols become the focus of the prior research as well as aims of new inhaler design. Effects of initial positions are largely neglected in the literature although effects of aerosol size, velocity and breath patterns are well studied. Typically, particle initial condition was not deemed as a control parameter for prior industrial hygiene studies since subjects were expected to breath naturally in the experiments. While this parameter could be the dominant factor in aerosol therapy. In fact, various aerosol therapy strategies (i.e., open-mouth vs. close-mouth method, the distance between inhaler and mouth, shape and opening o f the mouth, breath control, etc.), various inhaler and spacer design (i.e.,

cross-sectional geometry, spray angle, propellant pressure, etc.) will precisely change the particle's initial velocity, entrance position and angle, and therefore, results in distinct deposition patterns.

Recently, Lin et al. (2001) reported an experimental work on the effects of mouthpiece diameter on deposition efficiency in an oral airway cast. Their results showed that the effects were significant and depend on particle size. Lin et al. (2001) pointed out that the diameter may alter the airflow characteristics (i.e., air velocity and turbulence) for a given flow rate, leading to difference in deposition efficiency. In fact, the diameter will not only alter the airflow patterns, but also change the initial positions of inhaled aerosols relative to the oropharyngeal airway passage. Their experiments strongly supported our hypothesis that to manipulate inhaler designs can have significant effects on aerosol delivery efficiency.

3. Computer simulation of flow patterns and particle trajectories in human oral-oropharyngeal airway system is needed. Computational fluid simulation becomes an important research tool in the field of biomedical engineering. Current experimental techniques are not able to provide detailed information such as airflow patterns and particle trajectories in airways due to limited measurement resolution as well as associated costs. Velocity profiles and particle trajectories provide explicit information on flow-particle interactions and particle locations from launching to deposition points. Without such information, it is nearly impossible to conduct the deposition mechanistic study.

Although a 3-D computational oral airway model was first reported by Perzl in his Ph.D. dissertation (Perzl, 1997), there is no other publications available in the literature. The concentration of Perzl's work is on the development of the computational model. Results described in the thesis are limited t o steady state, and low Reynolds number (<1000) flow

simulations. Computer simulations will be used as a supplement tool for initial screening and preliminary examination of the key design parameters.

Important research needed in computer simulation is the development of a new particle trajectory method. It is noted that particle trajectory software built in most commercial CFD package as well as most trajectory publications neglected the effects of particle diffusion. The Monte Carlo method, which typically used in the literature, does take particle Brownian diffusion into account; however, the inherent 'random' nature of the method makes the computing of particle deposition efficiency difficult. Particles ejected at the same location in the steady flow would always follow different paths and ended up at different destinations for each simulation. Therefore, this method can't be used to provide the explicit particle destination information. The establishment of aerosol destination map is a key component.

Knowledge of particle transport within human airways is very important in the field of aerosol medicine therapy. The dose delivered to airway cell is a critical parameter in addressing the therapeutic effects of inhaled phatraafxslocal agents and also the potential irritant or -side effects elicited by the inhaled aerosols will depend on the relative quantities delivered to the airway tissues. Subsequent to deposition, the biophysics of pharmacokinetic processes and the biochemistry of reactions within cells can be studied on *a* dose-response basis.

Deposition sites of inhaled aerosol medicines are mostly influenced by levels of respiratory intensity as defined by coupled tidal volumes and breathing frequencies and particle parameters such as geometric size, shape, and density. The phenomenon of particle deposition in the human airways are strongly affected by the very nature of the fluid motion in which they are entrained and transported. The total amount of aerosol deposited in the human lung can be represented as the product of aerosol volumetric concentration, respiratory volumetric flow rate

and lung particle Deposition efficiency.

It is well known that the current efficiency of the aerosol medicine delivery using drag inhaler through month is very low. More than 90% of the drug particles will deposit in mouth and back of throat due to high velocity of aerosol cloud from MDT (Meter dosed-Inhaler), The initial launch location of the particle also play important roles in the deposition efficiency. In other words, the shape design of the inhaler nozzle has great impact on the drug deposition efficiency.

To understand all of the experiments and procedures one needs to understand the following: human oral airway geometry consists of three parts. Part one has fifteen segments, each segment or slice has thickness of 3 mm. All the segments in part one have been sliced perpendicular on the Y axis, so each segment has constant Y value (Some of the sections are seen as Figs. 34A-H) shows all the cross section shapes in the part one for scale factor one. Part two has eighteen segments, each segment or slice has been sliced every 5 degree. All the segments in part two have been sliced perpendicular on the 0 axis (cylindrical coordinates), so each segment has constant 0 value. (See Figs 35A-L) shows all the cross section shapes in the part two for scale factor one. Part three has twenty eight segments, each segment or slice has thickness of 3 mm. All the segments in part one have been sliced perpendicular on the Z axis, so each segment has constant Z value. (See Figure 36K-L)shows all the cross section shapes in the part one for scale factor one. This oral geometry has been supplied to us by Lovelace Respiratory Research Institute, Albuquerque, NM. This human oral airway geometry represents a normal oral airway position not the oral airway during the inhalation process.

Tongue position has a great influence on the deposition in the human airway. The tongue can take different positions according to the mouth opening and the respiratory flow rate. As we can see in **Figure** 27(**#69**-See part 3, Figure 27), the tongue can take different positions and different shapes, these positions/shapes will influence the deposition efficiency of the aerosol drug such as pMDI.

SUMMARY OF THE INVENTION

The objective of this project is to understand the characteristics of respiratory flow and particle transportation patterns during aerosol therapy and to develop a high efficiency, portable, light, reliable, inexpensive, disposable, adaptable and easy-to-use ancillary devices for use with various aerosol therapy system, especially for inhalers. This will be conducted by means of computer simulations and experimental investigations using extrathoracic airway models. The specific aims of the study are a) to identify and quantitate those components of aerosol therapy that are subject to manufacture manipulations and/or spatient use, b) to optimize the inhaler mouthpiece configurations design, and c) to improve the efficiency of aerosol delivery by a minimum of 200% (i.e., from current average of 10% to 30%), within the typical range of respiratory flow rate and aerosol size encountered during aerosol therapy.

Aerosols emitted from various cross-sectional location of mouthpiece have different destinations as demonstrated in our computer simulation. The efficiency of drug delivery can be significantly improved if an ancillary device (such as a specially configurated extended mouthpiece) is used to channel aerosols from where they are most likely to penetrate through the extrathoracic airways. This objective can be achieved by a good design of inhaler ancillary devices, including design of cross-sectional configuration, outside diameter, tapered angle, and distance extended into the mouth. Aerosol delivery efficiency is defined as the number ratio of the aerosols that went through the extrathoracic airways to the aerosols that ejected from the inhaler.

It is worth noting that the focus of the invention is the reduction of the aerosol deposition in extrathoracic airways, specifically, the oral-pharyngeal-laryngeal (OPL) airways. The

proposed optimized inhaler configuration may or may not change (positively or negatively) the aerosol deposition patterns beyond the OPL airways. However, the OPL airways act as the first of a series of artificial filters that aerosol will encounter before reaching the targeted lower airway lung region. It should be the first and necessary problem to be addressed. Also, for propellant driven inhalers, aerosol velocities and sizes decrease drastically after the spray. Typically, the measured velocities are about 50 m/s at the nozzle orifice and close to 20 m/s when reach the back of throat. Thus, if aerosols can survive the OPL airways and enter thoracic region, their velocities and sizes are significantly reduced. A much smaller impaction force can be expected downstream of OPL and therefore, the aerosol deposition by the mechanism of inertial impaction (the dominant mechanism that cause massive aerosol deposition at the back of throat).

One object of this invention is to understand the characteristics of respiratory flow and particle transportation patterns during aerosol therapy and to develop a high efficiency, portable, light, reliable, inexpensive, disposable, adaptable and easy-to-use ancillary devices for use with various aerosol therapy system, especially for inhalers. This will include computer simulations and experimental investigations using extrathoracic airway models. The hypothesis of the research is that since aerosols emitted from certain area of inhaler cross-section will not reach the targeted lung region, the efficiency of delivery can be significantly improved if the inhaler only ejects aerosols from where they are most likely to penetrate through the extrathoracic airways. We also hypothesize that this objective can be achieved by a good design of inhaler ancillary devices, including design of cross-sectional configuration, outside diameter, tapered angle, and distance extended into the mouth. The specific aims of the study are a) to identify and quantitate those components of aerosol therapy that are subject to manufacture manipulations and/or spatient use, b) to optimize the inhaler mouthpiece configurations design,

and c) to improve the efficiency of aerosol delivery by a minimum of 200% (i.e., from current average of 10% to 30%), within the typical range of respiratory flow rate and aerosol size encountered during aerosol therapy.

A three-dimensional body-fitted airway grid system, including oral cavity, oropharynx, larynx and trachea airways has been constructed. Several cases of low Reynolds number flows have been simulated. Providing initial validation, the simulated velocity profiles in the trachea airways at three different flow rates agree well with the detailed experimental measurement of Zhao et al. (1992).

Another objective is design an innovative nozzle shape design for the drug inhaler. The purpose of the nozzle design is to launch/spray the particles from where they are most likely to go deep into the lung and therefore reduce the unwanted aerosol deposition in the throat.

There are many unanswered questions in the area of aerosol medicine delivery and provide the motivation for this project.

These and other features and objectives of the present invention will now be described in greater detail with reference to the accompanying drawings, wherein:

DESCRIPTION OF THE FIGURES

FIG. 1 is a schematic of various inhaler mouthpiece configurations;

FIG. 2 is a spray jet spreading structure;

FIG. 3 illustrates the velocity profiles in an oral passage at an inspiratory flow rate of 15 L/min, which corresponds to the breathing rate at a light activity condition;

FIG.4 is a map of particle destination distribution;

FIGS. 5A and 5B show a schematic particle generation systems;

FIG. 6 shows a fabricated airway cast;

FIG. 7 shows a fabricated airway cast;

FIG. 8 is a breakaway of an inhaler nozzle;

FIGS. 9A-C are a front end view, a sectional view and rear end view of FIG. 8, respectively;

FIGS. 10 are a front end view, a sectional view and rear end view of an alternative embodiment, respectively;

FIGS. 11A-C are a front end view, a sectional view and rear end view of an alternative embodiment, respectively;

FIGS. 12A and B are front and rear views of still an alternative embodiment;

FIG. 13 is an oral airway model consisting of the mouth cavity, the pharyngeal cavity and the pharynx ;

FIG. 14 the three different parts of the airway geometry;

FIG. 15 shows the oral airway clay segments;

FIG. 16 shows a human oral airway mold and cast ;

FIG. 17 a dummy commercial inhaler;

FIG. 18 a canister charging system;

FIG. 19 illustrates experimental apparatus ;

FIG. 20 is a measurement calibration curve;

FIG. 21 is a line graph of flow rate of a mouthpiece having a Diameter of 20mm;

FIG. 22 is a line graph of flow rate of a mouthpiece having a Diameter of 16mm;

FIG. 23 is a line graph of penetration efficiency;

FIG. 24 is a line graph of the diameter effects of a flow rate of 90 L/min;

FIG. 25 is a line graph of the diameter effects of a flow rate of 60 L/min;

FIG. 26 is a line graph of the diameter effects of a flow rate of 30 L/min;

FIG. 27 is a line graph of particle penetration efficiency;

FIG. 28 is a line graph of particle penetration efficiency;

FIG. 29 is a line graph of particle penetration efficiency;

FIG. 30 is a line graph of particle penetration efficiency;

FIG. 31 is a line graph of particle penetration efficiency ;

FIG. 32 is a line graph of particle penetration efficiency;

FIG. 33 is a line graph of particle penetration efficiency;

FIG. 34A-H are cross sections of a human airway ;

FIG. 35 A-L are cross sections of a human airway;

FIG. 36 A-L are cross sections of a human airway

FIG. 37A-H illustrate different positions of a tongue:

FIG. 38 are three positions of tongues:

FIG. 39 is graphs of Aerosol Penetration Efficiency with Original Mouthpiece where d = 16 mm and 20 mm respectively;

FIG. 40 is a graph of aerosol penetration efficiencies with a need structure;

FIG. 41 show various inhaler adaptors made of straight channels with upward, angl-cuts of various degrees;

FIG. 42 is a graph of the Flow Rate on the Efficiency of MDI with a 20 Degree Angle Cut Mouthpiece (D=20mm); and

FIG. 43 is a graph of the Effect of the Flow Rate on the Efficiency of MDI with a 20

Degree Cut Mouthpiece (D=20mm).

DESCRIPTION OF THE INVENTION

An innovative breath simulator needed for transient experiments has been fabricated. This is a linear-motor controlled piston-cylinder device capable of controlling flow rate (covering the whole flow rate range of humans and animals), breathing frequency, amplitude and profile functions (with any profile displayed on the PC screen). All the aerosol generators, neutralizers and aerosol counters needed in the experiments have been calibrated.

Aerosols emitted from various cross-sectional location of mouthpiece have different destinations. The efficiency of drug delivery can be significantly improved if an ancillary device (such as a specially configurated extended mouthpiece) is used to channel aerosols from where they are most likely to penetrate through the extrathoracic airways which can be achieved by a good good design of inhaler ancillary devices, including design of cross-sectional configuration, outside diameter, tapered angle, and distance extended into the mouth. Aerosol delivery efficiency is defined as the number ratio of the aerosols that went through the extrathoracic airways to the aerosols that ejected from the inhaler.

The focus is the reduction of the aerosol deposition in extrathoracic airways, specifically, the oral-pharyngeal-laryngeal (OPL) airways. The optimized inhaler configuration results may or may not change (positively or negatively) the aerosol deposition patterns beyond the OPL airways.

For propellant driven inhalers, aerosol velocities and sizes decrease drastically after the spray. Typically, the measured velocities are about 50 m/s at the nozzle orifice and close to 20 m/s when reach the back of throat. Thus, if aerosols can survive the OPL airways and enter

thoracic region, their velocities and sizes are greatly reduced. A much smaller impaction force can be expected downstream.

Fig. 1 shows the schematic drawings of various inhaler mouthpiece configurations. 'Close-mouth' method, in which the lip encloses a mouthpiece, is used for the purpose of demonstration. Fig. 1A shows a typical design of an existing inhaler mouthpiece configuration. Most current inhaler mouthpiece has a circular or an oval cross sectional geometry with uniform tube thickness.

Panel B of Fig. 1 demonstrates an improved cross sectional configuration design that might improve aerosol delivery efficiency. The inner cross-sectional shape of the mouthpiece matches the contours of particle penetration zone revealed from computer simulation and experimental verification, while the outer configuration might still maintain the circular geometry for manufacture convenience or patient comfort.

Further improvement of design can be seen in Panel C of Fig. 1. The mouthpiece has sloped roof configuration facing the downward direction. When airflow exits the mouthpiece, the mainstream air levels out while the entrained aerosols near the top will continue their downward motions due to inertial forces. These are the same forces causing the aerosols deposited on the back of the throats. The downward angle will facilitate particles passing through the 90-degree downward bend of the oropharyngeal airway. Therefore, it will reduce the deposition at the back of throat caused by particle inertial impaction. This design is a three-dimensional optimization: 1) the inner passage can has a variable as well as a simple linearly sloped cross-sectional geometry, 2) aerosols enter the mouth in a downward direction, 3) this design can be achieved by design a 3-D optimum mouthpiece adaptor connected with most existing mouthpiece, 4) a simple version of the 3-D design can be achieved by placing a 2-D optimized plate configuration in front

of a: straight downward regular circular tube.

A preferred embodiment of the inhaler mouthpiece configuration is displayed in Panel D of Fig. 1. In this design, not only the aerosol initial position and angle, the inhaler distance extended into the oral cavity as well as the outer diameter of the mouthpiece is also optimized. It is noted that for most conventional designs, the distance of inhaler intruded into the mouth not only varies between patient to patient, but also changes between every therapy for the same individual. The outer diameter of a mouthpiece also plays an important role by controlling the opening of the mouth, therefore, it affects the shape of oral cavity.

There is a wide range of brands of inhaler and spacers available on the market. In principle, the aforementioned design concepts can be applied to all aerosol medicine delivery system, including MDI, DPI, nebulizer, as well as spacers and chambers. It is desired to have a universal inhaler ancillary device. Essentially, this device is a hollow, flexible and has an extended mouthpiece with an optimum configuration. It will easily hook up to mouthpieces of most current inhalers, spacers and other aerosol delivery systems. The optimum mouthpiece configuration assures high efficiency while extension places the inhaler at a greater distance from the mouth and thus further diffuses the aerosol velocity. The hollow and see-through structure minimizes the drug loses in the device and simplifies clean up.

For conventional spacer design, the objective is to be a good 'large aerosol filter' while the principals of this design are first to reduce the aerosol size and then to guide the aerosols through the oral cavity. The inhaler adaptor design is high efficiency, portable, light, reliable, inexpensive, disposable, adaptable and easy-to-clean. It is also designed to universally fit most aerosol therapy systems, especially for portable inhalers. The design features are described as follows:

1. Adaptor design with a slightly upward angle.

The computer simulation and experiments show that placing the inhaler with a slightly upward angle can significantly decrease the particle deposition in the airways cast. An optimum angle of about around 20 degrees exists which can maximize the particle penetration efficiency through the oral airway. Subsequently experiments show that the angle effects are not sensitive to the oral airway geometry.

Experimental Measurements:

To ensure full simulation of the commercial aerosol plume characterization, the commercial inhaler, PROVENTIL MDI, is used in the experiments to mimic the realistic inhaler spray. The suspension of dry green fluorescent polymer micro spheres of 7 micron (Duke Scientific, Corp., Excitation 468 nm; Emission 508 nm) and R134-a are charged into the PROVENTIL canister. Various (5) kinds of tests are conducted repeatedly throughout the experiments to assure the accuracy and consistency of the experimental system.

2. **Aerosol Spreading Structure Design**

A significant improvement in aerosol delivery efficiency can be obtained by using a novel spray jet spreading structure shown in Figure 2. The experiments are conducted at the typical aerosol therapy condition with the respiratory flow rate at 30 L/min and particle diameter equal 7 micron, respectively. Test shows a significant enhancement in overall efficiency, from 15% to 33%, and in oral delivery efficiency, from 15% to 55%.

Comparison of inhaler Ancillary Devices

PERFORMANCES / PRODUCTS	Delivery Efficiency	Cost	Drug losses Inside device	Clean Expediency	Portability	Adaptability
AEROCHAMBER	Intermediate	High	High	Low	Low	Intermediate
MICROSPACER	Low	Intermediate	Intermediate	Intermediate	Intermediate	Intermediate
PROPOSED DEVICE	High	Low	Low	High	High	High

Computer simulations will produce series of particle distribution maps. An ancillary device will be attached to inhalers. Thus, aerosol patterns similar to the predicted profiles of passing-through zone will be generated at the entrance of oral airway model. Various particle entrance conditions are therefore created. Due to characteristics of turbulent flow, the idealization of boundary conditions, the limitations of aerosol transport model as well as many numerical approximations used in equation solving, current computer simulations will only qualitatively predict a particle passing-through zone. Trial-and-error procedures are always needed in experiments for searching of an optimum configuration.

Airway Model Construction

The model of the human oral airway tract begins at the mouth entrance and continues through oral cavity, pharynx, larynx, and ending at the trachea. The cross-sections of the airway passages are based on the geometry published by Cheng et al. (1997), which is the identical geometry used in the computer simulation. The oral portion of the airway system was molded from a dental impression of the oral cavity from a human volunteer, while the other airway

portions were modeled from a cadaver.

The construction of the oral airway model will follow the same procedure as that used to build the nasal airway model (Lennon, et al., 1997). Clay models of the oral airway passage were developed first. These clay segments were taken separately and suspended within an open glass holding box. A silicone rubber compound was then poured over the suspended clay model. After the rubber solidifies, the mold was cut in half and the clay model was removed. Hot wax is then poured to create a wax model with the same geometry as the original clay model. After the wax solidified, the solid wax cast was carefully taken out. Many identical solid wax models can be made from the same production mold. To minimize the effect of electrostatic deposition, an electrically conductive silicone rubber compound (KE 4576) was applied to the wax cast to make the airway models. After a curing period, the hollow airway rubber model was obtained by removing the wax in boiling water. Before the experiments, the inside surface of the airway model was coated with an aqueous solution (Lin et al., 2001) containing 1% carboxymethylcellulose sodium (Spectrum Chemical Mfg. Corp., Gardena, CA) to simulate the mucus layer and to minimize the particle bounce.

Fig. 3 shows the velocity profiles in an oral passage at an inspiratory flow rate of 15 L/min, which corresponds to the breathing rate at a light activity condition. The condition of free inhalation (or without the mouthpiece) and steady breathing were simulated. Various characteristics of oral airway flows, including boundary layer flows, creeping flows, bend flows and jet flows were clearly displayed.

Fig. 4 displays a map of particle destination distribution. Aerosols were inhaled through a mouthpiece attached to the inhaler. The mouthpiece/spacer had a circular cross sectional geometry and was attached to the mouth (or zero distance extended into the oral cavity). The map

was compiled based on the results of some 400-particle trajectories at inspiratory flow rate of 45 L/min and particle size of fourteen microns. Inert particles with breath-activated conditions were simulated. The aerosol entering condition corresponds to dry-powder inhaler (DPI) applications, where aerosol initial velocities were approximately the same as flow velocity, and particle sizes are relative large. Particles entering the mouth from various cross-sectional location of mouthpiece follow different paths demonstrate that aerosols will either be deposited in the mouth cavity (15.8%), oropharynx (20.3%), laryngeal airway (33.0%), or go beyond extrathoracic airways (30.9%). The corresponding particle destinations are marked by different shadings indicated on the figure legend. Only a fraction of particles (30.9%) were able to pass through the oral-pharyngeal-laryngeal passages and deposit into the targeted lung region.

The concept of an optimum design is such that a high efficiency inhaler ancillary device will be able to guide particles to where they are most likely to penetrate extrathoracic airways, and therefore reduce unwanted aerosol deposition in the oral passages. The objective of the prevailing inhaler design is to reduce the aerosol impaction parameter (or to reduce particle size, mass and velocity). Typical cross-sectional geometry of inhaler nozzles is of a circular or oval shape. For closed-mouth aerosol therapy, the shape of the mouth opening bears the peripheral shape of the inhaler mouthpiece. This may not be the optimum shape of the inhaler design. One can speculate that if the configuration of an inhaler mouthpiece (or similar ancillary device) matches the contour of the particle passing through zone, the efficiency of aerosol medicine delivery can be significantly enhanced.

A schematic of the experimental setup is shown in Fig. 5. Two kinds of particle generation systems were used in the experiments to simulate two different type of aerosol delivery system. They are shown in Fig. 5, Panel A. Breath-activated System and Panel B. Propellant-driven

System, respectively. The initial velocity of a breath-activated aerosol was approximately the same as that of the flow at the oral entrance. Aerosol inhalation through a mouthpiece or spacer attached to the inhaler can be approximated as breath-activated system.

Monodisperse polystyrene fluorescent microspheres (specific gravity of 1.05) suspended in distilled water are atomized and dried within a Tri-Jet Aerosol Generator (Thermal System Inc.). The fluorescent particles exiting the aerosol generator were first neutralized by using an aerosol neutralizer (Richmond Static Control) and mixed with a steady flow of filtered room air. The flow then entered into the experimental containment where it was uniformly dispersed by a small mixing fan mounted within the box. The experimental box was a plexi-glass holding unit for most of the airway cast. The trachea extends outside the box through a hole in the bottom surface. The box also includes six holes that allow the positioning of particle sampling probes throughout the unit. An inhaler spacer/mouthpiece with tapered cross sectional geometry similar to the predicted profiles of passing-through zone were placed inside (or in front) of mouth entrance.

The trachea was the last segment of the experimental respiratory system, and this is where the exhaustion concentration readings were taken. The flow then entered a 3.5 in (8.9 cm) diameter hard plastic duct that connects to a filter. The exit duct was connected to a blower, which draws air through the experimental airways to simulate inhalation from a person breathing. A flow meter was placed at the outlet of the blower to measure the volumetric flow rate, which was controlled by regulating the voltage supplied to the blower motor. For transient experiments, a breather replaced the blower.

Two types of particle deposition measurements were taken simultaneously during the experiments, i.e., total particle deposition measured by particle counters and regional particle

deposition measured by a fluorescent spectrophotometer. For total particle deposition measurement, particle sample probes were connected to Climet Instrument CI-225 Optical Particle Counters by clear rubber tubing. The output of the Optical Counter was sent to a CI-220 Multi-Channel Monitor every 8 seconds. The Multi-Channel Monitor contains a 7805-5 input board that has eight input channels, which are each set to record various particle size readings. The data that was collected by the Multi-Channel Monitor and sent every 84 seconds to an IBM computer, which stored the data for future analysis.

Regional particle deposition was measured by a fluorescence method. After the desired amount of experimental data was collected, the airway cast was removed from the plexi-glass box. A fixed volume of distilled water was rinsed into predetermined locations of the airways for at least 5 times, and the mixture of distilled water and fluorescent particles collected. The particle concentration in these samples was measured with a fluorescent spectrophotometer (Hitachi Model F-2000) which was preprogrammed according to the fluorescence properties of the monodisperse polystyrene microspheres. Then, the uncertainty analysis was performed.

For the experiments with propellant-driven aerosol generator system, the MDI inhaler was used. These aerosol inhalers were provided by pharmaceutical companies. These aerosol inhalers were mounted on inhaler trigger devices to imitate the coordination of hand action and inhalation. The trigger actions were controlled by solenoid valves. The actuation time of the solenoid valve were controlled by a personal computer (PC). The distances/angles between the inhaler and mouth were easily adjusted to duplicate actual inhaler applications.

A filter (WI) was placed in one line and the airway model was placed in another line followed by a filter (W2). Identical flow rates were used in both lines during the experiments. The desirable cyclic air movement through the surrogate airway casts was induced by the

reciprocating motion of a piston in a piston-cylinder type device called a human breath simulator. The motion of the piston was actuated by a linear motor, which is in turn was controlled by electrical signal input. These electrical signals were converted from different breath profiles displayed on the PC screen. During the experiments, the particles were collected on the aforementioned filters for 10 - 20 minutes. The particles deposition values were obtained by measuring the weight of filters W1 and W2. An OHAUS Model AP210S precision analytical scale will be employed. The accuracy and readability of the scale was 10e-5 gram. The deposition efficiency d is calculated from the weight of filter (W1) and the filter after the airway cast (W2): d = 1 - W2 / W1. To account for a possible uneven split of flow in the system, we will measure the difference in particle collections by placing filter (W2) ahead of the airway cast before starting each new experiment. Monodespersed fluorescent particles were mixed with liquid R134a and sealed in the container of a MDI. It is understood that there will be differences between the fluorescent particle and actual drug aerosols.

Experiments with flow rates between 15 L/min and 60 L/min, particle size between 1 to 10 microns were conducted to study effects of inhaler configuration design and breathing profiles. For the applications of the propellant-driven inhaler, the effects of trigger time relative to the breathing profile were an additional parameter. The fabricated airway cast were similar to the ones shown below **See Figures 6 and 7** .

Computational fluid dynamics (CFD) researchers are always skeptical of using the software that they have not developed themselves. It is very difficult to customize another person's code to one's own problems. Even more hazardous is not understanding some aspect of the code that has not been documented properly.

For all flow simulations and particle trajectory simulations in proposed research, the CFD

commercial software package CFX 5.1 (AEA Technology Inc., Pittsburgh, PA) was used. It is general-purpose software for fluid flow simulation consisting of pre-processor, solver, and post-processor. All kinds of flow scenarios can be modeled and the user can choose among a variety of solution techniques. CFX-3D is one of the leading CFD software that comprises decades of research and development. Therefore, much of discussion herein refers to and is adapted from the CFX 5.1 Flow Solver User Guide (2001). The following description of the modeling will concentrate on the work that needs customized coding and user input.

The respiratory air stream is treated as viscous, homogeneous, and incompressible fluid. Its motion is governed by the Navier-Stokes equations (consisting of three partial differential equations in a three-dimensional coordinate system) and the continuity equation. In order to solve these equations numerically, these continuous differential equations must be discretized on the grid nodes distributed within the airway geometry by using various approximation methods to obtain a system of simplified algebraic equations. The control-volume scheme based on the principals of mass, energy and momentum conservation is mainly used in CFX-3D software for numerical discretization.

The extrathoracic airflows consist of both laminar and turbulent flows. Generally speaking, most laminar flows problem can be numerically solved without encountering major difficulties. However, turbulent flow problems are most difficult to analyze. It is almost impossible to directly simulate the instantaneous turbulent flow eddies with today's computer technology. A common approach in the literature is to describe turbulent motion in terms of time-average quantities. One of the many turbulent models incorporated into the CFX-3D is the two-equation k-e model. This model has been highlighted in most fluid dynamics textbooks. The k-e model is based on Reynolds average equations and the eddy-viscosity concept. The general k-

e model is not that effective in near-wall region. Therefore, a low Reynolds number and two equation k-e model coupled with a near-wall modeling scheme built in CFX 5.1 will be used in our flow simulations.

The effects of mucus layer, elastic wall, and site-specific tissue absorptivity were not included in the simulation. No slip and constant concentration boundary conditions were applied. During aerosol therapy, the geometry of extrathoracic airways is generally stationary. Extrathoracic airways are upstream conducting airways while respiratory flows are induced by lung volume changes downstream, it can be assumed that effects of moving-boundary or elastic wall of extrathoracic airways are not important, as suggested in all of the prior numerical and experimental studies.

The uniform velocity distribution, or plug flow, at the inlet of mouthpiece/spacer (or at mouth entrance for propellant-driven aerosol system without using mouthpiece/spacer) was used for all the simulations. Since the mouthpiece/spacer is connected to an aerosol generation device, the actual flow at the inlet of mouthpiece/spacer becomes an unknown developing flow. To solve this problem, the length of mouthpiece/spacer used in the computer simulation and experiments were slightly longer than the actual size, in order to duplicate a developing flow conditions. Zero gradient and mass flow (mass conservation) conditions were used at the outlet of the airway system. Both the steady flow and transient flow were simulated. Various breathing profiles during the transient flow will be studied which including profiles of nollual breathing, sine breathing and controlled linear-curve breathings.

The most time-consuming part of the computer simulation is construction of the grid system that resembles realistic 3-D oral-oropharyngeal-laryngeal airway geometry. A 3-D body-fitted oral airway grid system was constructed and simulated several cases for low

Reynolds number flows. The computational oral airway geometry was reconstructed based on the information published by Cheng et al. (1997). The grid test was conducted to minimize numerical truncation errors. A final grid size was chosen for the production runs as a compromise between computational accuracy and the cost.

Different flow rates (between 15 L/min to 60 L/min) were simulated. The preliminary results of velocity profile in the trachea airways agree well with the detailed experimental measurement of Zhao et al. (1992).

As discussed before, two major aerosol generation systems are used in aerosol therapy. These are the breath-activated inhaler (i.e., DPI and nebulizer) and the propellant-driven inhaler (i.e., MDI). Inhalation through a spacer/mouth-piece can be approximated as the breath-activated aerosol therapy. The initial velocity of a particle at the mouth entrance will be quite different between these two systems. Particle deposition as a function of breathing rate, particle size, initial speed, entrance angle and locations (both in traverse and longitudinal directions) were systematically studied for both systems. At each fixed parameter, arrays of 25x35 (approximately 700, in the preliminary study, 20x20 is used) particles, which are uniformly distributed in the cross-sectional area of the mouth entrance, were launched simultaneously. The positions of these particles in the airflow was then be computed and tracked all the way to deposition point. The total and regional particle deposition efficiencies was computed.

A discrete Lagrangian approach was used to model the motion of particles in the oral airway flow. It is assumed that the particles are sufficiently dilute that the particle-particle interactions can be neglected. Also, break-up or coalescence of particles were excluded from the model. The effects of turbulent force were included in the particle transport model. The continuum velocity in the particle momentum equations was taken to be the mean velocity plus a

contribution due to turbulent eddies. For detail, please refer to CFX 5.1 solution manual (2001).

The CFX-3D software serves the basic function of simulating particle trajectories. However, like most other commercial CFD software, the effects of Brownian diffusion were not included in the trajectory model. This effect could be important for submicron particle (i.e., some aerosols generated by nebulizer). Therefore, a customized trajectory code was needed. The Monte Carlo method was typically used in the customized code. It does take particle Brownian diffusion into account; however, the inherent 'random' nature of the method makes the deposition efficiency computing difficult, particularly for aerosols of smaller sizes. Particles ejected at the same location in the steady flow will always follow different paths and end up with different destinations at every-and-each simulation. Therefore, this method can't be used to generate the needed particle destination information, which is a key component of the proposed research.

A unique trajectory mapping approach was modified to predict particle deposition efficiency in airways. This involved certain works of modifying source code and incorporating this model into the software. Brownian diffusion was accounted for using an effective particle radius concept. This effective radius is defined such that the apparent size of a particle being tracked grows in time according to the probability of not finding its center inside an exclusion sphere. This approach was uniformly applicable to all particle sizes with diffusion influence diminishing in importance as physical particle size increases. This method takes into account the Brownian diffusion effects, and at the same time, provides detailed spatial particle deposition patterns.

Monte Carlo method was also used to provide the benchmark results for the proposed unified trajectory simulations. Monte Carlo method is a reliable and proven method, especially for larger particles. For the proposed unified trajectory method, there was a constant needed to be

determined. The physical meaning of the constant was the probability of aerosol that will diffuse to the outside the effective radius. This constant equals 0.65 for straight conducts (Zhang and Lessmann, 1997). It showed that this constant is insensitive to different variables and can be applied to a wide range of particle size (0.001 to 5 micron), different flow type (parabolic and plug), different pipe size, and different geometry (circular, square and other polygonal cross-sectional geometry).

There is a wide range of aerosol medications. Of particular interests to trajectory simulations are the physical properties such as particle velocity, density and size. Since the inertial impaction is the dominant mechanism for aerosol medicine deposition in human extrathoracic airways and the designs are to avoid such deposition, the impaction parameter would be the major dimensionless variable to be studied to reduce the number of computer runs. The second variable can be the sedimentation number.

The accuracy of the numerical simulation was verified by the experimental results. However, the verification was indirect and limited to particle deposition simulations. This is because currently there were no experimental measurements of velocity profiles and particle trajectories available in the literature, while there was some reported studies on particle deposition in oral airways as discussed previously.

Computer simulations were conducted to simulate the respiratory flow field and particle trajectories, Particles launched at various regions at the entrance of the mouth will be either deposited in the mouth cavity, throat, laryngeal airway or deep into the lung. A regional distribution map of particles at the launch site will be generated. This map is the function of particle size, density as well respiratory parameter. This map will be verified by the experimental measurement. This particle regional distribution map will be used in the commercial design of the inhaler.

The proposed design provide a noninvasive and inexpensive means to improve the aerosol drug delivery. It applies to the treatment of lung diseases using most types of aerosol medicine inhaler. This device can be operated by patients themselves or a doctor with minimum training for both at home therapy and in hospital treatments.

FIG. 8 is a breakaway perspective view of an embodiment of the invention. wherein an inhaler nozzle 10 is comprised of a housing 12. The inner surface 20 of the housing 12 is configured to facilitate the delivery of a medicated aerosol to the lungs of a user when the medicated aerosol is forced through the housing 12. The inner surface 20 comprises a lower arcuate section 30 and upper section 40. The upper section 40 comprises a first arcuate portion 42 and a second arcuate portion 44. The first arcuate portion 42 and the second arcuate portion 44 are joined together to form a ridge a ridge 46. Both the lower arcuate section 30 and the upper section 40 can extend along the entire length L of the housing 12 or optionally can extend along at least a portion of the length L of the housing. Alternatively, the lower arcuate section 30 can extend along the entire length L of the housing and the upper section 40 can extend along at least a portion of the length L of the housing or vice versa.

To visualize the full inhaler nozzle, various view have been included. FIG. 9A shows the front end view of FIG. 8. FIG. 9B is a sectional view FIG. 1 taken along lines 9B. wherein the upper section 40 extends downwardly along the entire length L of the inhaler nozzle 10 toward the lower arcuate section 30 at an angle within the range of between 5° to 40°, preferably 30°, to the vertical axis Y of the inhaler nozzle 10. And FIG. 9C is a rear end view of FIG. 8.

FIG. 10A is a front end view of an alternative embodiment of FIG. 1. FIG. 10B) is a sectional view of FIG. 10A taken along lines 10B wherein the upper section 40 extends downwardly along about half the length L of the inhaler nozzle 10 toward the lower arcuate section 30 at an angle within the range of between 5° to 40°, preferably 30°, to the vertical axis Y of the inhaler nozzle 10. FIG. 10C is a rear end view of FIG. 10A.

An alternative embodiment is shown in including the front end view, See FIG. 11A. FIG. 11B is a sectional view of FIG. 11A taken a long lines 11B, the housing 12 comprises a first segment 50 having a top and bottom surface 52, 54 and a second segment 60 having a top and bottom surface 62, 64. The top surface 62 extends upwardly from the top surface 52 at an angle within the range of between 5 ° to 40°, preferably 30°, from the horizontal axis X of the first segment 50. FIG. 11C is a rear end view of FIG. 11C.

FIG. 12A is a front end view of yet another embodiment of FIG. 1. FIG. 12B is a sectional view of FIG. 12A taken along lines 12B. Referring to FIG. 12B, the inhaler nozzle 10 comprises a collar 80 which collar 80 is adapted to frictionally receive a tube 70 having a length A. The length A is positioned at a right angle to the length L inhaler nozzle 10.

Suitable moldable materials used to construct the inhaler nozzle 10 include moldable plastics.

The oral airway model used in this study duplicates a physiologically realistic human airway morphology without any modifications. It was constructed from scanning pictures, which had been taken from a healthy human volunteer by using MRI (Magnetic Resonance Imaging) and provided by the Lovelace Respiratory Research Institute. It was then reconstructed into a three-dimensional configuration in our Laboratory both virtually (numerically) and physically. The oral airway model consisted of the mouth cavity, the pharyngeal cavity and the pharynx as shown in Fig. 13.

The airway model was constructed from 61 clay segments with a thickness of 3 mm each. The original database was in digital format containing tens of thousands of points which represent the whole oral airway geometry; these points have been divided into three parts, and each part has been sliced into different cross sections In the first part, all the points in each cross section have the same Y-axis value with a thickness of 3 mm each. In the second part, all the points in each cross section have the same angle (0) forming a 90-degree bends. In the third part, all the points in each cross section have the same Z-axis value with a thickness of 3

mm each, as it shown here in Figure 14.

All cross sections from the aforementioned three parts have been mapped onto the clay segments. The exact shapes of airway cross sections are carved out of the clay segments to leave a hollow impression of the oral airway cross section as shown in Fig. 15. The clay segments were then heated to ensure the hardness and the stability of their geometrical shape. Finally, all segments were glued together to form a duplicated hollow oral airway geometry..

The silicone rubber compound which was purchased in its liquid state, was prepared by mixing the rubber base with the silicone. The amount of the silicone was controlled at 10% of the weight of the base (rubber). The mix was stirred with a stiff, flat ended metal spatula and then placed into a vacuum chamber. The compound was evacuated to entrap the air from the mixture by achieving 30 inches of mercury vacuum through a vacuum pump. The mixture was kept in the chamber under vacuum for 15 minutes. The volume of the mixture grew fast while being placed the vacuum; therefore the mixing bowl should not be filled more than its one-third volume capacity. Then, the mixture was poured into the clay hollow slowly and steadily; thus minimize entrapped air bubbles during the pouring process. The clay cast and the poured mixture were placed on the shaker for 5-10 minutes to release any air bubbles trapped inside the clay cast. The silicone rubber compound must be allowed to cure for 16-24 hours before removing the rubber mold from the clay cast; a petroleum jelly is applied on the cast internal surface to make it easy to remove the rubber mold from the clay cast. The solid rubber mold must be allowed to stay in the air for 24 hours before using it to achieve a full cure.

The solid rubber mold was used to construct the oral air way cast by suspending the mold within an open glass box. The previous procedure for preparing the silicone rubber compound was used here. The silicon rubber mixture was poured in the glass box to construct the hollow human oral air way cast and used in our experimental study as shown in Fig. 16.

Preparation of Particle-R134a Suspension

One of the challenges in the experimental work was the preparation of a homogeneous

particle suspension in the pMDI propellant (134-a). Success in this step was very important to ensure that the uniform and identical amount of the fluorescent particles will be delivered with every puff of the pMDI. The goal was to uniformly suspend the solid fluorescent particles in the liquid propellant and place the suspension inside the inhalers. The commercial inhaler, PROVENTIL MDI, is used in the experiments to mimic the actual inhaler spray and to ensure full simulation of the commercial aerosol plum characterization.

Dry green fluorescent polymer microspheres (reference), which are made of polystyrene divinylbenzene (DVB), have a density of 1.05 g/cm^2, and they were used to prepare this suspension. 30 mg of fluorescent particles were mixed with 0.5 ml ethanol (95%) and placed in the sonicator for about 5 minutes to ensure fully dispersion of the agglomerated fluorescent particles in the ethanol. The volume of the prepared suspension is equal to 5% of the total volume of the commercial dummy inhaler See Fig 17. The prepared suspension was injected in the dummy commercial inhaler, and the whole system was then charged by 134-a by using the canister charging system. A mechanical shaker was used to mix the suspension with the 134-a.

To ensure that the ethanol had no effect on the stability of the fluorescent dye which covered the outer surface of the micro spheres, 5 mg of fluorescent particles were mixed with 2 ml ethanol, and this sample was left for 24 hours, next, the ethanol was separated from the suspended particles by using centrifugal separator. A sample of the ethanol was measured by using the spectrophotometer to detect any dissolved fluorescent dye in the ethanol sample; and no reading was detected, which is an indication that the use the ethanol has no influence on the stability of the fluorescent dye, which indicated that the spectrophotometer readings were caused by the existence of the fluorescent particles in the sample under the measurement.

The fluorescent particle stayed fully dispersed in the propellant after using the mechanical shaker for 2-3 minutes, apparently this should be sufficient for one set of puffs, to ensure a full dispersion of the fluorescent particles during the spraying time, stainless steel spheres of the

diameter of 2 mm were inserted inside the commercial canister, to be used before the spraying of any puffs, and prevent any particles agglomeration inside the dummy canister.

The dummy inhaler as it shown in Fig. 17 consists of three parts, the first, is the commercial canister, the second, is a clear tube, the third part, is a ball valve. These three parts connected to each other through pipe fittings. The commercial canister will be used as storage for more than 200 puffs and it is also consists of the metered dose valve, which is connected to the plastic actuator through the stem. The main reason for the clear plastic tube is to provide us with visual sight about the quality of the suspension inside the commercial canister. The ball valve was used as a shutoff valve to terminate or allow the propellant flow during the charging process. The dummy commercial inhaler was a good simulator to the actual commercial inhaler in the market.

The canister charging system is a mechanical device which is used to charge or pressurize the dummy inhaler with the HFA propellant (134-a). This system consists of several parts as it shown in Fig. 18. this system contained three valves, valve I, valve II and valve DI, valve I is used to control, terminate and release the pressurized propellant from the propellant can to the dummy inhaler, valve II was connected to a vacuum pump, which was used to evacuate the dummy inhaler from the air before starting to inject the fluorescent suspension inside the dummy inhaler, valve III is used to release the prepared suspension under the vacuum pressure through this valve to the dummy canister. A pressure gauge was installed next to the propellant can as an indicator to the level of the propellant inside the can. A pressurized 134-a propellant can is used to as storage to be used to charge the dummy canister when needed, this can has a shut off valve to control and terminate the propellant flow.

The charging of the dummy canister process contained different steps, first, was to open all the shut off valves from the pressure gauge till the dummy canister (there were four valves to control the propellant flow), the second, was to apply a vacuum pressure through valve III to evacuate the air from the dummy canister, the third, was to allow the vacuum pressure to release the prepared suspension into the dummy inhaler through valve II, the

fourth, is to open the can's valve to fill the dummy canister with the HFA 134-a, the fifth, is to close all the shut off valves and separate the dummy canister from the charging system. The dummy canister was filled with the propellant, and was easily seen through the clear tube.

The experimental apparatus contained the oral airway model, the inhaler, inhaler positioning device, a vacuum pump, a flow meter, a flow rate regulator, valves, two expansion balloons and two breathing chambers as shown in Fig. 19. The reference breathing chamber was used to measure the reference/benchmark. This chamber was connected to a vacuum pump through the opening at the back. An expansion bag (the reference balloon) was placed inside the chamber and connected to the front opening from the inside. The front opening was exposed to the ambient pressure. When the vacuum pressure was applied to the chamber, the expansion bag expanded inside the reference breathing chamber and sucked the air and induced the air flow to the front opening. Four puffs was sprayed into the reference expansion bag during the expansion process of Fig. 19.

The cast breathing chamber was connected to the vacuum pump through a side opening and to the oral airway cast through the top opening from the outside opening. An expansion balloon was placed inside the breathing chamber and connected to the outlet of the oral airway cast. When the vacuum pressure was applied, the cast expansion bag expanded; the degree of vacuum determined the rate of balloon expansion, and in turn determined the rate of respiratory flow through the oral airway passage. Again, four puffs were sprayed into the oral airway geometry during the expansion of the cast balloon for aerosol deposition measurement.

A flow meter was connected to the vacuum tube to measure the respiratory air flow rate. The flow meter was calibrated before the starting of the experiments. An air flow regulator was used to control the air flow rate representing a wide range of flow rates encountered in the aerosol therapy.

An inhaler-positioning device was designed to hold and control the position of the dummy inhaler during the spray process. The device can position the dummy inhaler at different x-y-z positions as well as injection angles, which allowed one to study the effects of the

mouthpiece position on the inhaler efficiency. With this structure, it was convenient to investigate the entrance angle effect, and the effects of lateral and the axial movement of the mouthpiece with respect to the entrance of the oral airway cast.

Expansion bags (balloons) were used to collect the deposited fluorescent particles and to measure indirectly the particles deposited in the oral airway cast. The expansion bags have an aerodynamic similarity with the human respiratory system. It was a simple, accurate and effective method in collecting the deposited fluorescent particles.

The most common method used in in-vitro aerosol human airway deposition measurement reported in the literature is the filtering method. A filter or filters are placed downstream of the airway models and collect the penetrated aerosols particles such as (Cheng, Y. S., Yazzie, A. S., Gao J., 2003). The quantity/percentage of particles penetration would be measured by either comparing the weights of the filter before and after the aerosol deposition experiment, or by measuring the fluorescent intensity of particles captured by the filter. If the radioactivity-labeled particles were used, the intensity of the radioactivity were measured. There are several disadvantages of this approach including: 1) the micron size particle filter creates a large pressure drop and thus limited the maximum respiratory flow rate driven by the fixed pressure differences between the vacuum and the ambient, and 2) to reduce the pressure drop and increase the flow rate, a large filter surface was required. Many inhaler puffs were therefore needed to create a detectable difference in weight/fluorescence measurement. However, each puff or spray caused a slight temperature drop of the canister due to the evaporation of the R134-a. As numbers of spray increased, the characterization of the spray become inconsistent due to temperature changes, 3) it was difficult to rinse off all the particles captured in the mini-pore of the filter and therefore, introduced at additional measurement errors. To overcome this problem, some researchers employed the forced air or flow blowing system instead of the vacuum system so large pressure differences could be used to drive the air to pass the filter. However, it created the problems of different flow conditions at the mouth inlet. Furthermore, the inhaler working condition would be unrealistic.

The expansion balloon method used in our experiments has many advantages: It is cost-effective in terms of time and money; it is easy to design, fabricate and control; it creates the least amount of pressure drop and therefore experiments can be conducted in a wide range of flow rate; it needs only minimum number of inhaler puffs; and it provides a more accurate measurement because 100% of the fluorescent particles penetrated through airway cast will be captured inside balloon and can be easily ring-off for fluorescent intensity measurement.

Balloons of approximately 16-inch diameter were used in the experiments. One balloon was attached to outlet of the airway model and placed inside the cast breathing chamber. Another balloon was attached to the inlet of the reference breathing chamber. Respiratory flow rates (including both steady and transient airflows) were controlled by the rate of the balloon expansion, which is in turn controlled by the vacuum pump. All fluorescent particles were deposited inside the reference balloon or penetrated through the airway model to the cast balloon were captured inside the surface of these balloons. After the pre-determined number of inhaler puffs, the vacuum pump was stopped and balloon released air (or shrunk) at the controlled rate until it reached its natural un-inflated shape. Then, fixed amounts of DI water was poured into and ring-off the aerosols deposited on the balloons surfaces. Four puffs were sprayed into the reference balloon and washed down by 3 ml of DI water. This sample solution was measured by using the spectrophotometer (Hitachi Model F-2000), which gave the reference reading (Np). Another four puffs were sprayed inside the human oral airway cast under the identical flow conditions, and the penetrated particles to the cast balloon were ring-off by 3 ml of DI water. This sample was also measured by using the same spectrophotometer, which gave us the cast balloon reading (Np). The penetration efficiency was calculated using the following formula:

$$\text{Penetration efficiency} = \left(\frac{N_P}{N_t}\right) \times 100\%;$$

Similarly, the particle deposition efficiency of the oral airway cast is defined as:

$$\text{Deposition efficiency} = \left(\frac{N_t - N_P}{N_t}\right) \times 100\%;$$

A calibration curve was obtained for measuring particle mass concentration vs. spectrophotometer readings, which is shown in Fig. 20. Figure 8 shows that there existed a linear relationship between the spectrophotometer reading and the particle volume fraction. The calibration curve was used to quantify the various deposition measurements, such as the human oral airway deposition fraction, fraction of the particles penetrating the cast, and spacer deposition fraction. Fixed volumes of DI water were used to wash out the particles deposited either in the collecting balloon, or in the oral cast, or in the reference balloon for various measurements.

Several tests on the experimental setup were carried out to verify the accuracy of the measurement. In each-test, the sum of the spectrophotometer readings for the particles deposited in the oral airway cast and those collected in the collecting cast balloon were compared with that for the particles collected in the reference balloon. The relative errors in the particle mass fraction measurements were found to be $\pm$ 5%.

Furthermore, the effect of the balloon shrinking (air releasing) time was carried out; spectrophotometer reading showed that when the balloon shrinking time was controlled to be more than 10 minutes, the amount of fluorescent particle escaped from the balloon during the air releasing was negligible. The balloon air releasing times were controlled to be more than 10 minutes in the experiments. Consistency is a significant factor in evaluating any measurement method; therefore, consistency test was carried out to verify the accuracy of this new measurement method. Four puffs were sprayed into each five balloons, and the fluorescent particles were washed down by DI water and measured by spectrophotometer. The variations of fluorescent intensity in all 5 balloons were less than $\pm$4.2%. Therefore, it was concluded that the released fluorescent particles with each puff are consistent. This test was repeated and periodically done through the whole experimental time. When the readings variation increased to more than $\pm$5% during the experimental period;

changing of the dummy canister was effective to bring back the readings variation less than 5%.

The spectrophotometer readings were directly correlated to the fluorescent particles existence. To assure there was no existence of fluorescent before hand, 3 ml of DI water was used to ring inside the balloon before it was used in the experiment. The spectrophotometer reading, which called 'back ground readings' was negligible. It was also found that the balloons materials used had no effect on the spectrophotometer readings.

Although, the DI water was the only washing media used to ring off the particles inside the experimental balloons, it was observed that ethanol gave the same spectrophotometer reading if it was used *as* a washing media. In this study, 16" white balloons have been used all the time. One of the observations was found by this experimental study, is the colored balloons (any color but white) can't be used in such study; the main reason for this observation was the commercial colored balloons doesn't have a negligible background reading since fluorescence was added. A large error will be introduced to the experimental by using these balloons.

The prepared fluorescent-R134a suspension was not sensible to the time. Same balloon spray and measurement procedures were repeated two weeks apart under the other identical conditions, the difference in spectrophotometer readings is less than + 5.6%.

Before each test had begun, the human oral airway cast must be cleaned by using the Ethanol to remove excess dust and dried fluorescent particles. The oral airway cast was first coated by Ethanol and scrubbed by using brush. This washing and scrubbing procedure was repeated several times, and the cast was left to dry out, then the inner surface of the human oral airway cast was coated by petroleum jelly to prevent the fluorescent particles from bouncing off the surface and reentering the respiratory flow during the experiments.

The two halves of the oral cast were then properly aligned and fastened together by using silicon rubber compound. The cast was then left for 24 hours to allow full cure of the silicon rubber compound. The cast balloon was then attached at the lower end of the oral cast. This balloon was washed down first and dried to remove any excess powder inside the balloon.

The oral cast and the attached balloon was placed at the top of the cast breathing chamber inlet and sealed by using silicon rubber compound. This balloon will be called "cast balloon". The oral cast will be outside the chamber and the cast balloon will be inside the chamber.

Another balloon was placed at the inlet of the reference chamber. This balloon will be called "reference balloon". The air flow rate was adjusted through the air flow controller (valve). The reference and the cast balloons were allowed to expand and the shrinking time was recorded (must be 10 minutes to proceed with the experiments). The dummy inhaler was placed on a mechanical shaker to disperse any agglomerated fluorescent particles; the time between shaking the dummy inhaler and spray inside the cast or the reference balloon is less than 30 seconds. The dummy inhaler was placed on the inhaler holder before spraying inside the cast balloon. Four puffs were sprayed inside the reference and the cast balloon respectively after the balloon expansion was steady. Next, the balloons were allowed to fully shrink. The two balloons were removed from the breathing chambers. 3ml of DI water was used to wash down particles off these balloons. These balloons were constantly shook and rubbed during the washing. The sample DI water solutions with the suspended fluorescent particles were measured by the spectrophotometer. The spectrophotometer reading was used directly to calculate the penetration efficiency.

For experiments with different inhaler positions, each balloon were labeled, and the particles-DI water solution be collected by using a clean syringe. The concentration of the fluorescent particles in the collected samples was then measured by the fluorescence spectrophotometer. The fluorescent spectrophotometer operated according to the guidelines of the currently loaded program. A specific program had to be developed and tested for the fluorescent particles under study. Concentration readings are recorded for each sample and this completes the procedure for each experiments.

Experiments of inhaler delivery efficiencies with effects of respiratory flow rate mouthpiece diameters and particle entrance effects were conducted. Fluorescent particles in the size of 7μm, which had the dominant mass fraction in this size range for a typical MDI

spray (Purewal, Tol. S., Grant, David J. (1998). Metered Dose Inhaler Technology), were used in all experiments. Different respiratory flow rates L/min ranging from 30 to 90 L/min were studied. The flow rate of 30 L/min represents a lower end and 90 L/min represented a higher end of the respiratory flow rate among the typical asthma patients, respectively. Mouthpiece diameters, 16mm and 20 mm inside diameter, were used in experiments which were also used by Lin et al, 2001. To investigate the effect of the inhaler's entrance angle on the aerosol penetration efficiency, five different entrance angles, the angle between the horizontal position of the mouth opening and mouthpiece outlet, were used in the experiments. These entrance angles were 0°, 10°, 20°, 30° and 40°, respectively.

Six sets of experiments were completed to investigate the effects of respiratory flow rate effects. Line graph charts of Fig. 21 and Fig. 22 show the particle penetration efficiencies for the flow rates of 30 L/min, 60 L/min and 90 L/min, with mouthpiece diameters equal to 20 mm and 16 mm, respectively. It is noted that flow rate of 30 L/min represents the typical breathing intensity for a human adult at the light activity and 60 L/min represents that at the heavy activity,

As it shown in Figs. 21 and 22, the particle penetration efficiencies decreased with the increase in flow rates. The particle-R134a suspension sprayed out of the inhaler nozzle have a much higher initial velocity than that of the respiratory flow and gradually slow down by the surrounding air flow due to flow shear stress or drag force. The lower of the air flow rates, the larger the difference between the air velocity and particles initial velocity, and therefore, and the greater drag force will be. As a result, the velocity of the aerosol particles will be reduced. It is known that the inertia impaction is the dominant mechanism of particle deposition in oral airways. It is known that the particles need to pass 90 degree bend in the oral airway to reach the targeted area, fluorescent particles with high inertia impaction will not be able to follow the air streams through the 90 degree bend and will end up getting deposited at the back of the throat. The inertial parameter is function of particle density, particle diameter and air flow rate. The parameter of inertia impaction is defined as:

Inertial Parameter = pd^2Q

As shown in the above equation, particle velocity is the major variable in the inertia impaction parameter. By reducing the particle velocity and consequent the inertia impaction parameter, the depositions of particles on the back of throat due to inertia impaction decrease and more particles will turn around the 90-degree bend and pass through the oral airway to the targeted lung region. This explains why higher penetration efficiency is associated with the lower flow rates.

Experimental results displayed in Figs 21 and 22 showed that the correlations of the particle penetration efficiencies with the airflow rates are highly nonlinear. For both cases of 20-mm mouthpiece diameters in Fig. 21 and 16-mm diameter in Fig 22, penetration efficiencies are almost tripled (from 6.1% to 15.8%) when flow rates decreased from 90 L/min to 60 L/min in the case of 16 mm diameter, The further enhancements in penetration efficiency become smaller; it is less than doubled (from 15.8% to 25.8%) when flow rates decrease from 60 L/min to 30 L/min in the case of 16 mm diameter. Fig. 23 shows the relative increasing in the penetration efficiency at different respiratory flow rates in both diameter 16 mm and 20 mm. flow rate 90 L/m will be the reference in calculating the relative increase in the penetration efficiency. Relative increase is defined as:

$$\text{Relative increase at 60 L/m} = \frac{\eta_{60} - \eta_{90}}{\eta_{90}} * 100$$

$$\text{Relative increase at 30 L/m} = \frac{\eta_{30} - \eta_{90}}{\eta_{90}} * 100$$

Effects of mouthpiece diameter on particle penetration efficiency, with respiratory flow rates of 90 L/min, 60 L/min, and 30 L/min, are shown in Fig. 24, Fig. 25 and Fig. 26, respectively. The experimental measurements clearly demonstrate the effects of mouthpiece diameter on penetration efficiency, which confirms the study of Lin et al, 2001, Fig. 27 shows their results. Both results agreed qualitatively (both have the same trend) and

quantitatively in the case of 90 L/min. Although their results have the same trend but totally different in the way of generating the aerosol particle, in the results pMDI was used as an aerosol generator but in their study they used multi diameter aerosol generator (liquid particle suspended in the air) which was closer to the Nubulizer than pMDI. In their experimental study the aerosol particle has velocity equal or less than the air velocity which is can't simulate the pMDI because of lake of similarity and different characterization. Results showed that the 20-mm mouthpiece consistently has higher penetration efficiencies than those of 16-mm mouthpiece diameter at all flow rates we studied. The relative enhancement of particle penetration efficiencies are 16.14%, 9%, and 10.6% at the respiratory flow rate of 90 L/rain, 60 L/min and 30 L/min, respectively see Fig. 28.

The effects of mouthpiece diameter on particle penetration efficiency may be explained as follows: Based on the principle of mass conservation for an inhaler puff (it is assumed that each puff generates the same amount of flow and mean density of the fluid is unchanged), it can be shown that the mass flow rate along channels of different diameters must be a constant, or, r^2u = C, where r and u are channel radius and mean velocity, respectively. Therefore, particle velocity is inversely proportional to the square of the channel size. The 20-mm mouthpiece diameter will result in a lower aerosol droplets velocity than that of the 16 mm-mouthpiece diameter. Lower velocity associates with lower inertia impaction parameter, thus, less fluorescent particles will deposited in the oral airway.

Effects of particle entrance angles relative to horizontal position on particle penetration efficiencies were demonstrated in Figs. 29-33). Respiratory low rates of 90, 60, and 30 L/min and mouthpiece diameters of 16 mm and 20 mm were used in the experiments. Particle entrance angles vary from 0 to 40 degree with 10 degree increment. Results of particle penetration measurement using the 16-mm diameter mouthpiece are shown in Figures 29, 31, and 33 with the flow rate of 90 L/min, 60 L/min and 30 L/min, respectively. The results of 20-mm mouthpiece are shown in Figures 30, 32 and 34 with the flow rates of 90 L/min, 60 L/m and 30 L/min, respectively.

It is noted that all the experimental results display similar trends: particle penetration efficiencies increase monotonically from 0 degree entrance angle to 20 degree angle, reach the maximum value at about 20 degree angle, and then decrease monotonically when the entrance angle increase further. **Figure 23** (**#65**-See part 3, Figure 23)demonstrate the relative efficiency enhancement when the entrance angle increased from 0 degree to 20 degree. Figure **23** also shown that the entrance angle effect is very apparent at higher flow rates (90 L/min) compare with lower flow rates (30 L/min) The relative efficiency increasment from 0 degree angle to 20 degree angle is 193.8%, 40.8% and 15.5% at 90 L/min, 60 L/min and 30L/min respectively at mouthpiece diameter of 16mm. On the other hand, at mouthpiece diameter of 20 mm, the relative efficiency increasment is 152.1%, 45.5% and 9.8% at 90 L/min, 60 L/min and 30L/min respectively.

The effects of inhaler mouthpiece angle were caused by the position of the tongue. The airway morphology used in this study is obtained under the natural breathing condition. The top surface contour of the tongue and the roof of the mouth cavity form a curved and concave downward shallow passage as shown in Figs. 34-36. Assuming the human head model is positioned vertically, particle ejected at the zero degree mouthpiece entrance angle (or when the mouthpiece outlet is placed horizontally), will be partially blocked and a fraction of the aerosols will deposited on the surface of the tongue. Increase the entrance angle will facilitate aerosol streams bypass the tongue surface and therefore increase penetration efficiency through the mouth cavity. However, excessive entrance angle increase (i.e., greater than about 20 degree in our experiments), will aim the aerosol streams directly to the roof of the mouth cavity and increase the deposition there.

In most of the previous experiments, either simplified airway geometries are used or researchers are purposely positioned the inhaler at the zero degree angle. It is also noted that 1) the tongue shapes and positions are subject to great inter-subject variability as demonstrated in Fig. 37 it is also flow rate dependent. During the deep breathing, the tongue tents to pull back and positioned near the throat as shown in Fig. 38. The higher the respiratory flow rate,

the more the tongue will move back. Therefore, more studies are needed to study the effects of mouthpiece entrance angle with consideration of inter-subject variability and flow rate dependence drug inhalation.

The depositions of fluorescent particles (7μm) within a silicon rubber model of the human oral airways with different respiratory flow rates, mouthpiece diameters and mouthpiece entrance angles were investigated. Particle penetration efficiencies, which is a directly indication of the inhaler performance are measured.

A new expansion balloon-based particle human airway deposition experimental system has been successfully developed. Compared with the traditional aerosol filter system, it is simple, quick, accurate, and cost-effective.

Respiratory air flow rates have great influences on the pMDI aerosol delivery efficiency. The lower flow rate has a higher aerosol penetration efficiency compared with the higher flow rate. The penetration efficiency was highest for the case of the lowest flow rate (i.e. 30 L/min) used in the experiments, while the greatest particle penetration enhancement by reducing the flow velocity occurs at the higher flow rate (i.e., 90 L/min). This conclusion is independent of the mouthpiece diameter.

Increasing the mouthpiece diameter has a moderate and positive influence on the particle penetration efficiency of the pMDI. The particle penetration efficiency associated with the larger mouthpiece diameter (i.e., 20 mm) was higher than that associated with the smaller mouthpiece diameter (i.e., 16 mm). This conclusion is independent of the air flow rate.

Placing the inhaler with an upward angle can significantly decrease the particle deposition in the airways cast. However, this conclusion was based on a particular oral airway geometry at a natural breathing condition.

The results of this research have the following implications to the design and implement of aerosol medicine therapy procedures:

1. The patient should use the deep and slow breathing.

2. The reduction of the particle velocity is an effective method to increase particle

penetration efficiencies.

3. A larger diameter mouthpiece design is preferred as long as it can be comfortably fit into the patient's mouth.
4. A high efficiency mouthpiece design should incorporate an outlet with slightly upward angle.

Previous research demonstrated that mouthpiece diameters, cross-sectional configurations and injection angles do have great impacts on aerosol penetration efficiency in oral airways. However, it is noted that these manipulations are passive means to modify aerosol transport patterns after the development of the strong R134a spray. There are more effective means to improve the inhaler efficiency by attacking the source of the problem: the high-speed aerosol spray. However, it is noted that the high velocity of the jet at the canister nozzle is essential for the process of the aerosol atomization: higher velocity jet, which is created by higher canister pressure and smaller nozzle diameter, will produce finer aerosol sizes and finer aerosol sizes correlate to high penetration efficiency. Therefore, the reduction of the spray velocity should be achieved only after the jet existing from the canister nozzle.

Fig. 1 shows an innovated simple needle-based jet spreading device located in side the mouthpiece. A needle of approximately 0.5 mm diameter is placed horizontally across the mouthpiece diameter with a distance approximately of 1 mm in front of the canister nozzle. High velocity R134a-particle jet rushing through the canister nozzle is divided into two streams when bypassing the needle. The needle serves two functions: it reduces the jet linear momentum by absorbing the direct impaction and it makes the spray more diffusive by slightly modifying the jet direction. Experimental measurement shows that the additional deposition of aerosols, on the surface of the needle and inner surface of the mouthpiece caused by the needle structure, is insignificant.

As shown in Fig. 39, Panels A and B are graphs of the aerosol penetration efficiency

using the original inhaler mouthpiece at flow rates of 30, 60 and 90 L/min with the diameters of 16 mm and 20 mm, respectively.

Fig 40 shows the improved aerosol penetration efficiencies with the attachment of the needle-based jet-spreading device. Aerosol penetration efficiencies have been enhanced in almost all range of flow rates (30 – 90 L/min) and mouthpiece diameters (D = 16 mm and D = 20 mm, respectively).

Table 2 compares the aerosol penetration efficiencies with and without the addition of needle jet-spreader structure. Except at flow rate of 30 L/min and D = 20 mm, aerosol penetration efficiencies have been enhanced at minimum of 75% for all other 5 cases. It is noted that, generally speaking, the percentage of the enhancement is directly proportional to the flow rate and inversely proportional to the mouthpiece diameter. The particle-R134a suspension sprayed out of the inhaler nozzle had a much higher initial velocity than that of the respiratory air flow and gradually slowed down by the surrounding air flow due to viscous shear stress or drag force. When the airflow velocity was lower, the difference between the air and particles initial velocity was greater. Thus, it resulted in a greater drag force, and as a result, the velocities of the aerosol particles reduced. Similarly, the larger mouthpiece diameter also corresponds to lower aerosol velocity. At a low flow rate (Q = 30 L/min) and a larger mouthpiece diameter (D = 20 mm), the velocity of aerosol spray is sufficient low that the effects of jet-spreader become ineffective. Our measurement shows that the aerosol penetration efficiency with the addition of the device is actually decreased.

Penetration Efficiencies	D = 16 mm Q = 30 L/m	D = 16 mm Q = 60 L/m	D = 16 mm Q = 90 L/m	D = 20 mm Q = 30 L/m	D = 20 mm Q = 60 L/m	D = 20 mm Q = 90 L/m
Original Mouthpiece	25.8	15.9	6.1	29.1	17.5	7.5

Mouthpiece with Jet Spreader	45.2	28.7	12.6	20.5	33.1	17.2
Percentage of Enhancement	75%	80%	107%	-30%	89%	129%

Table 2 Comparison of Aerosol Penetration Efficiencies

It has been shown that the Metered-Dose-Inhaler spray angle has a strong effect on the aerosol penetration efficiency through the oral airway cast. Placing the MDI inhaler with a slightly upward angle can significantly decrease the particle deposition in the oral airways cast. An optimum angle exists which can maximize the particle penetration efficiency through the oral airway. This conclusion is independent of respiratory rate and mouthpiece diameter.

It is generally known in the field of aerosol therapy that a great effort and time are needed to train the patients to compliance with the prescribed aerosol therapy procedures. Any additional new operational parameter, such as the angle of the inhaler spray during the aerosol administration, will add more complexity to the aerosol therapy application. To capitalize the importance of angle effects and not to complicate the patient compliance requirement, we designed a simple inhaler adaptor made of a straight channel with an upward angle-cut at the exit as shown in Fig. 41. The conception of the design is that an upward angle-cut at the outlet of the channel will naturally create an upward angle aerosol plume when it exit the adaptor and enter the oral airway.

Results of aerosol penetration efficiency with and without angle-cut mouthpiece adaptor are compared in Figure 5(**#75**-See part 4, Figure 5). It is noted that even with a straight channel (without the angle-cult at the exit) attach to the inhaler, it will act like a simple space; because it keeps the inhaler a distance away from the mouth and meanwhile allow the R134a spray more time to evaporate and slow down the momentum. Penetration efficiencies with flow rates between 30 L/min to 90 L/min are measured. **Figure 5** shows that similar to the results of using the adaptor of with a jet-spreading device as discussed, **Table 1**, the maximum

relative penetration efficiency enhancement for angle-cut adaptor is also at the highest flow rate. The relative enhancement increases from 7% at the flow rate of 30 L/min to 62% at the flow rate of 90 L/min.

The effects of flow rate on MDI efficiency using a mouthpiece adaptor with a 20 degree angle cut is shown in Figure 6(**#76**-See part 4, Figure 6). Again, similar to all the aforementioned studies, although the relative MDI efficiency enhancement is highest, the absolute value is always the lowest at the flow rate of 90 L/min.

In light of the foregoing, it will now be appreciated by those skilled in the art that various changes may be made to the embodiment herein chosen for purposes of disclosure without departing from the inventive concept defined by the appended claims.

We claim:

1. An inhaler adaptor which channels medication into the mouth cavity.

2. The inhaler adaptor of claim 1 which alters the flow rate of the medicine into the mouth cavity.

3. The inhaler adaptor of claim 1 wherein the adapter having an inner cavity of altered designs.

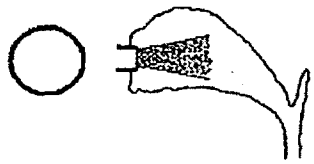

A Typical Existing
Mouthpiece Configuration

(A)

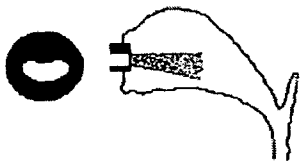

Inner Contour Matches
Aerosol Pass-through Zone

(B)

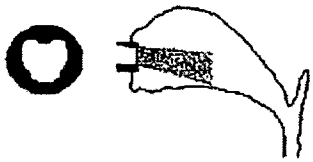

Sloped Roof Facilitating
Aerosol Downward Motion

(C)

Optimum Design With
Controlled Depth and Mouth Opening

(D)

FIGS 1A - D

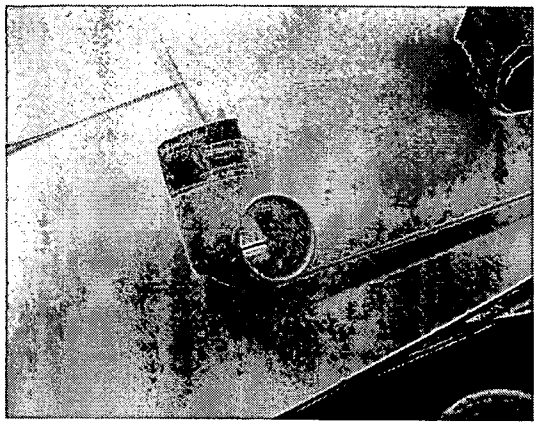

FIG 2

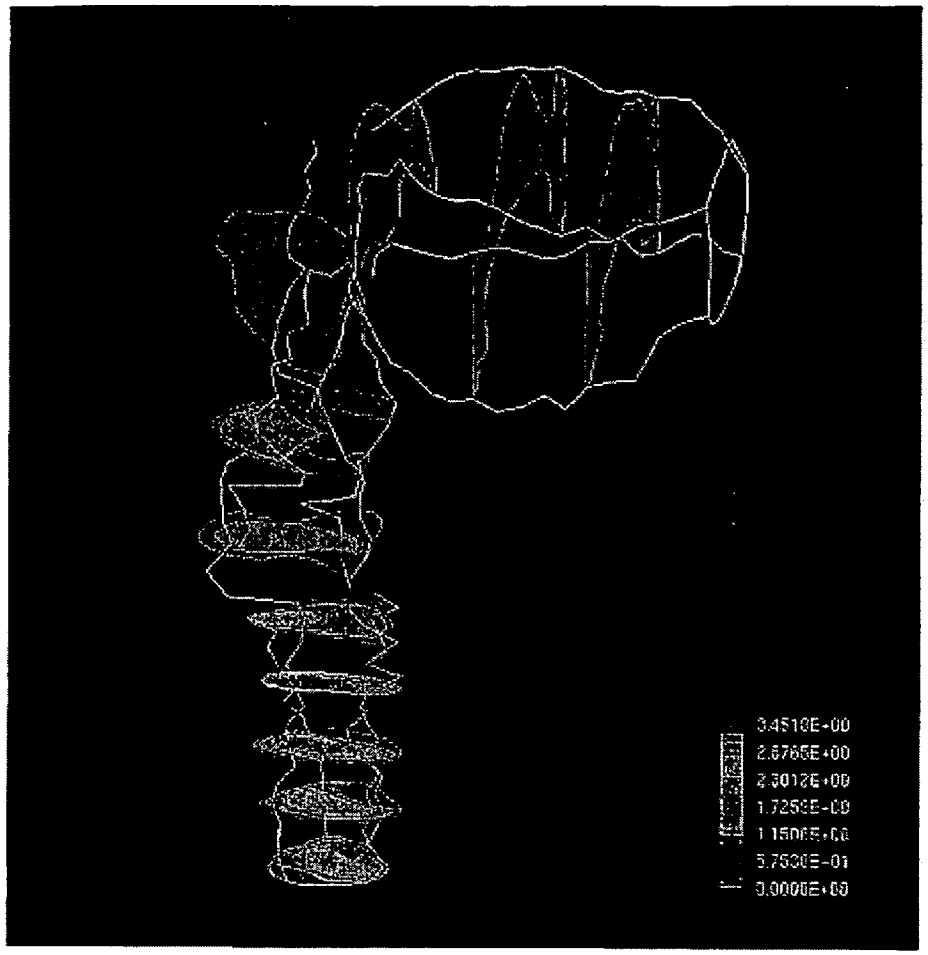
3.4510E+00
2.6765E+00
2.3012E+00
1.7259E+00
1.1506E+00
5.7530E-01
0.0000E+00

FIG 3

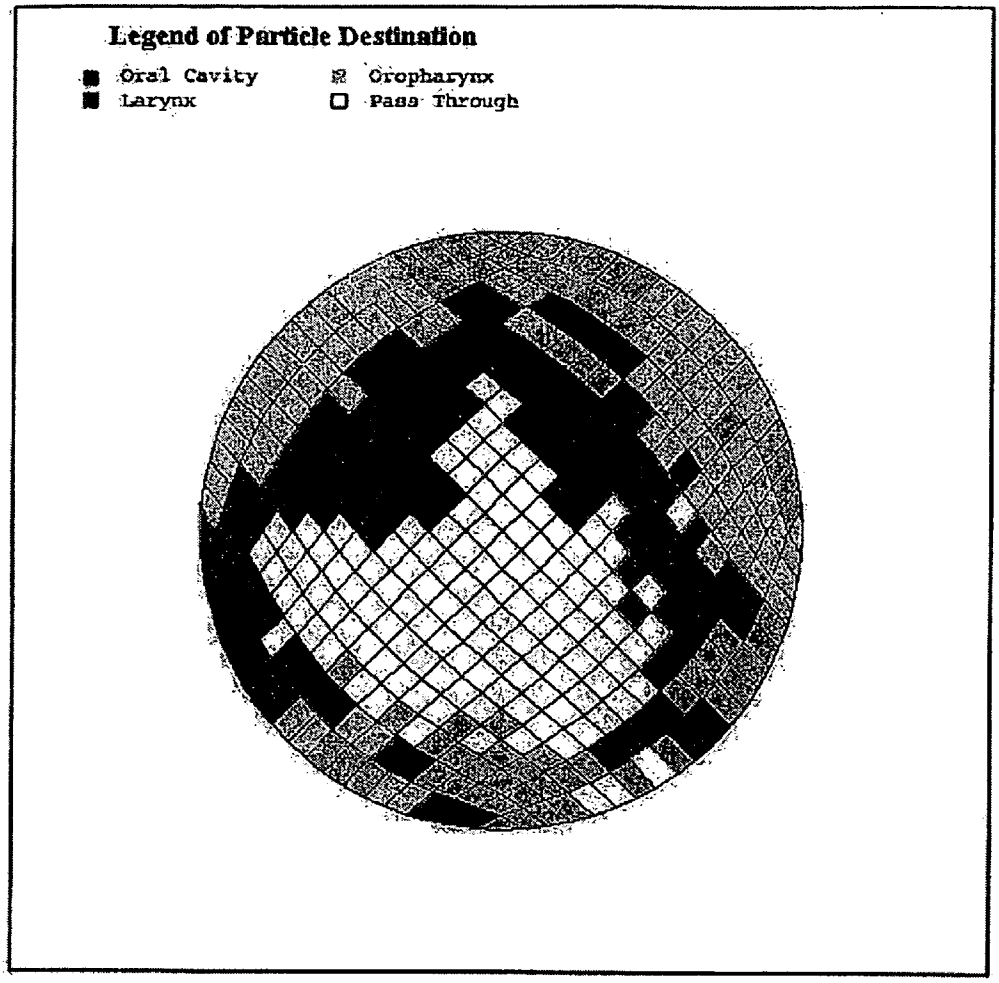
Legend of Particle Destination
Oral Cavity
Oropharynx
Larynx
Pass Through

FIG 4

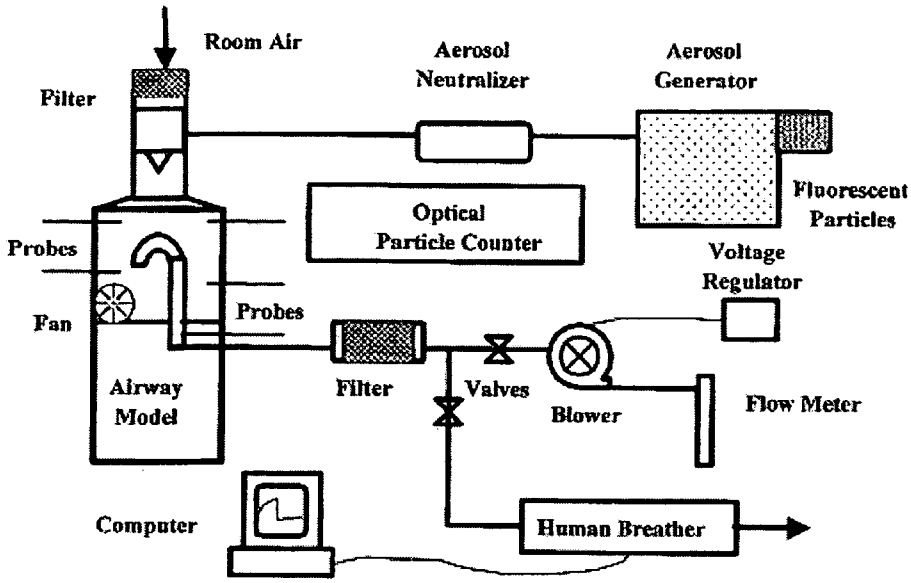

A. Breath-actuated System

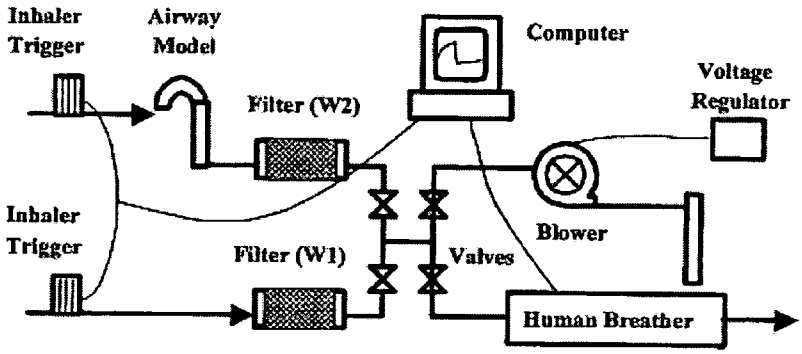

B. Propellant-Driven System

FIGS 5A and B

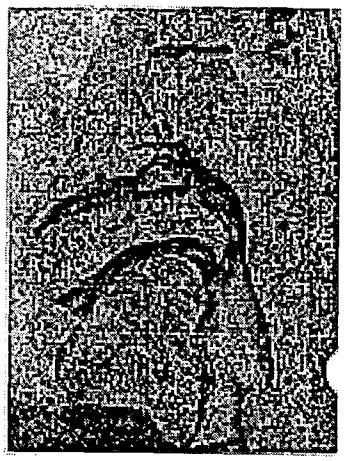

FIG 6

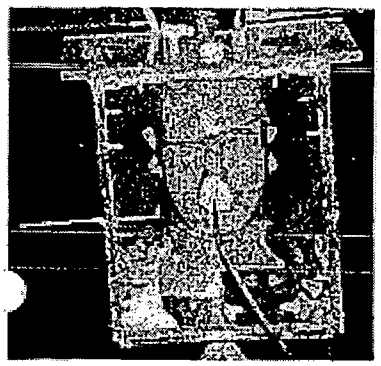

FIG 7

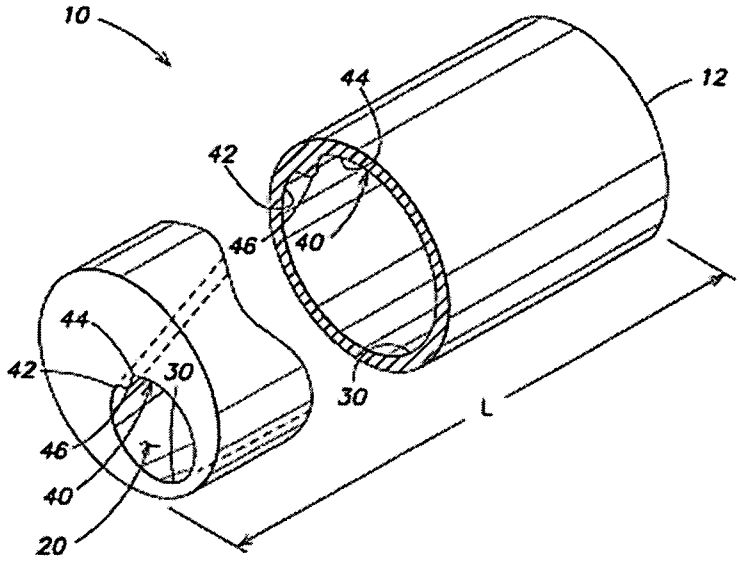

FIG. 8

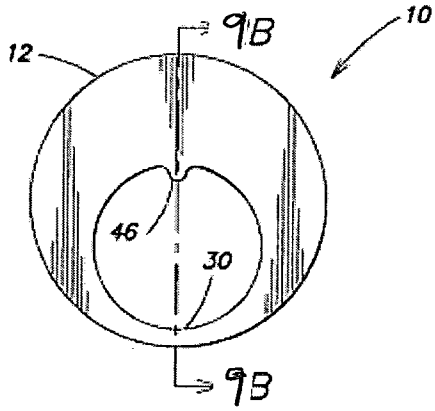

FIG. 9A

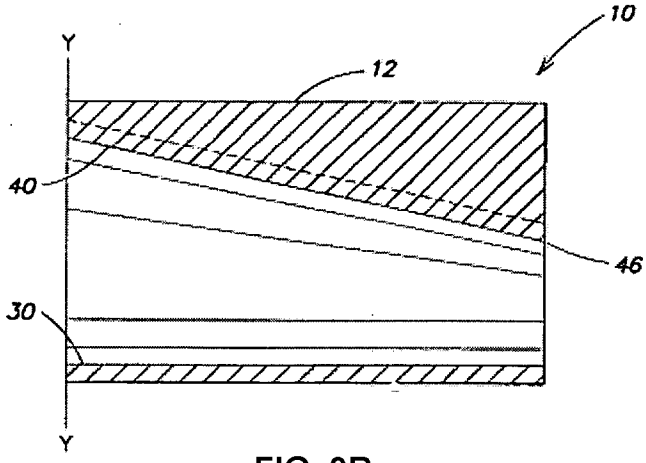

FIG. 9B

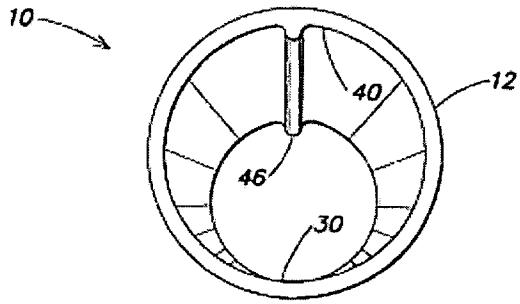

FIG. 9C

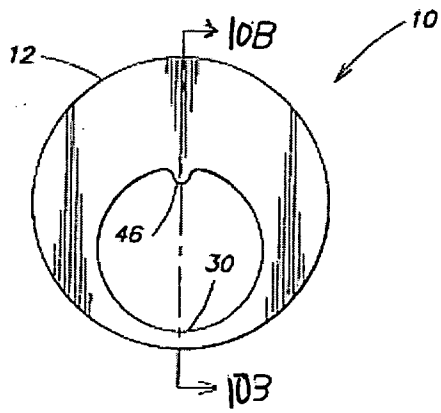

FIG. 10A

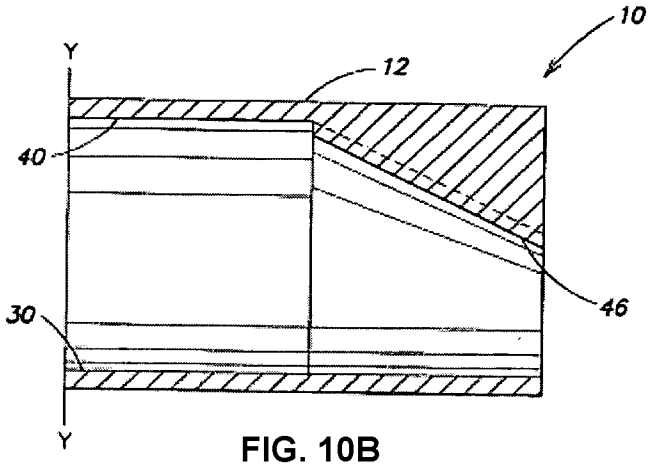

FIG. 10B

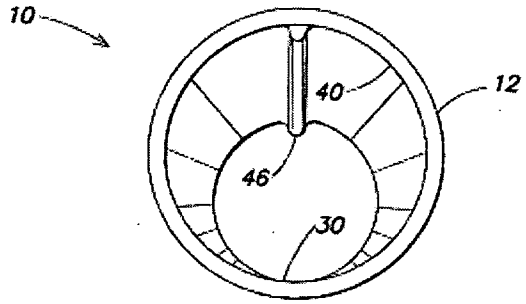

FIG. 10C

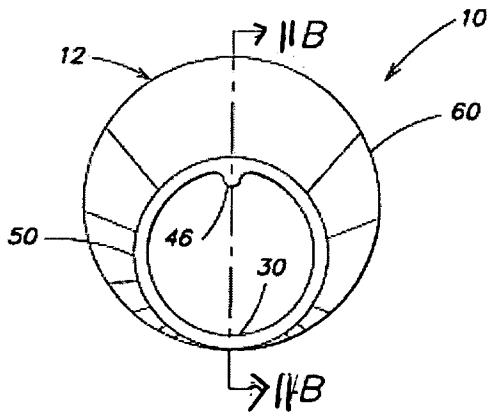

FIG. 11A

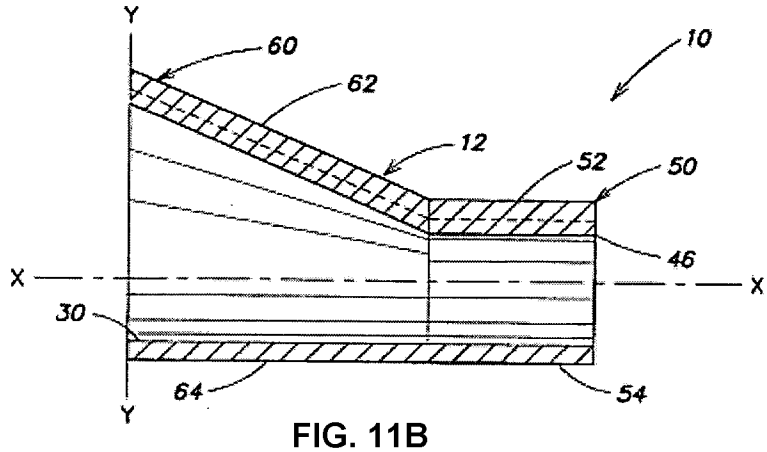

FIG. 11B

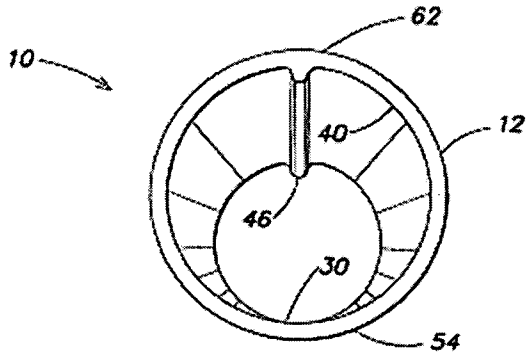

FIG. 11C

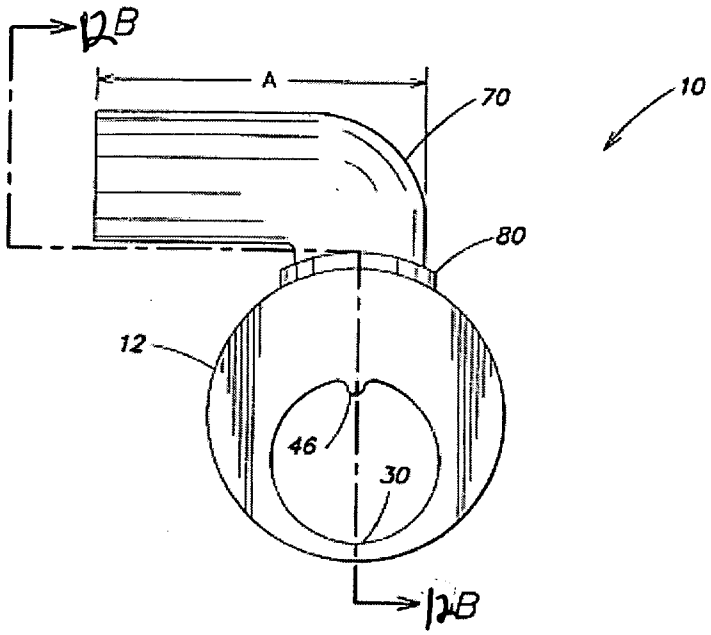

FIG. 12A

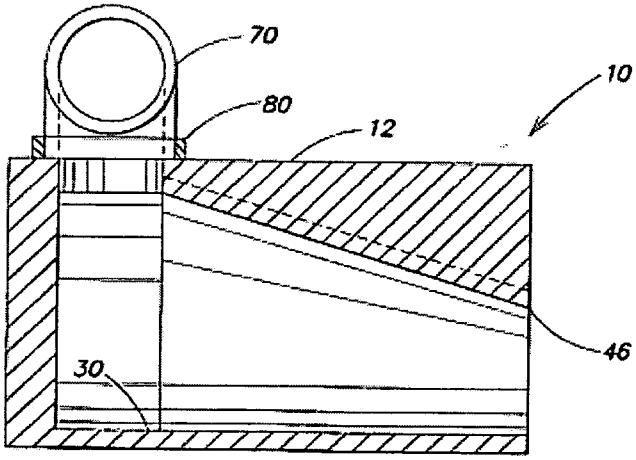

FIG. 12B

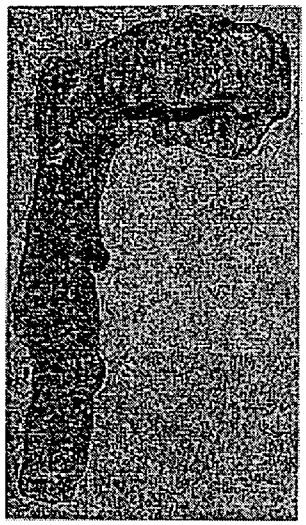

FIG. 13

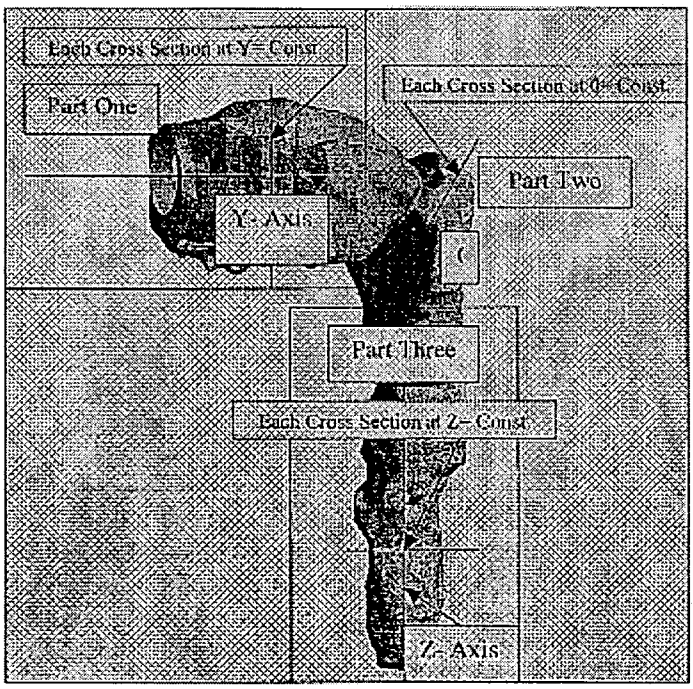
Each Cross Section at Y= Const.
Part One
Each Cross Section at θ= Const.
Part Two
Y- Axis
θ
Part Three
Each Cross Section at Z= Const.
Z- Axis

FIG. 14

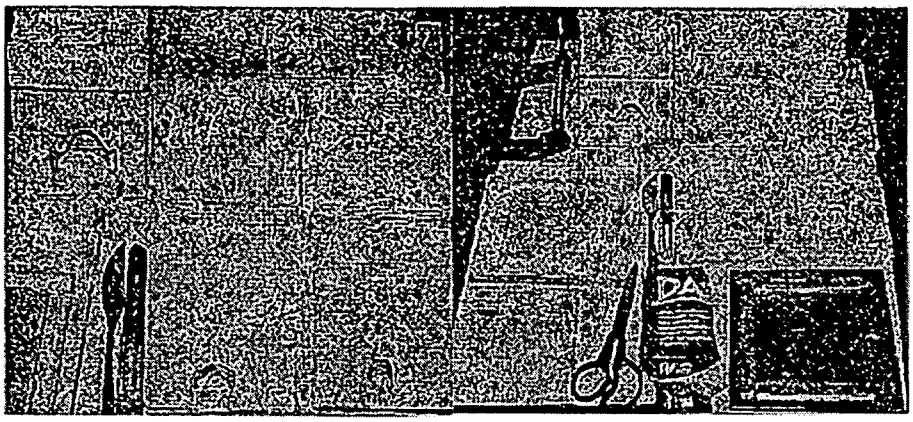

FIG. 15

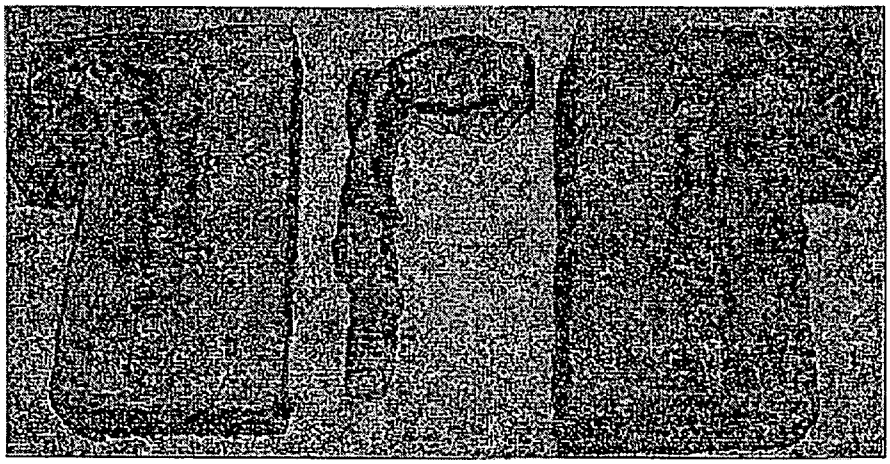

FIG. 16

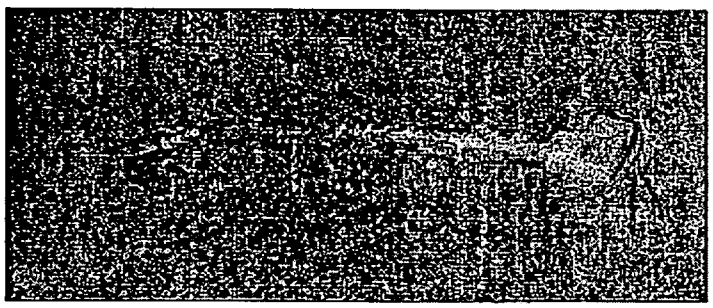

FIG. 17

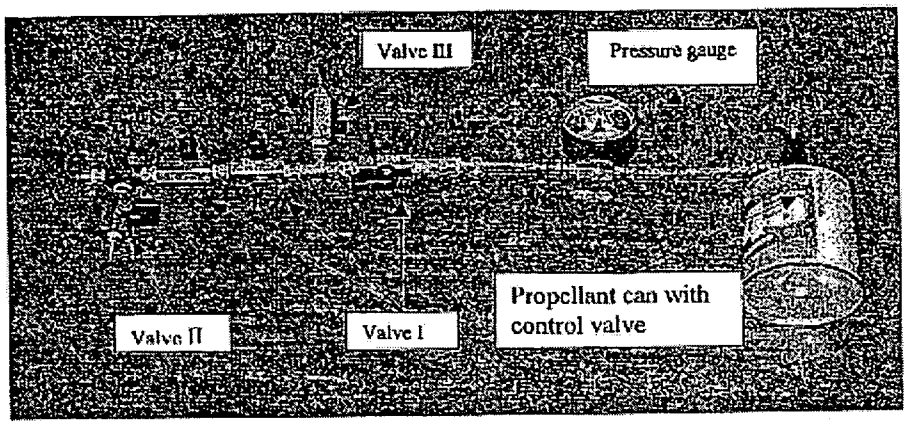
Valve III
Pressure gauge
Propellant can with control valve
Valve II
Valve I

FIG. 18

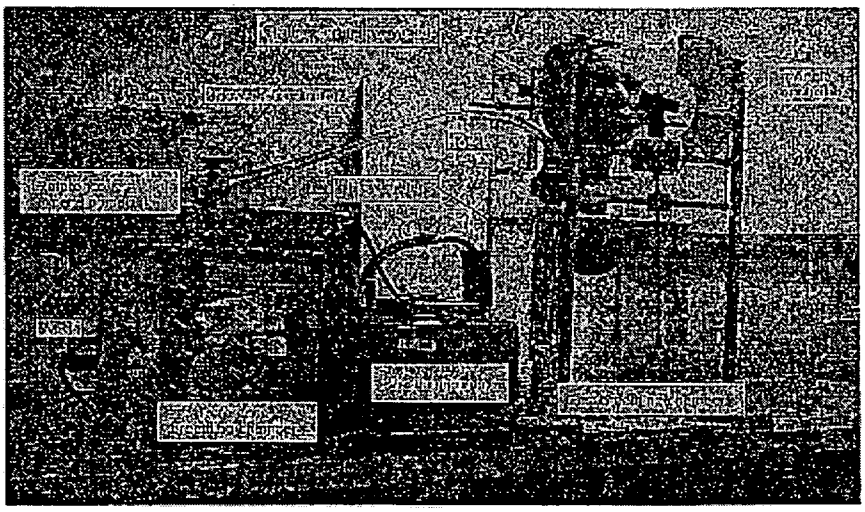

FIG. 19

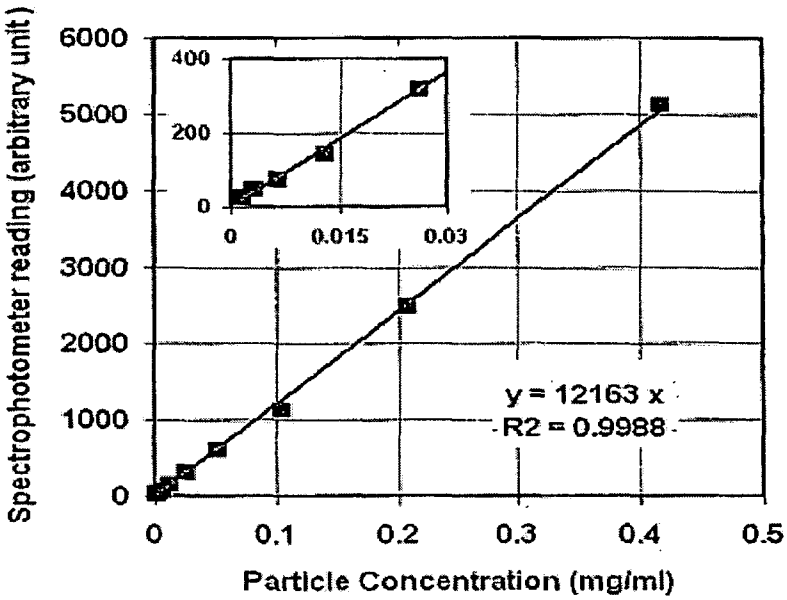
Spectrophotometer reading (arbitrary unit)
6000
5000
4000
3000
2000
1000
0
0
0.1
0.2
0.3
0.4
0.5
Particle Concentration (mg/ml)
y = 12163 x
R2 = 0.9988
400
200
0
0
0.015
0.03

FIG. 20

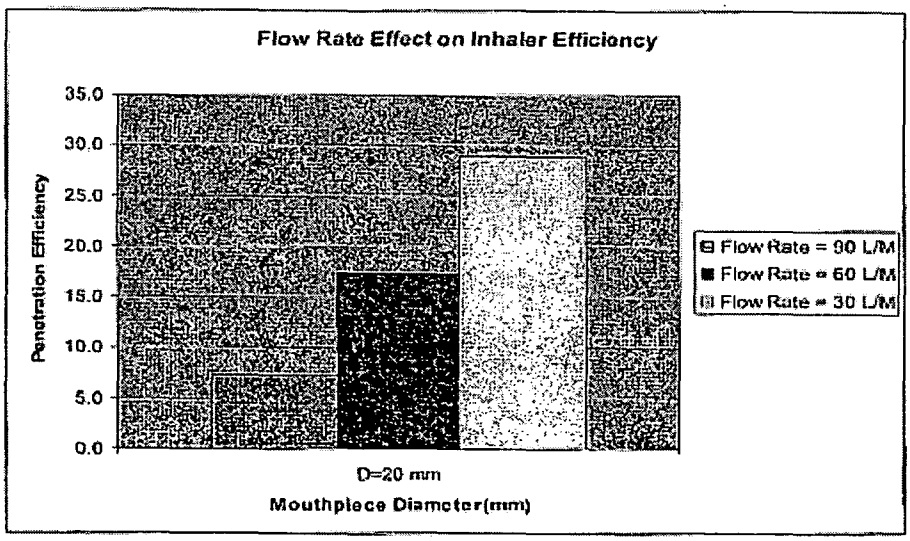
Flow Rate Effect on Inhaler Efficiency
Penetration Efficiency
35.0
30.0
25.0
20.0
15.0
10.0
5.0
0.0
D=20 mm
Mouthpiece Diameter(mm)
Flow Rate = 90 L/M
Flow Rate = 60 L/M
Flow Rate = 30 L/M

FIG. 21

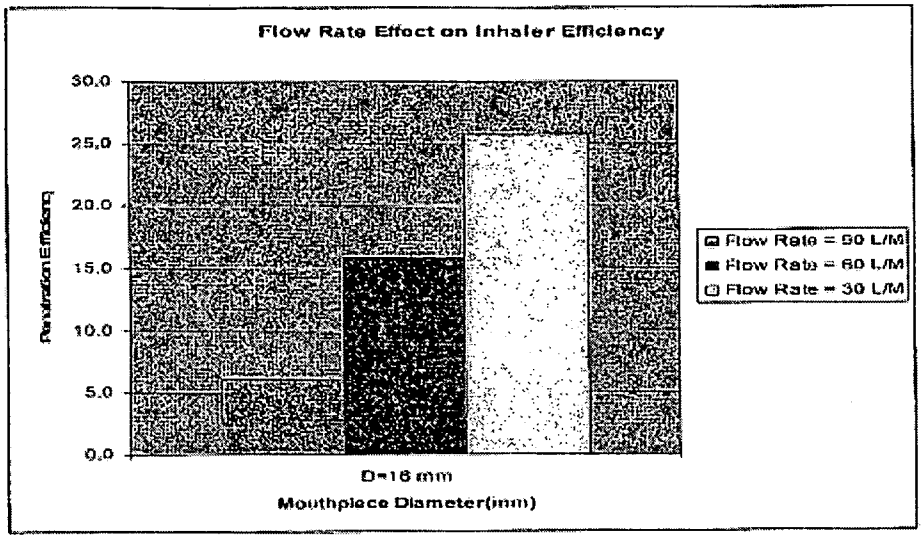
Flow Rate Effect on Inhaler Efficiency
30.0
25.0
20.0
15.0
10.0
5.0
0.0
Penetration Efficiency
Flow Rate = 90 L/M
Flow Rate = 60 L/M
Flow Rate = 30 L/M
D=18 mm
Mouthpiece Diameter(mm)

FIG. 22

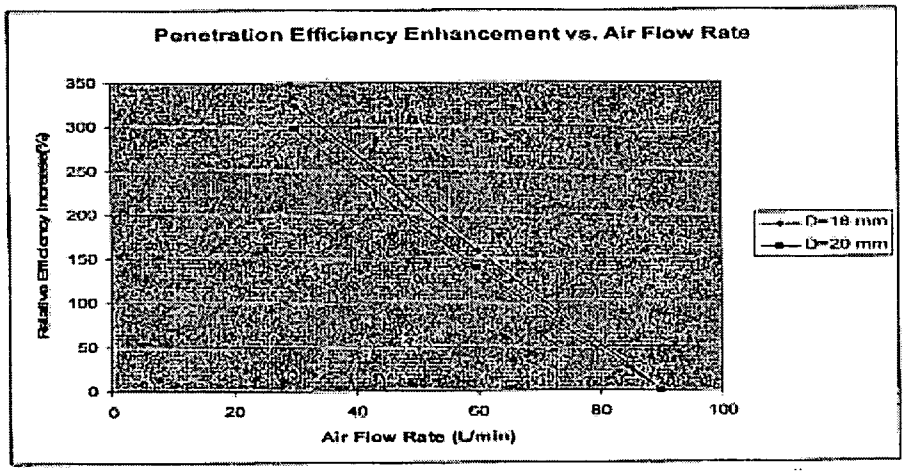
Penetration Efficiency Enhancement vs. Air Flow Rate
350
300
250
200
150
100
50
0
Relative Efficiency Increase(%)
0
20
40
60
80
100
Air Flow Rate (L/min)
D=18 mm
D=20 mm

FIG. 23

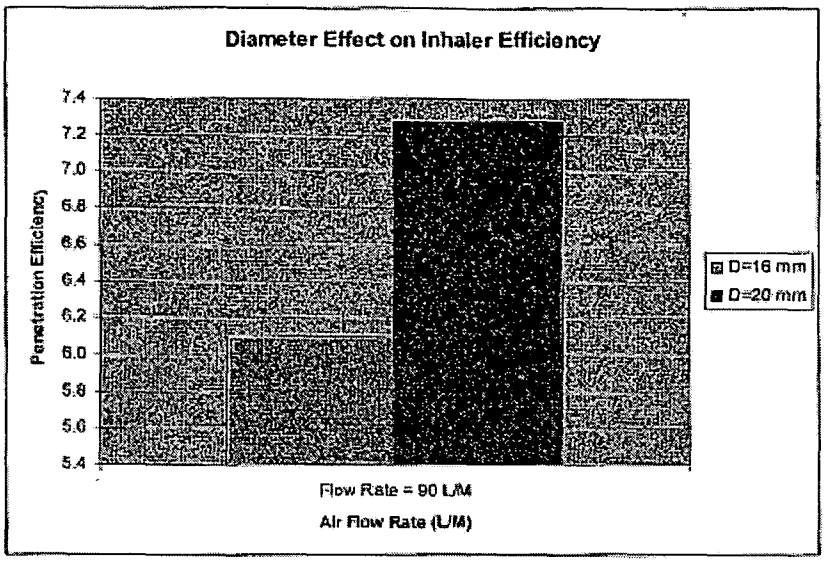
Diameter Effect on Inhaler Efficiency
Penetration Efficiency
7.4
7.2
7.0
6.8
6.6
6.4
6.2
6.0
5.8
5.6
5.4
D=16 mm
D=20 mm
Flow Rate = 90 L/M
Air Flow Rate (L/M)

FIG. 24

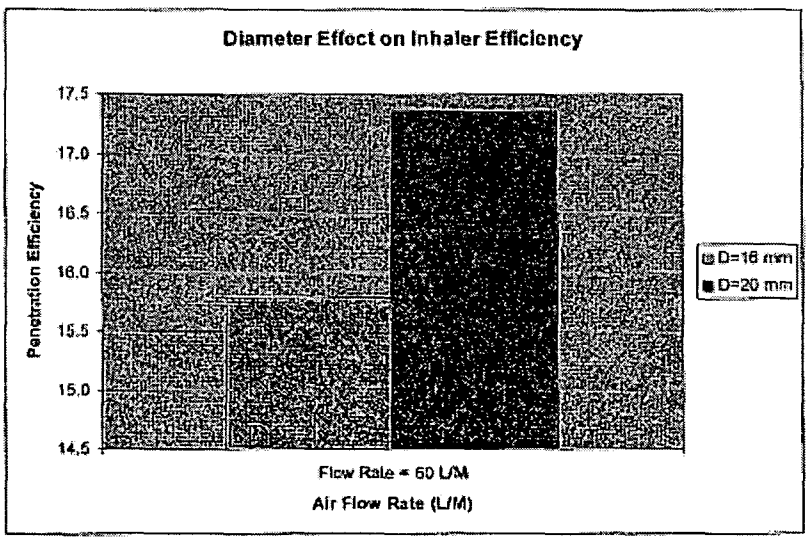
Diameter Effect on Inhaler Efficiency
Penetration Efficiency
17.5
17.0
16.5
16.0
15.5
15.0
14.5
D=16 mm
D=20 mm
Flow Rate = 60 L/M
Air Flow Rate (L/M)

FIG. 25

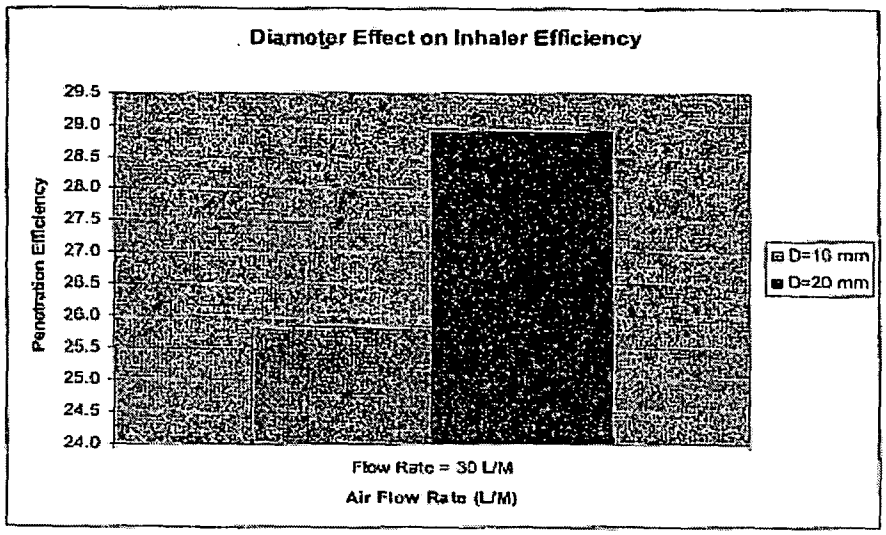
Diameter Effect on Inhaler Efficiency
Penetration Efficiency
29.5
29.0
28.5
28.0
27.5
27.0
26.5
26.0
25.5
25.0
24.5
24.0
D=10 mm
D=20 mm
Flow Rate = 30 L/M
Air Flow Rate (L/M)

FIG. 26

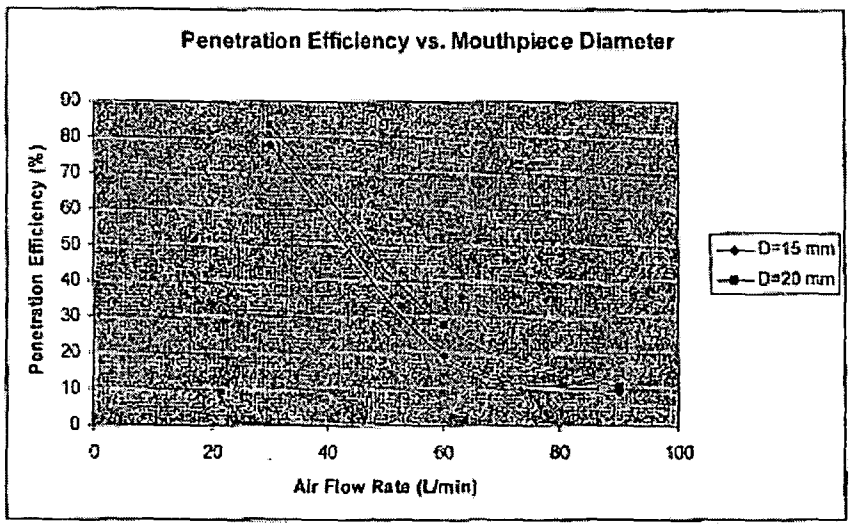
Penetration Efficiency vs. Mouthpiece Diameter
Penetration Efficiency (%)
90
80
70
60
50
40
30
20
10
0
0
20
40
60
80
100
Air Flow Rate (L/min)
D=15 mm
D=20 mm

FIG. 27

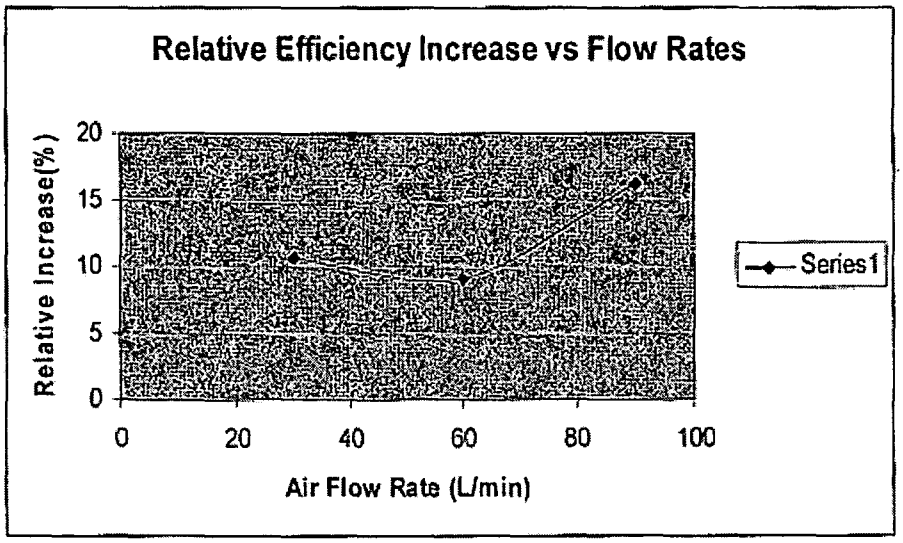
Relative Efficiency Increase vs Flow Rates
Relative Increase(%)
20
15
10
5
0
0
20
40
60
80
100
Air Flow Rate (L/min)
Series1

FIG. 28

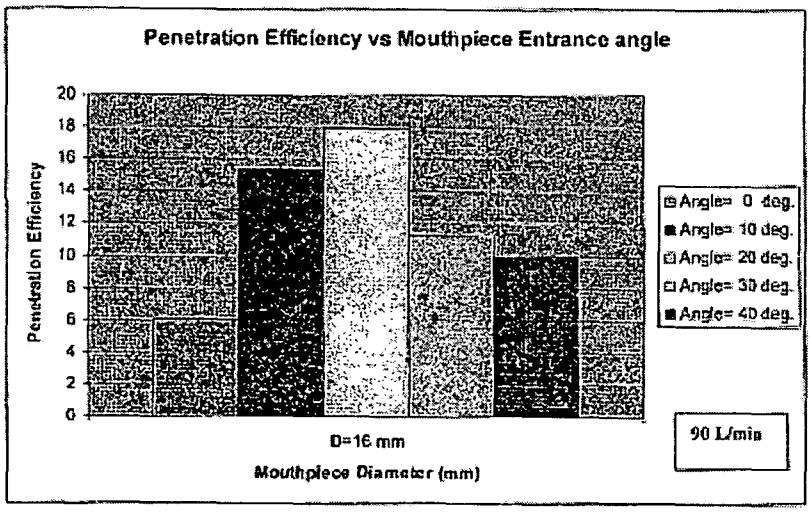
Penetration Efficiency vs Mouthpiece Entrance angle
Penetration Efficiency
20
18
16
14
12
10
8
6
4
2
0
D=16 mm
Mouthpiece Diameter (mm)
Angle= 0 deg.
Angle= 10 deg.
Angle= 20 deg.
Angle= 30 deg.
Angle= 40 deg.
90 L/min

FIG. 29

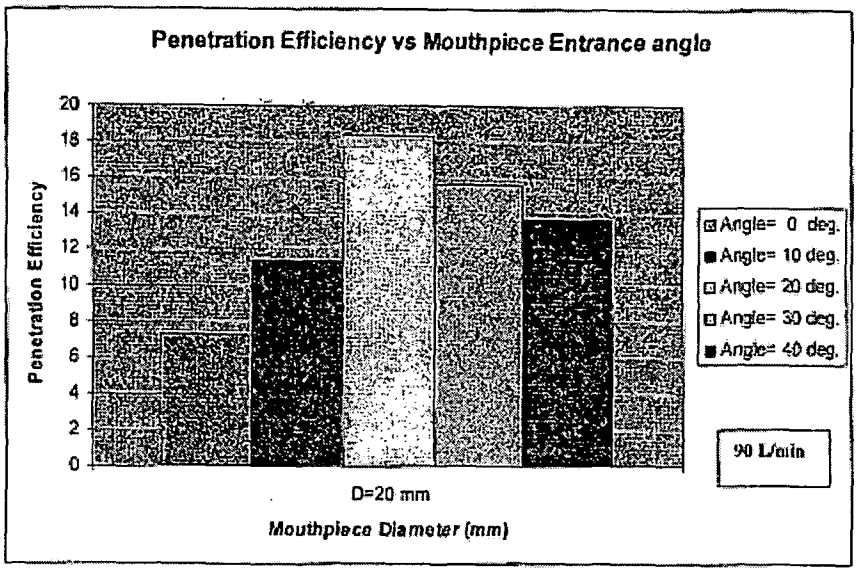
Penetration Efficiency vs Mouthpiece Entrance angle
Penetration Efficiency
20
18
16
14
12
10
8
6
4
2
0
Angle= 0 deg.
Angle= 10 deg.
Angle= 20 deg.
Angle= 30 deg.
Angle= 40 deg.
90 L/min
D=20 mm
Mouthpiece Diameter (mm)

FIG. 30

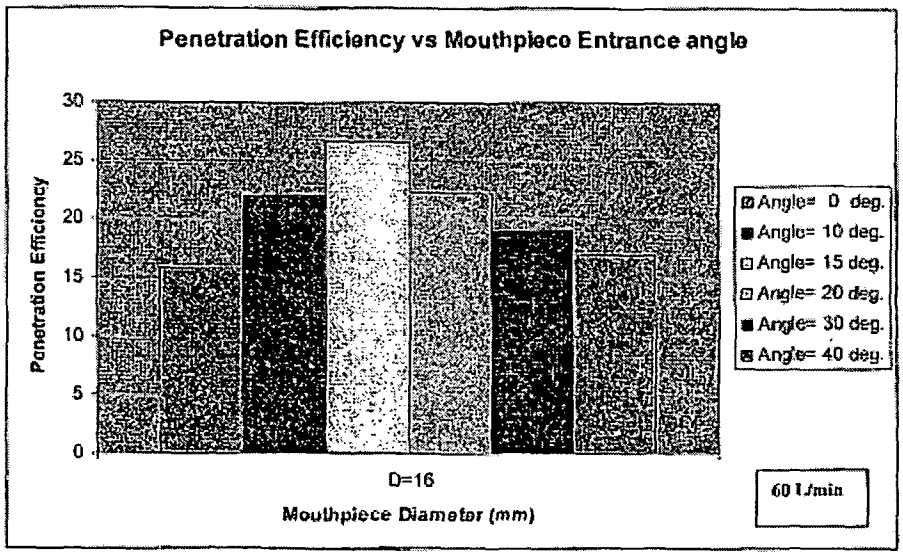
Penetration Efficiency vs Mouthpiece Entrance angle
Penetration Efficiency
30
25
20
15
10
5
0
Angle= 0 deg.
Angle= 10 deg.
Angle= 15 deg.
Angle= 20 deg.
Angle= 30 deg.
Angle= 40 deg.
60 L/min
D=16
Mouthpiece Diameter (mm)

FIG. 31

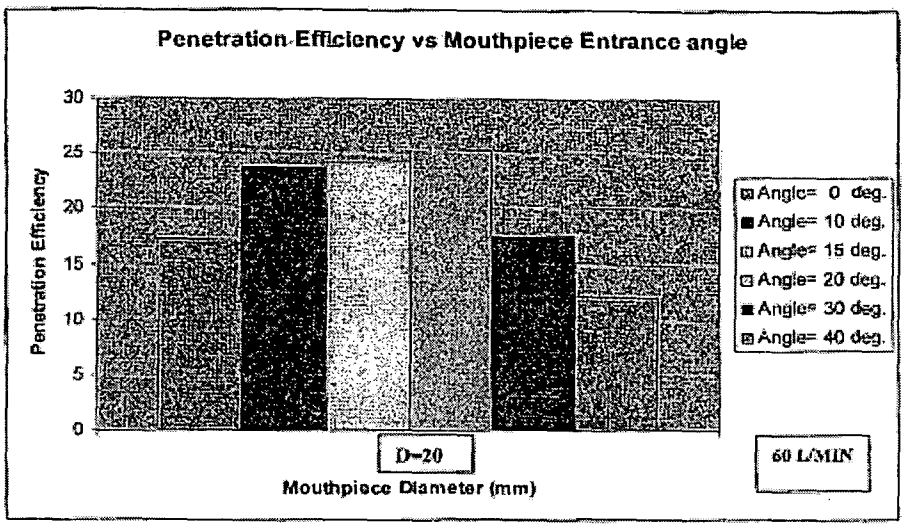
Penetration Efficiency vs Mouthpiece Entrance angle
Penetration Efficiency
30
25
20
15
10
5
0
Angle= 0 deg.
Angle= 10 deg.
Angle= 15 deg.
Angle= 20 deg.
Angle= 30 deg.
Angle= 40 deg.
D=20
Mouthpiece Diameter (mm)
60 L/MIN

FIG. 32

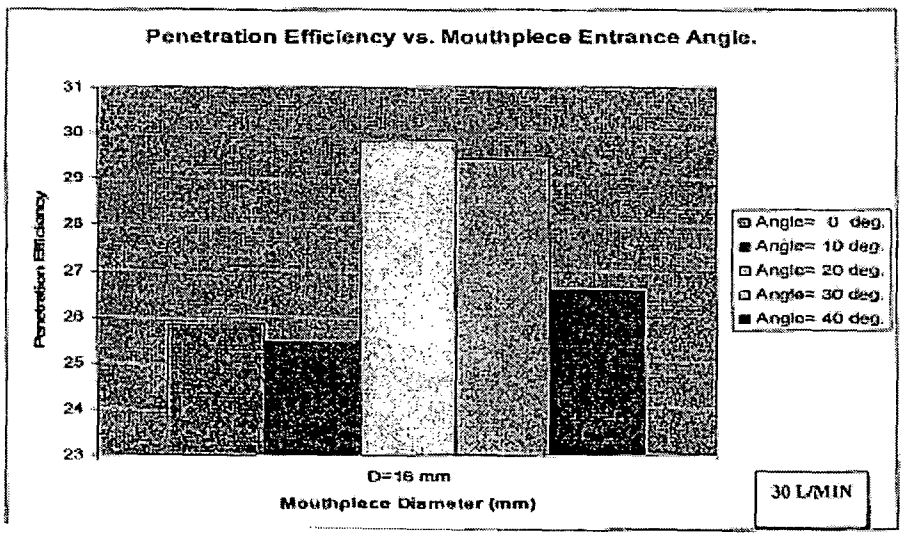
Penetration Efficiency vs. Mouthpiece Entrance Angle.
Penetration Efficiency
31
30
29
28
27
26
25
24
23
Angle= 0 deg.
Angle= 10 deg.
Angle= 20 deg.
Angle= 30 deg.
Angle= 40 deg.
D=16 mm
Mouthpiece Diameter (mm)
30 L/MIN

FIG. 33

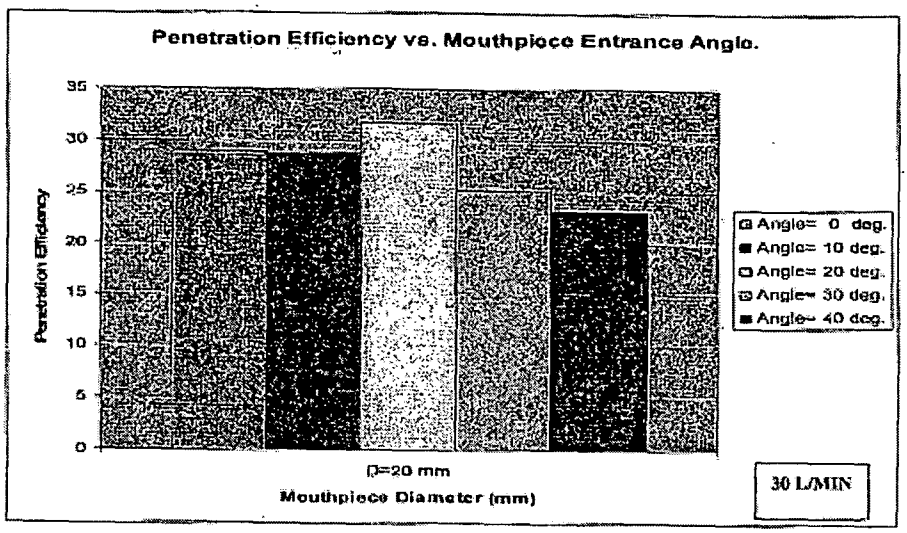
Penetration Efficiency vs. Mouthpiece Entrance Angle.
Penetration Efficiency
35
30
25
20
15
10
5
0
D=20 mm
Mouthpiece Diameter (mm)
Angle= 0 deg.
Angle= 10 deg.
Angle= 20 deg.
Angle= 30 deg.
Angle= 40 deg.
30 L/MIN

FIG. 34

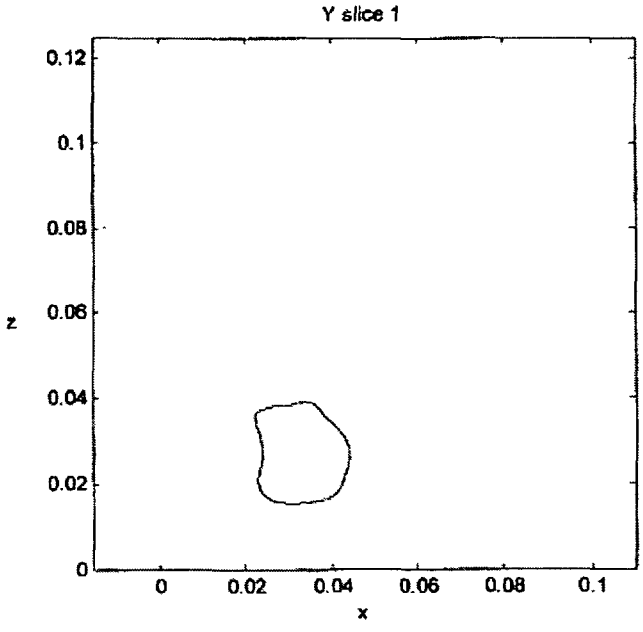

FIG 34A

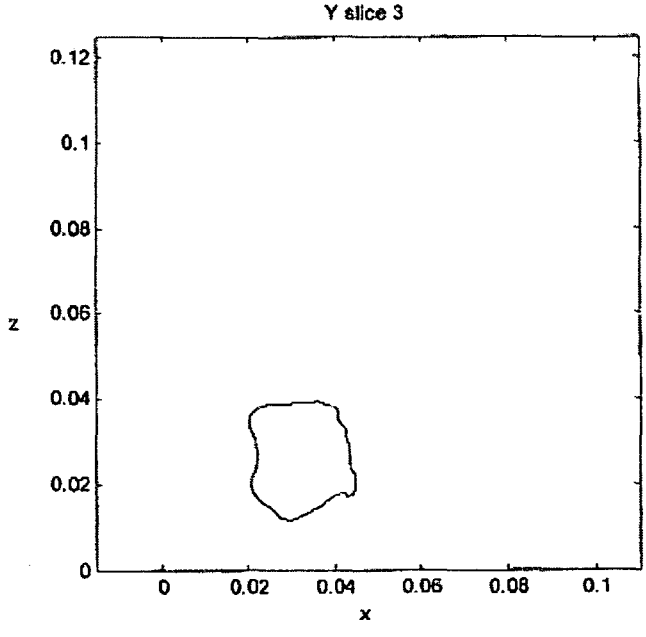

FIG 34B

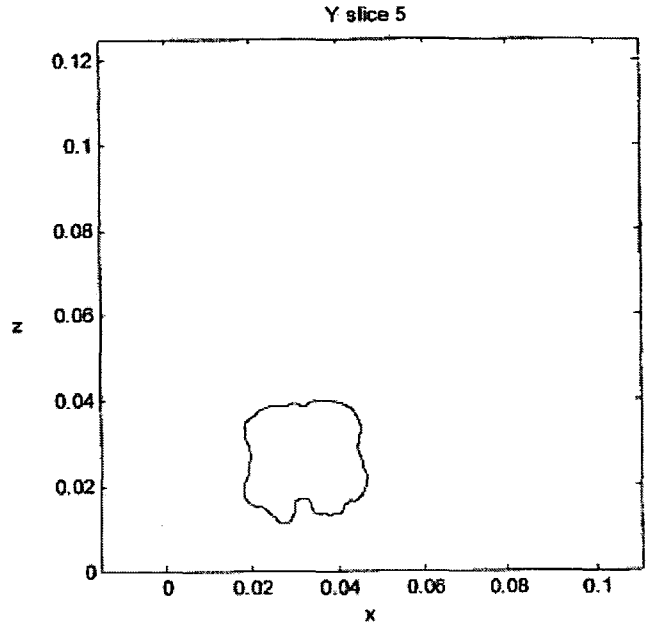

FIG 34C

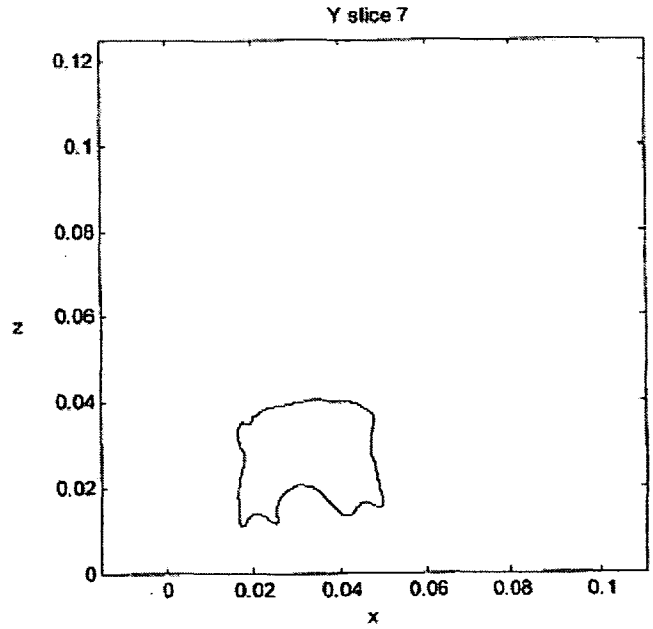

FIG 34D

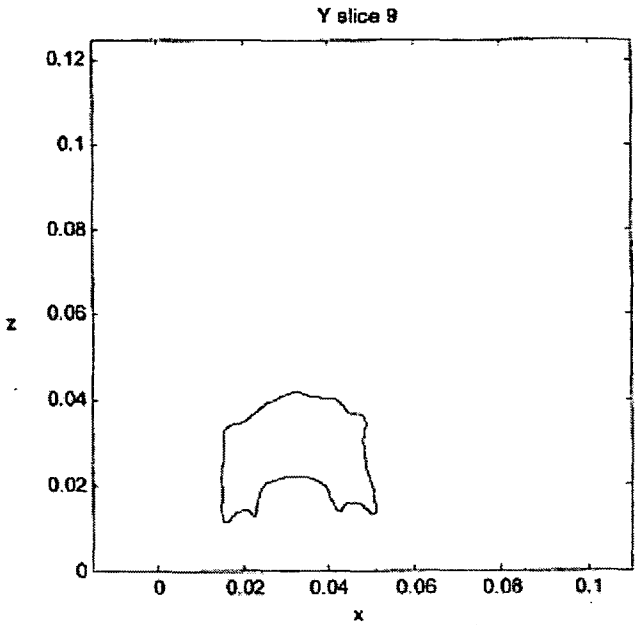

FIG 34E

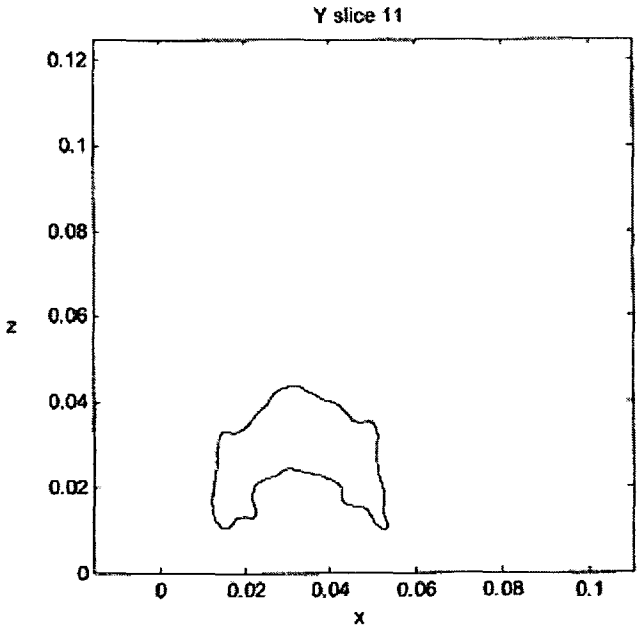

FIG 34F

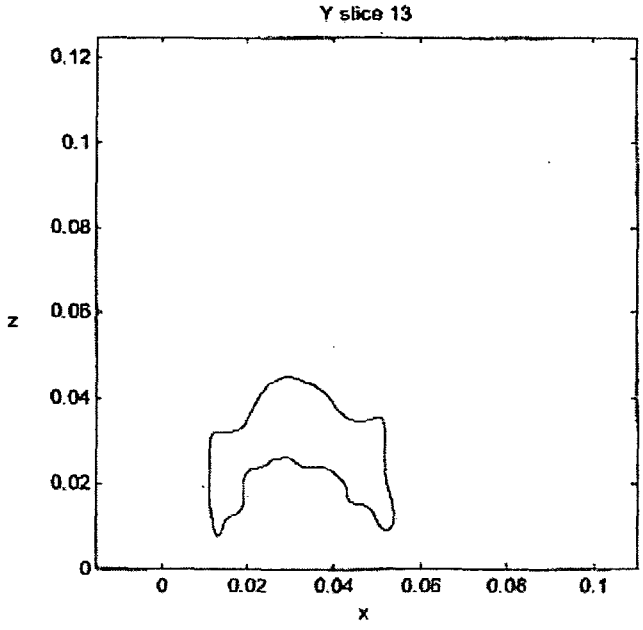

FIG 34G

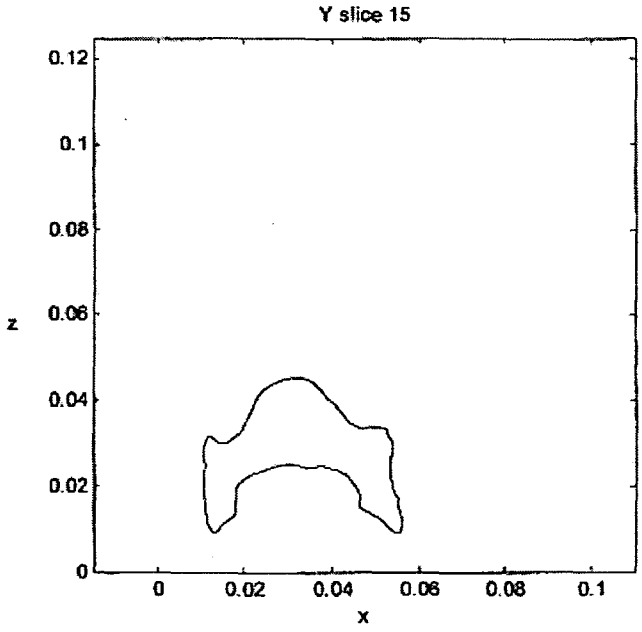

FIG 34H

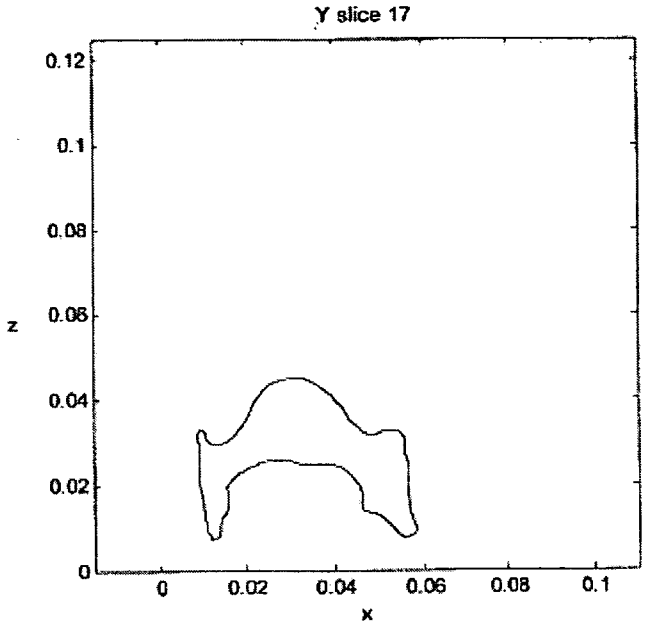

FIG 35A

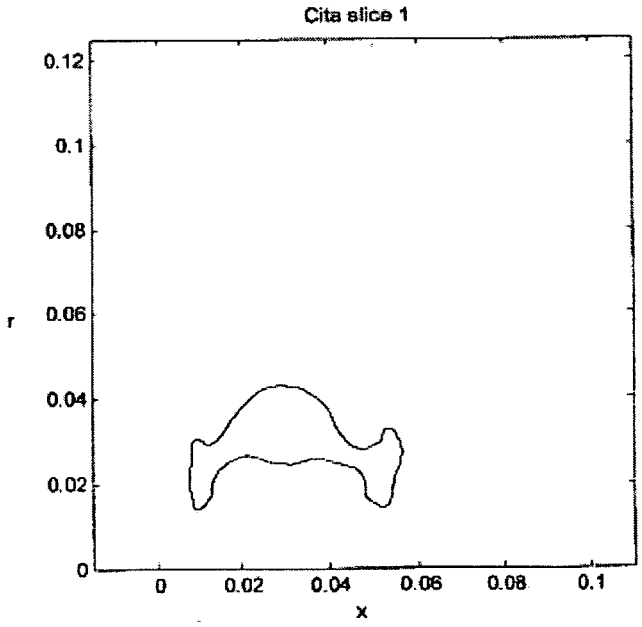

FIG 35B

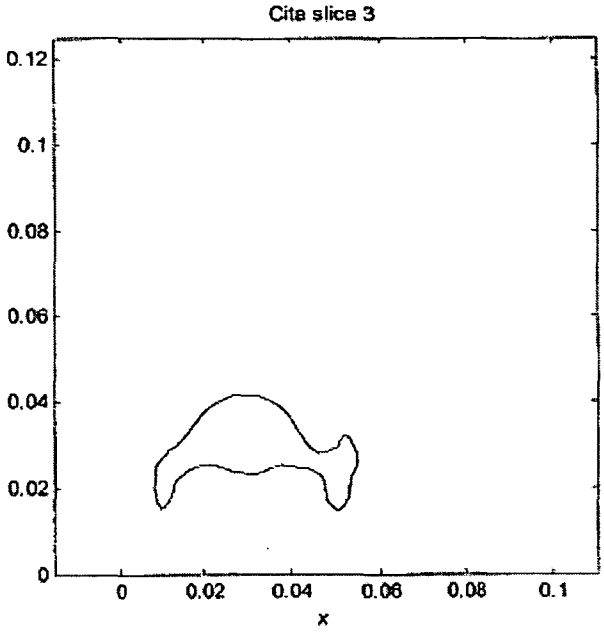

FIG 35C

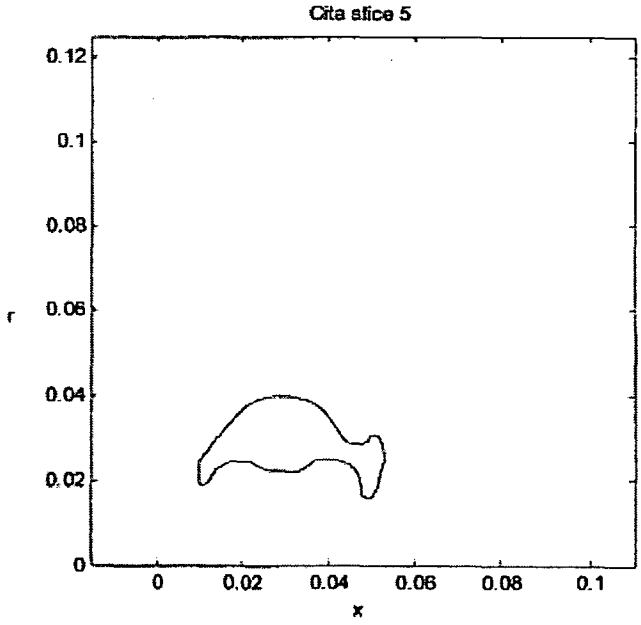

FIG 35D

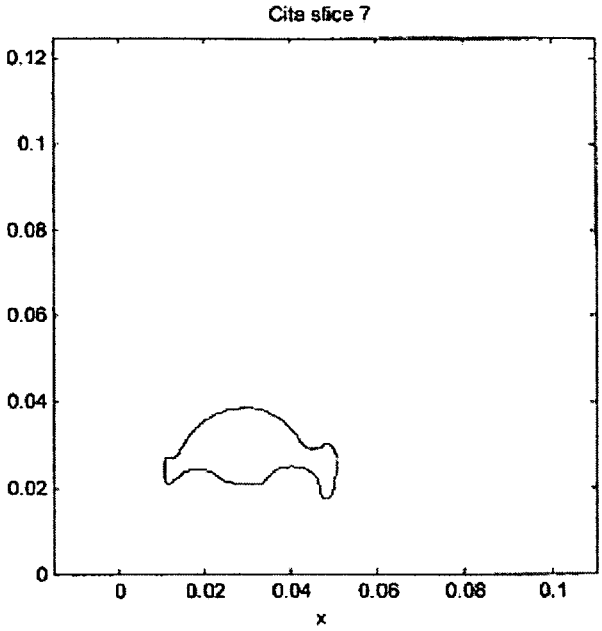

FIG 35E

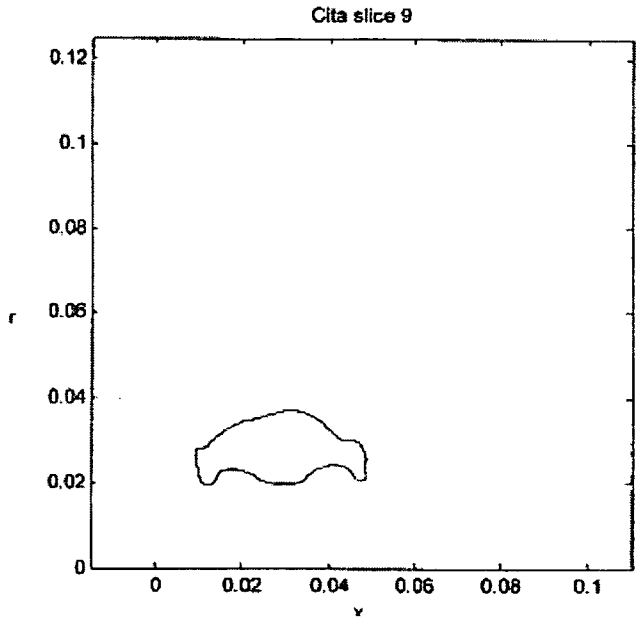

FIG 35F

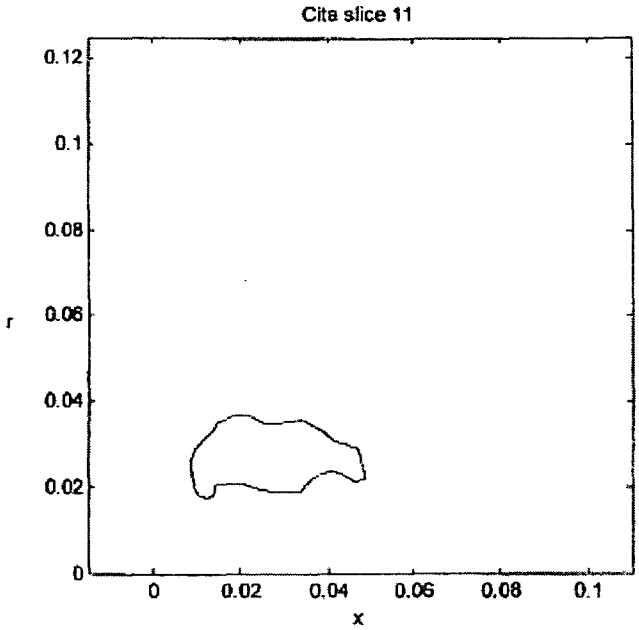

FIG 35G

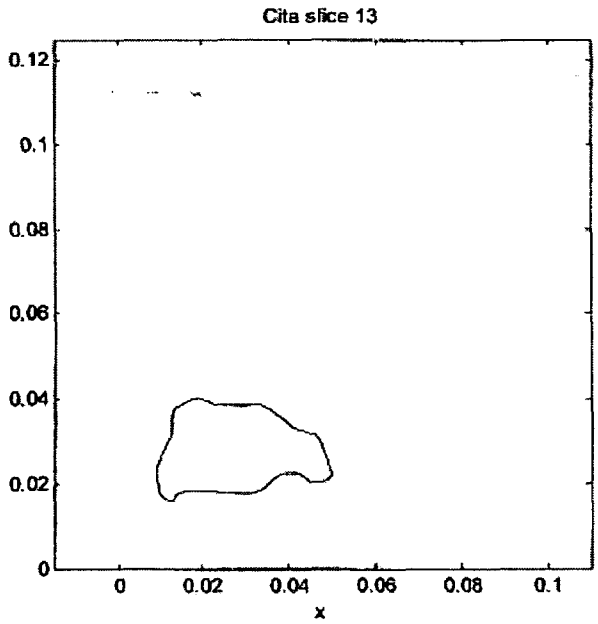

FIG 35H

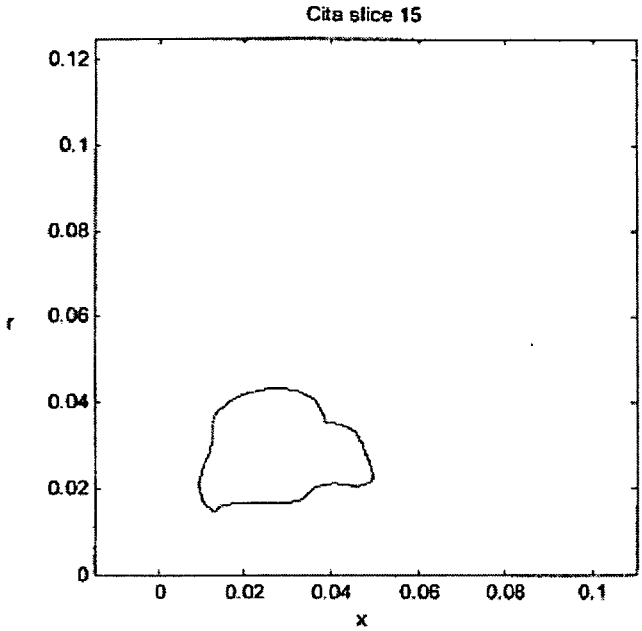

FIG 35I

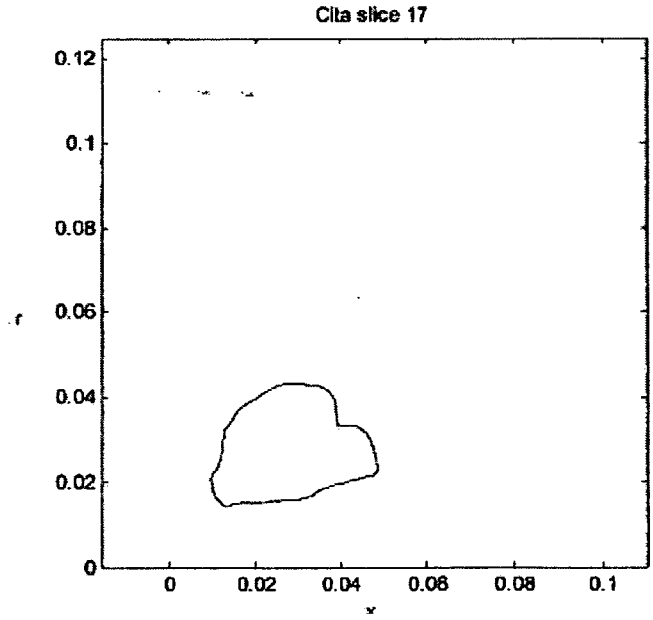

FIG 35J

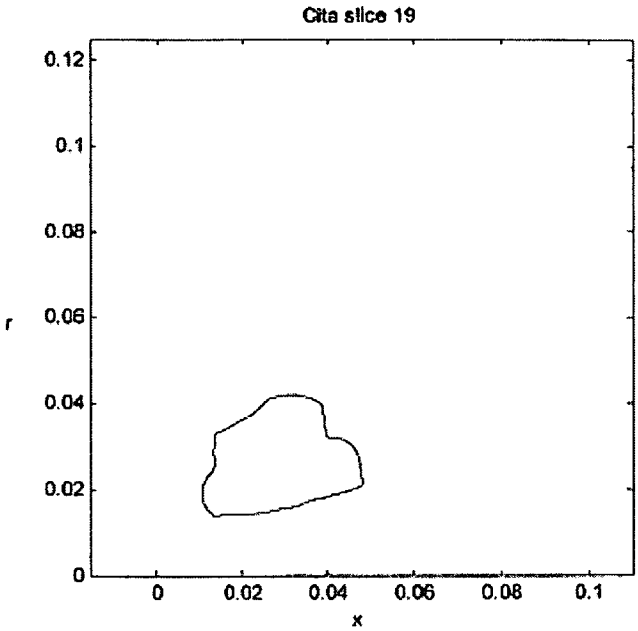

FIG 35K

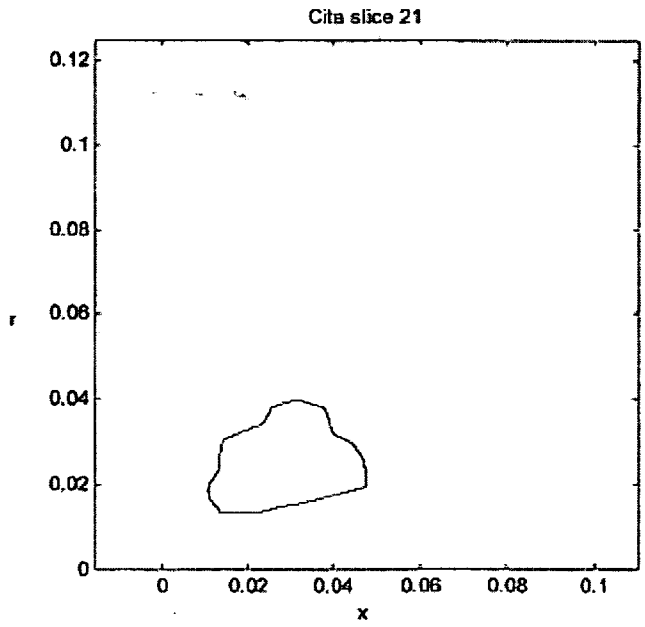

FIG 35L

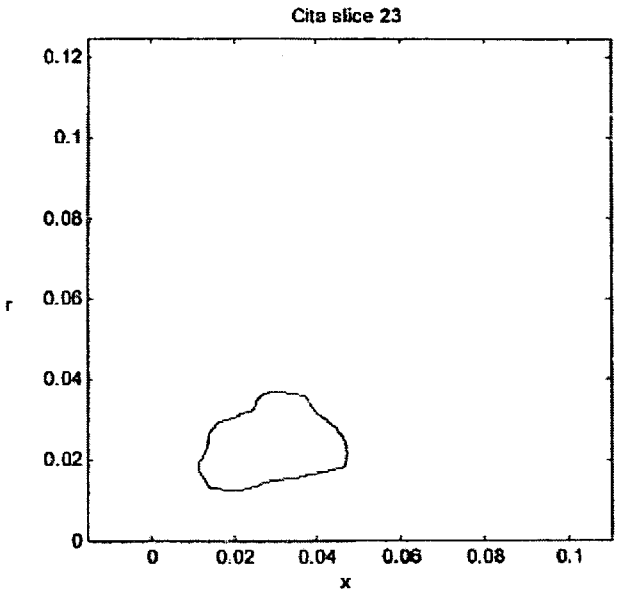

FIG 36A

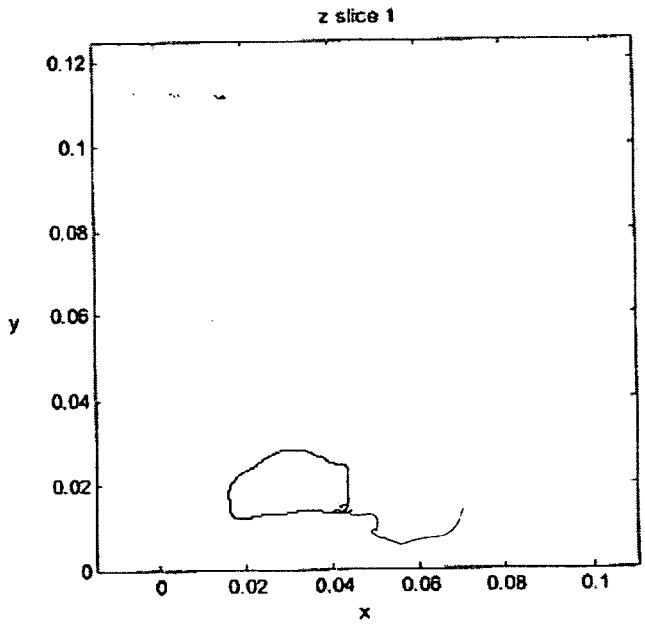

FIG 36B

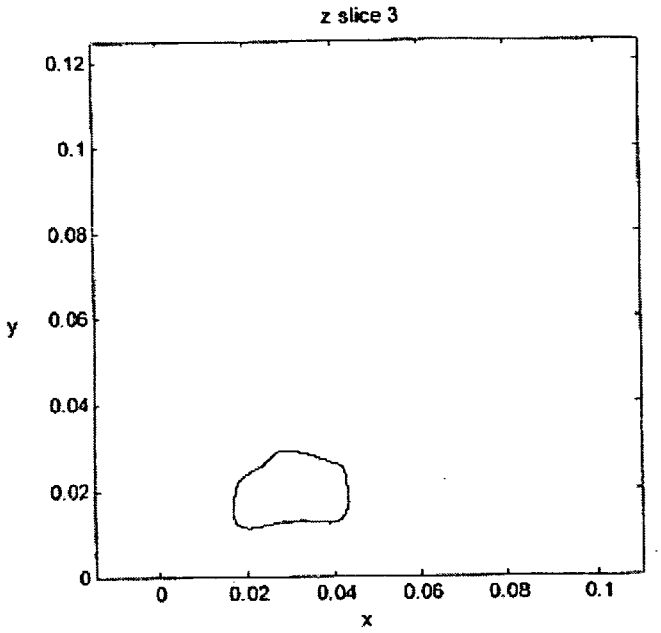

FIG 36C

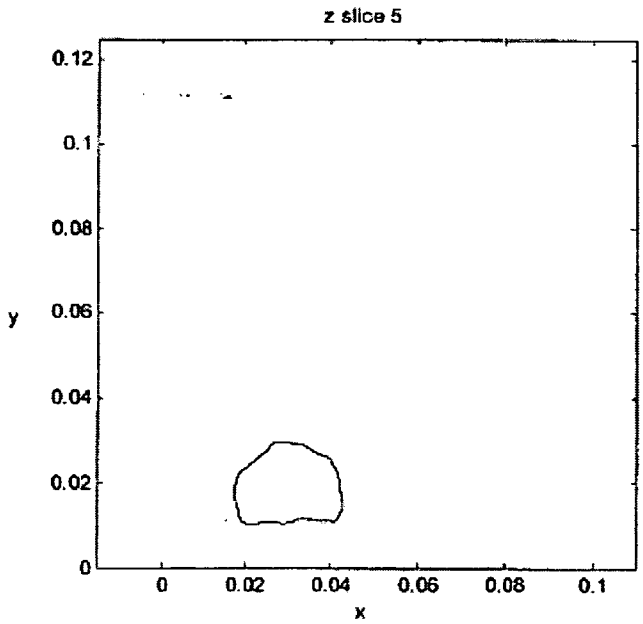

FIG 36D

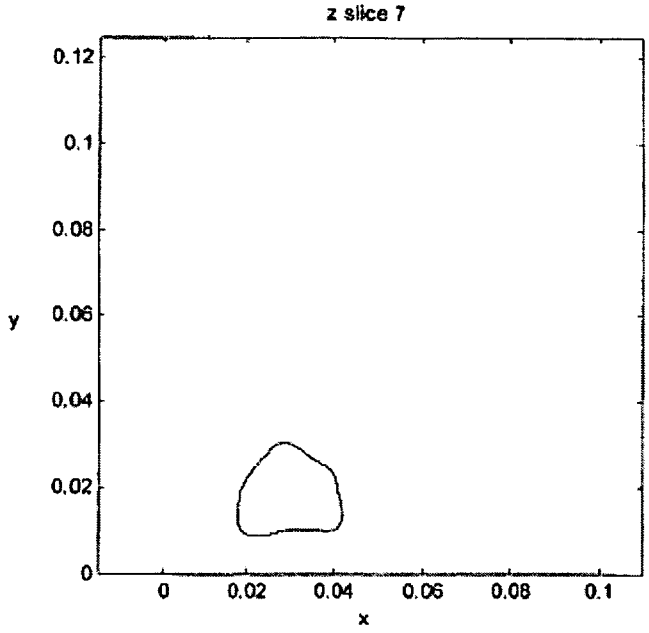

FIG 36E

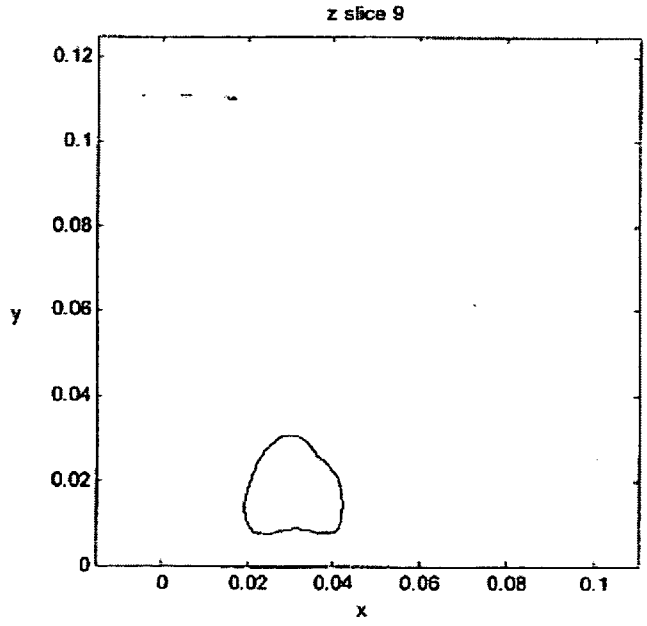

FIG 36F

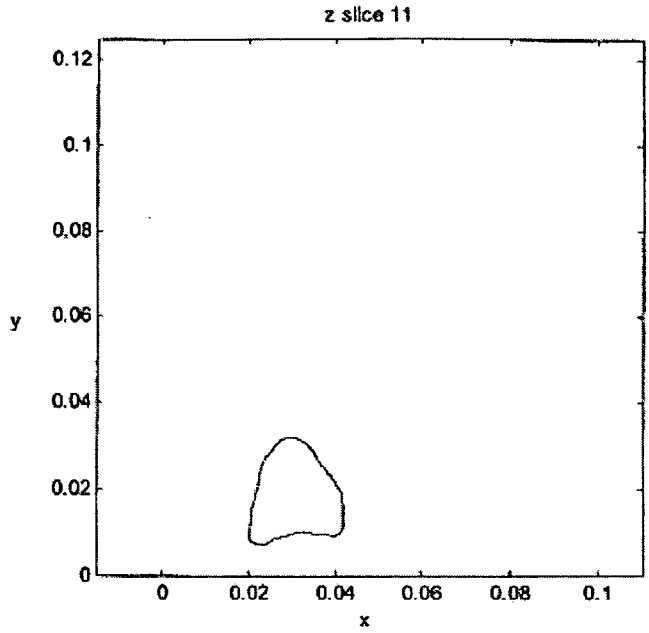

FIG 36G

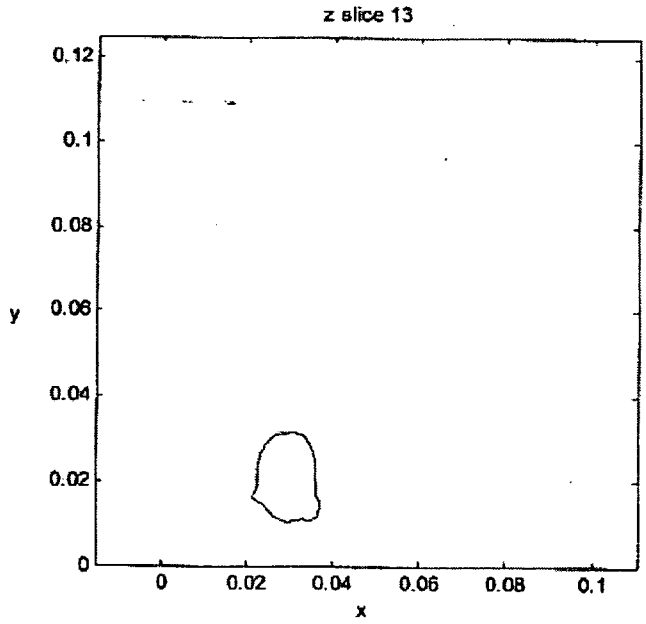

FIG 36H

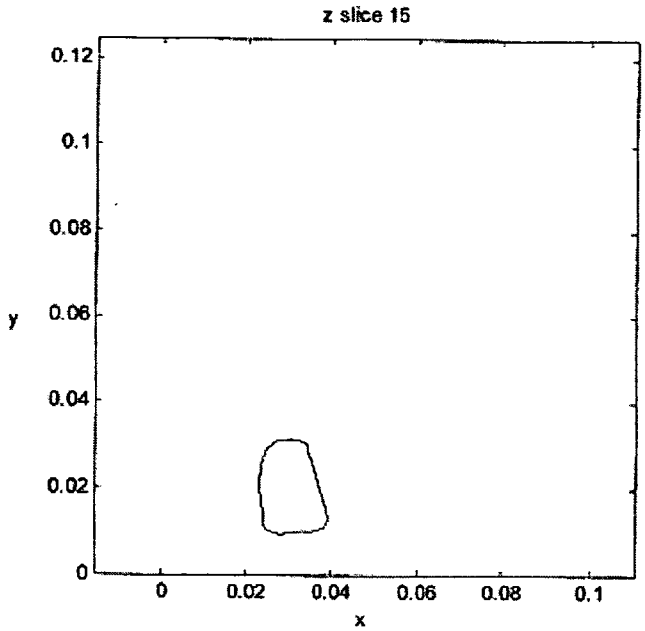

FIG 36I

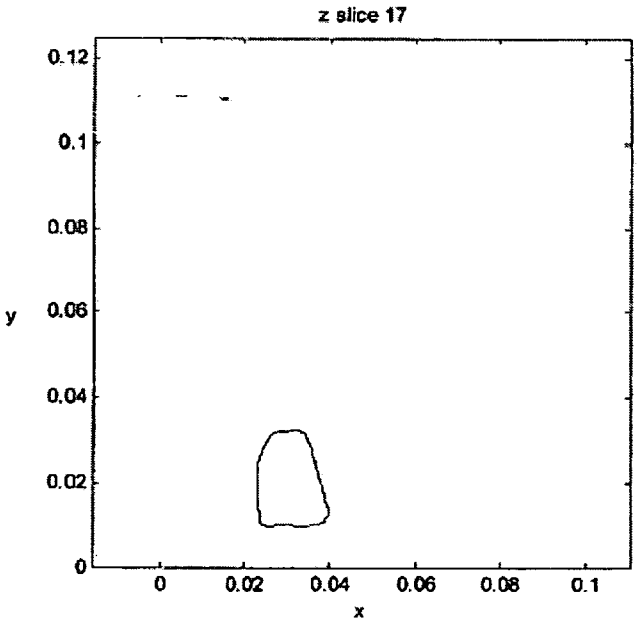

FIG 36J

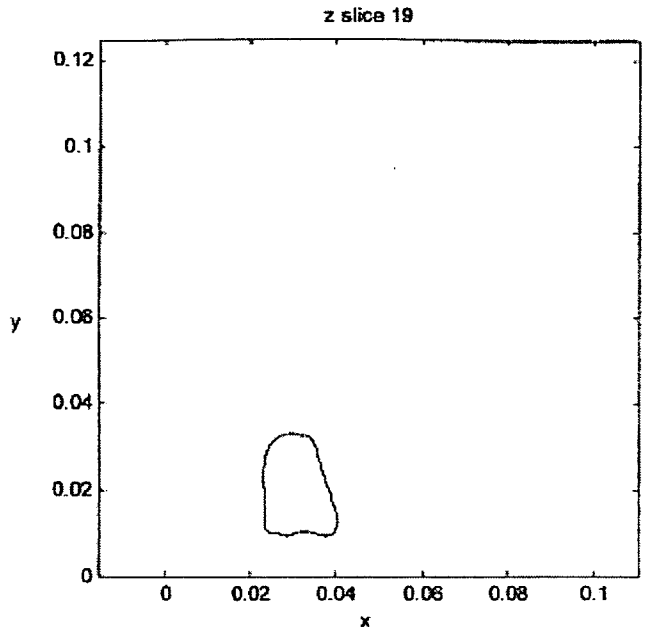

FIG 36K

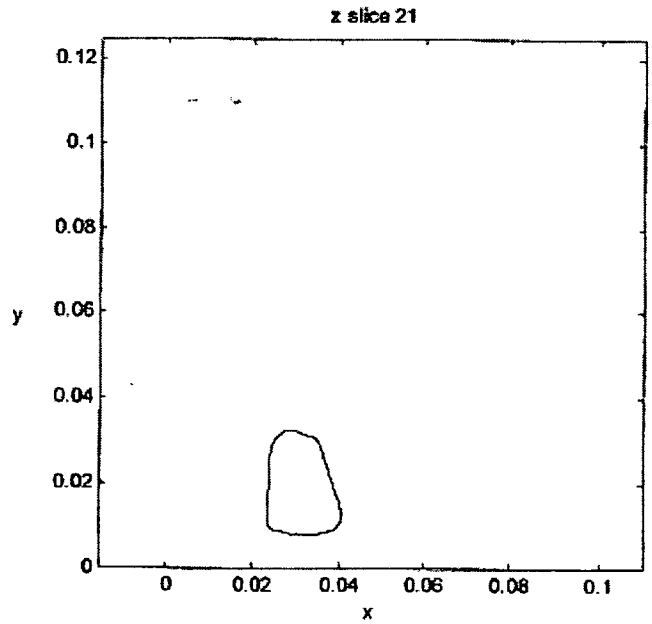

FIG 36L

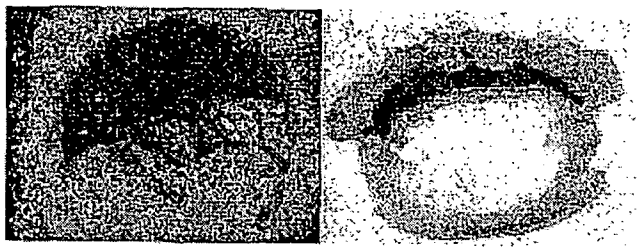

Fig. 37A

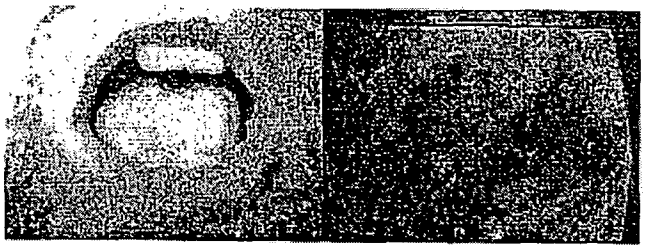

Fig 37B

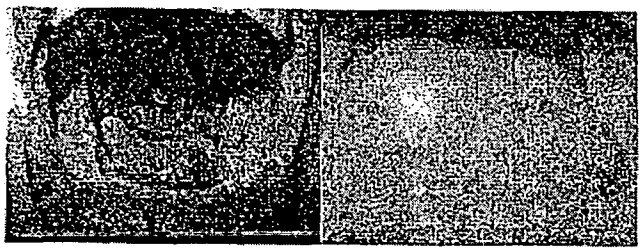

Fig. 37C

Fig 37D

Fig. 37E

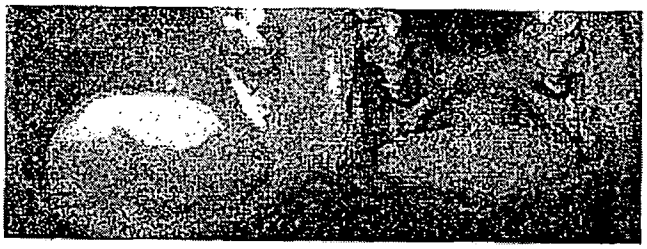

Fig. 37F

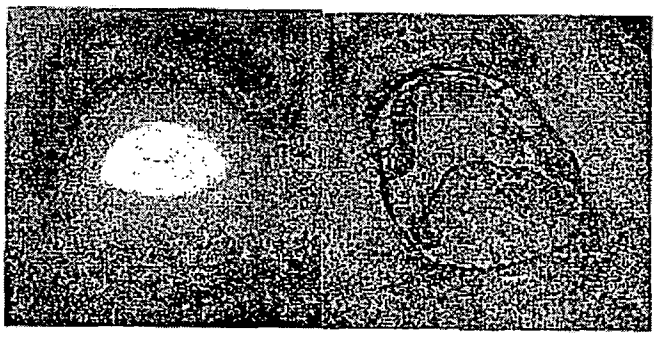

Fig 37 G

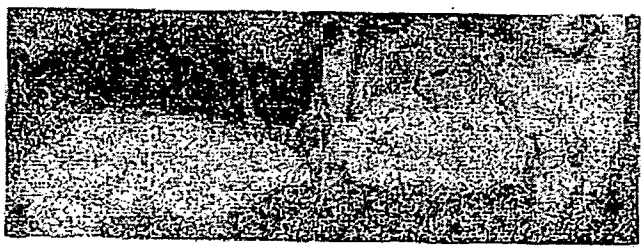

FIG. 37H

FIG. 38

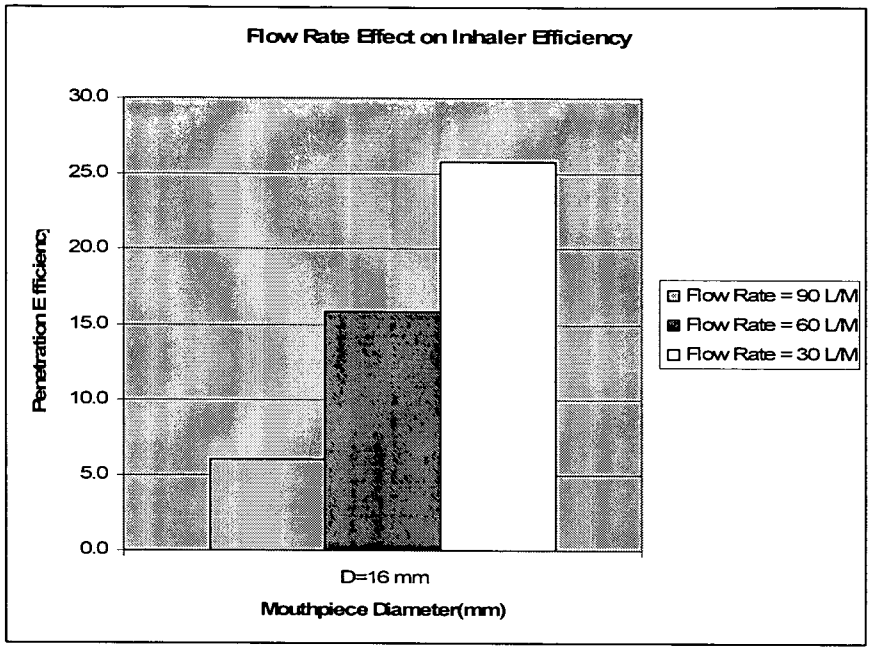

Fig. 39A. Aerosol Penetration Efficiency with Original Mouthpiece (d = 16 mm)

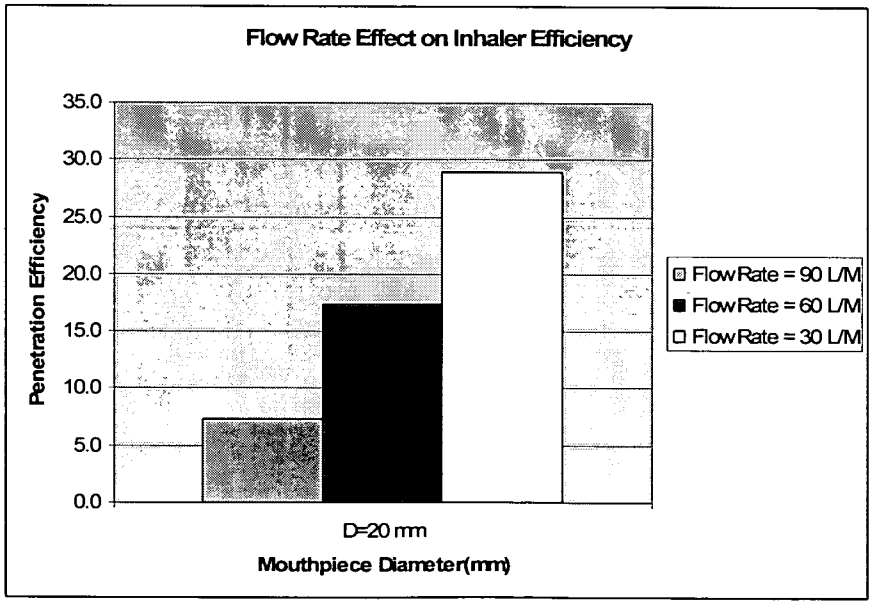

Fig. 39B. Aerosol Penetration Efficiency with Original Mouthpiece (d = 20 mm)

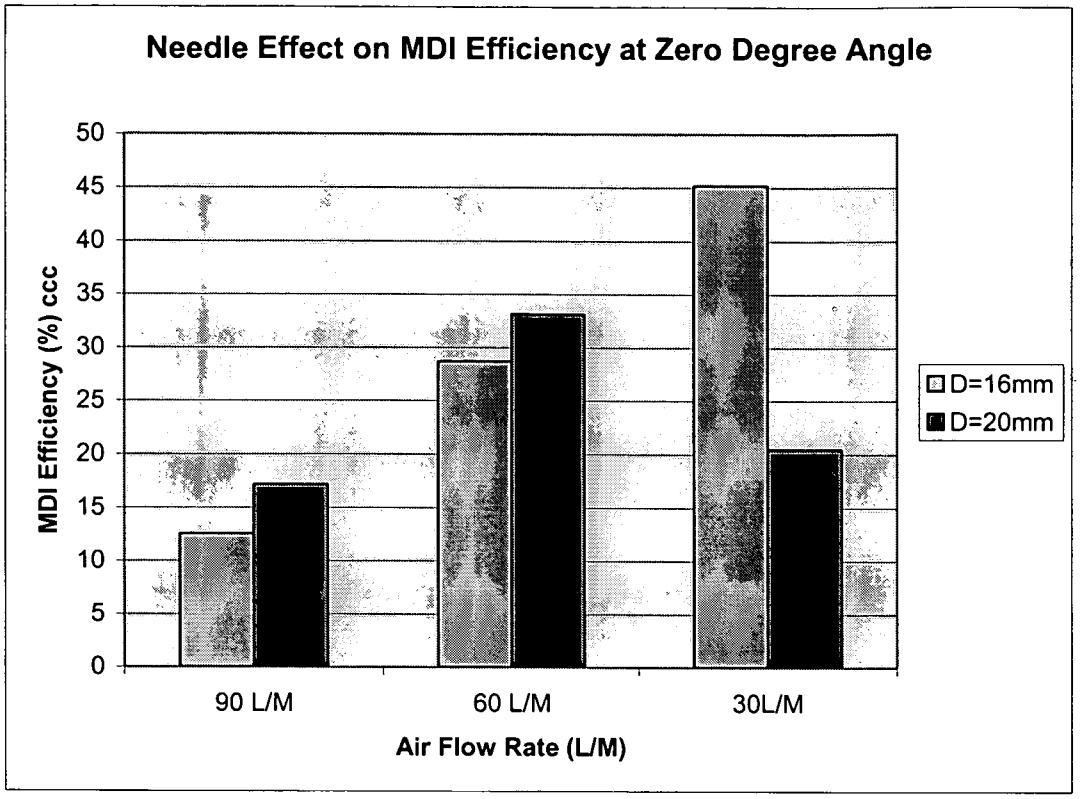

Fig. 40 Aerosol Penetration Efficiencies with the Needle Structure

Fig. 41 Inhaler Adaptors Made of Straight Channels with Upward Angle-Cuts of Various Degrees

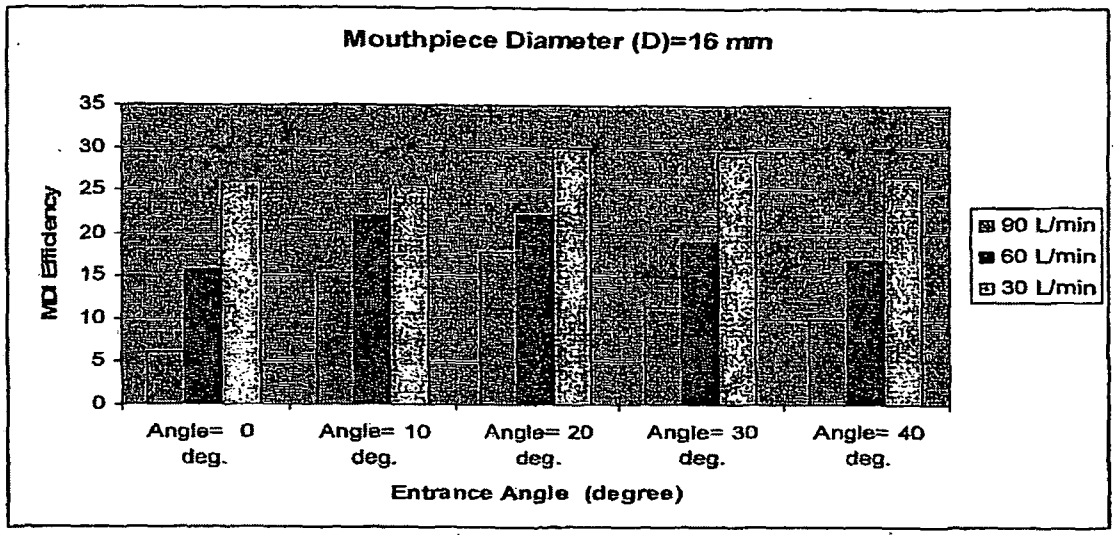
Mouthpiece Diameter (D)=16 mm
MDI Efficiency
35
30
25
20
15
10
5
0
Angle= 0 deg.
Angle= 10 deg.
Angle= 20 deg.
Angle= 30 deg.
Angle= 40 deg.
Entrance Angle (degree)
90 L/min
60 L/min
30 L/min

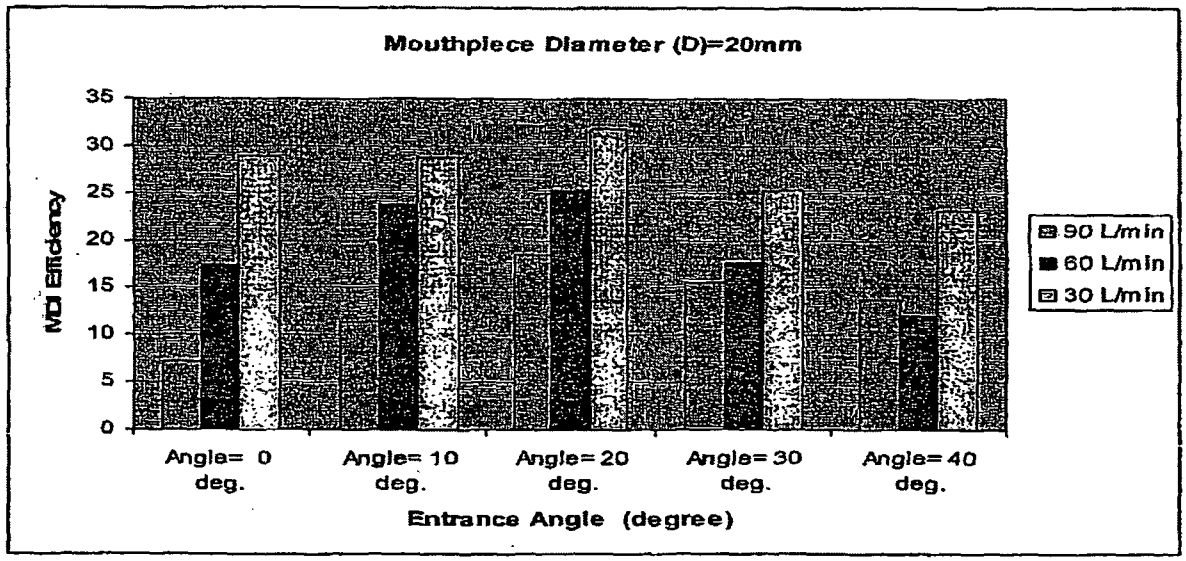
Mouthpiece Diameter (D)=20mm
MDI Efficiency
35
30
25
20
15
10
5
0
Angle= 0 deg.
Angle= 10 deg.
Angle= 20 deg.
Angle= 30 deg.
Angle= 40 deg.
Entrance Angle (degree)
90 L/min
60 L/min
30 L/min

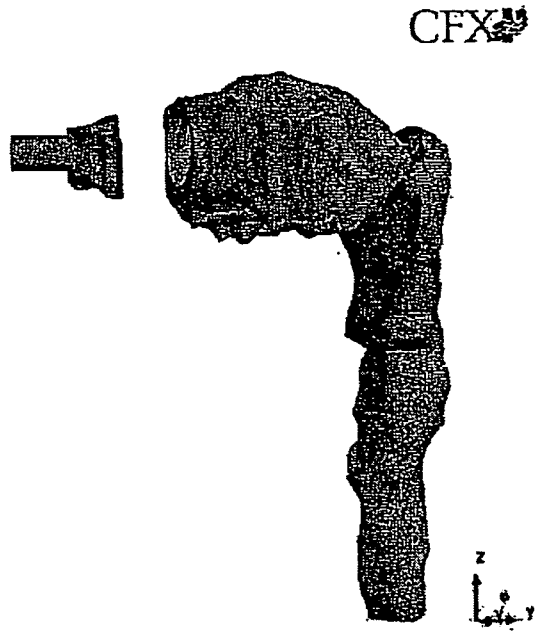
CFX
z
y

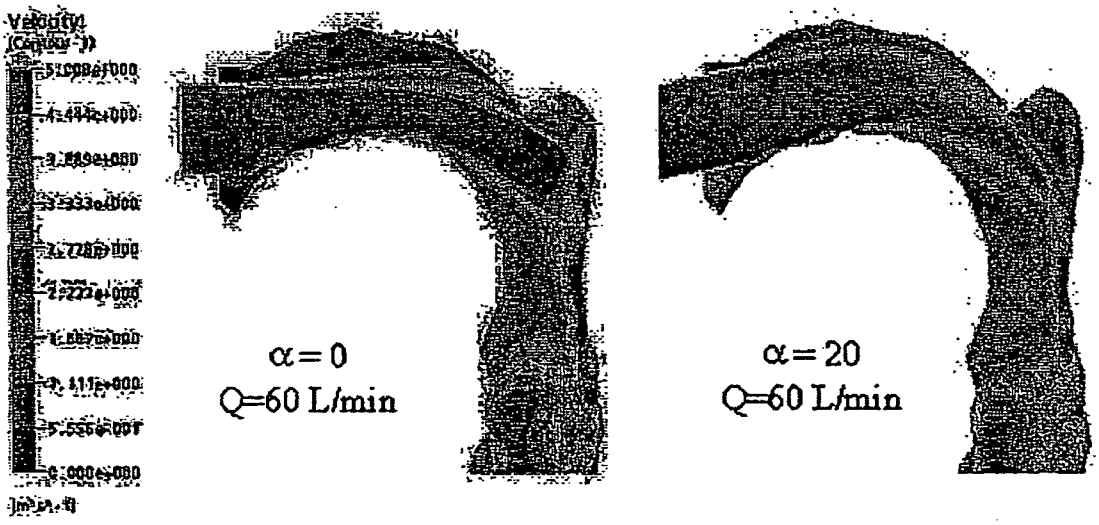
α = 0
Q=60 L/min
α = 20
Q=60 L/min

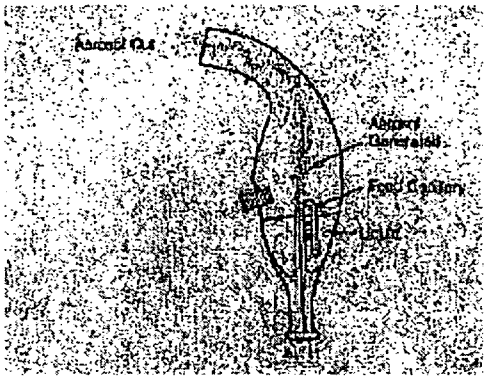

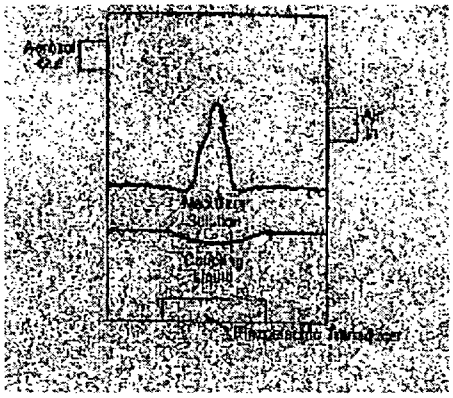

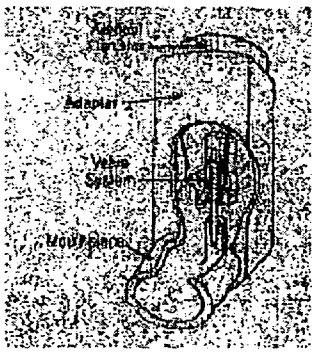

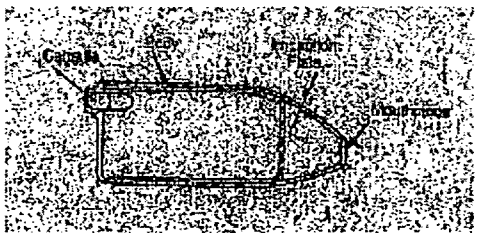

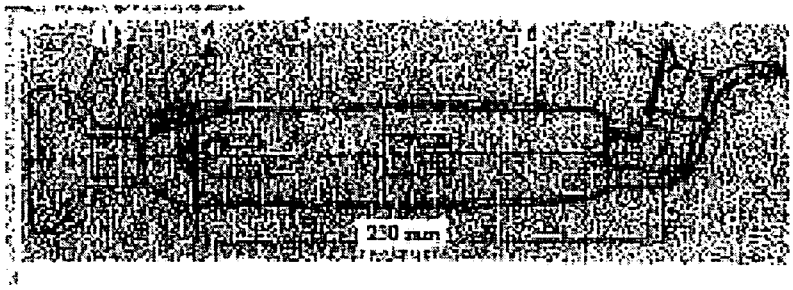

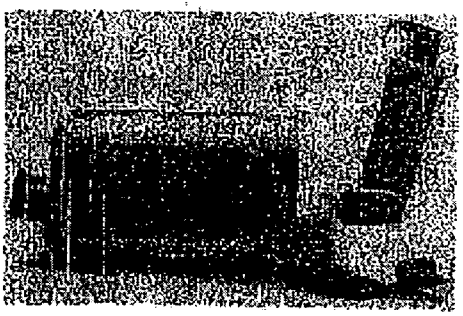

AEROSOL DEPOSITION MECHNISMS

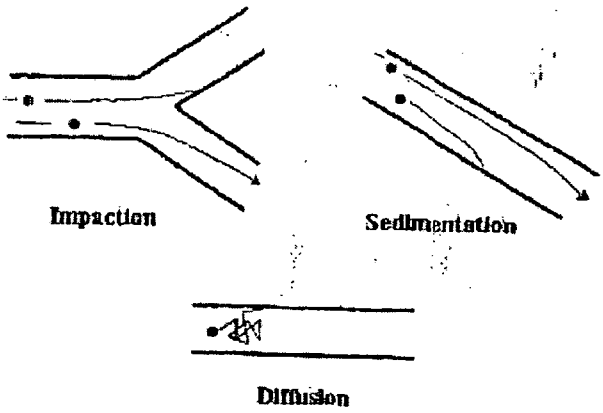

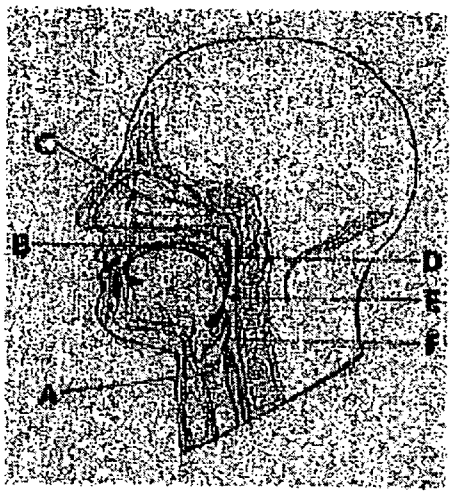
C
B
D
E
F
A

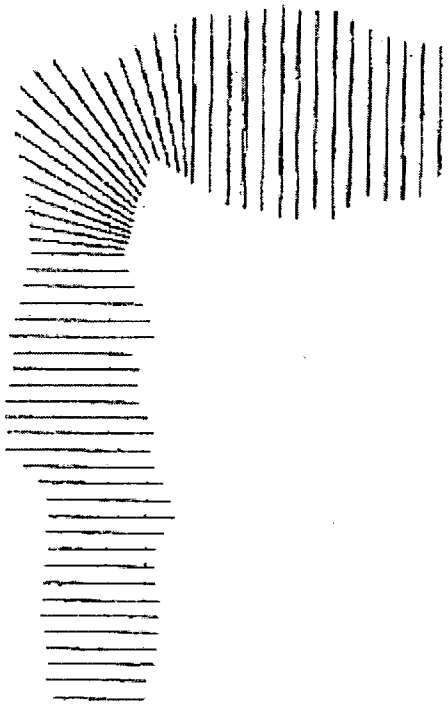

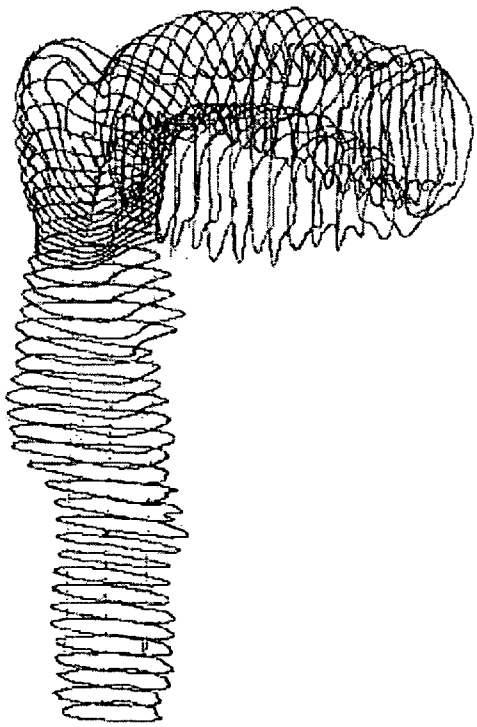

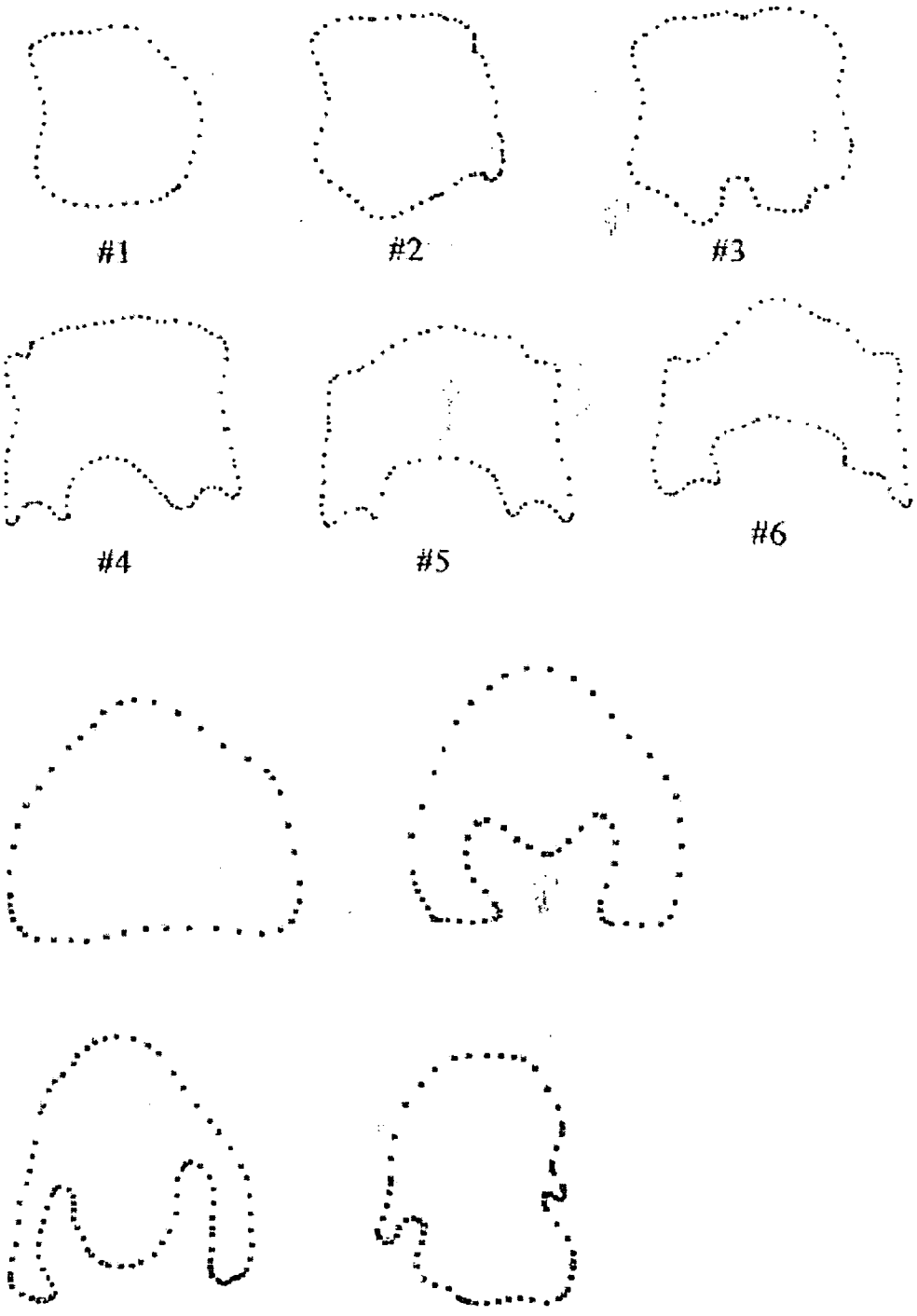
#1
#2
#3
#4
#5
#6

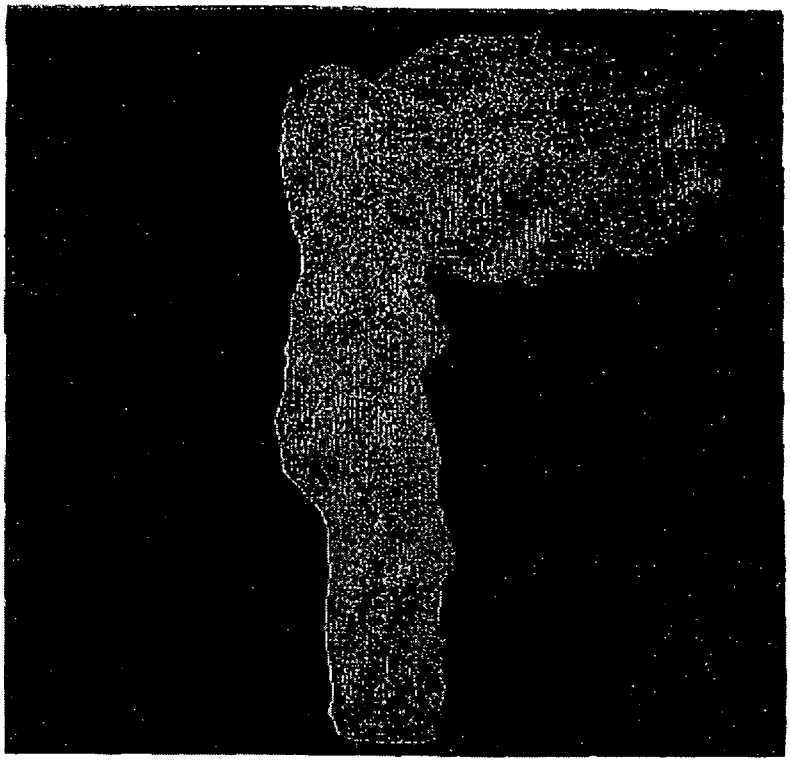

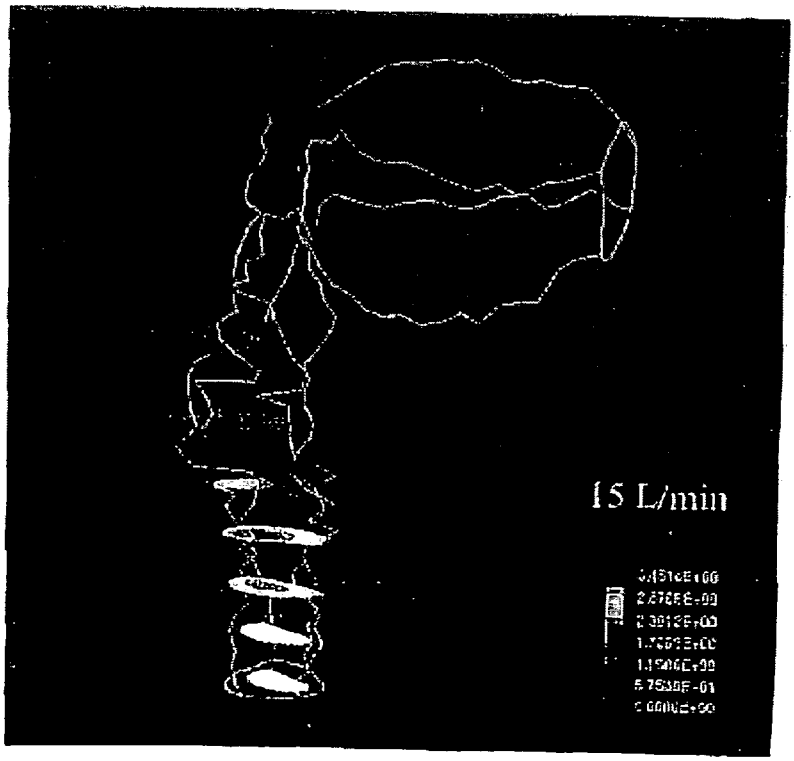
15 L/min

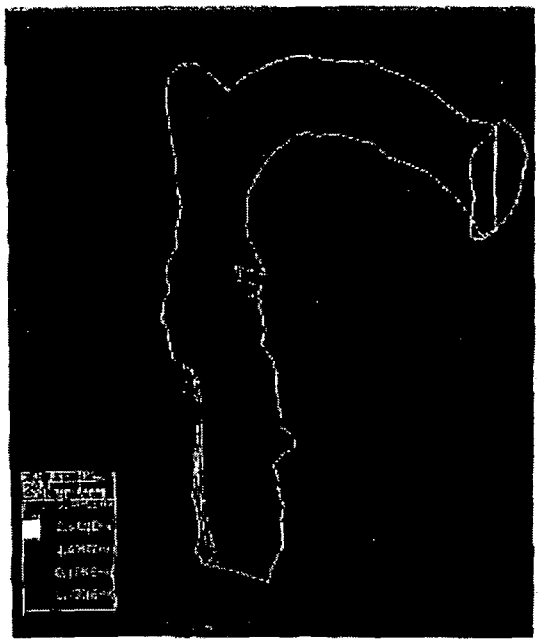

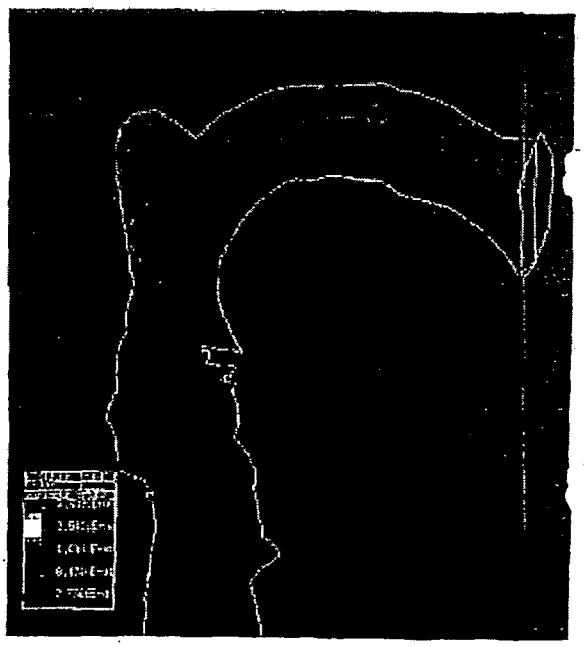

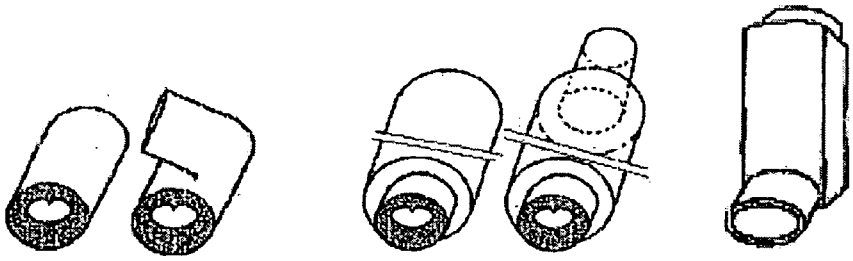

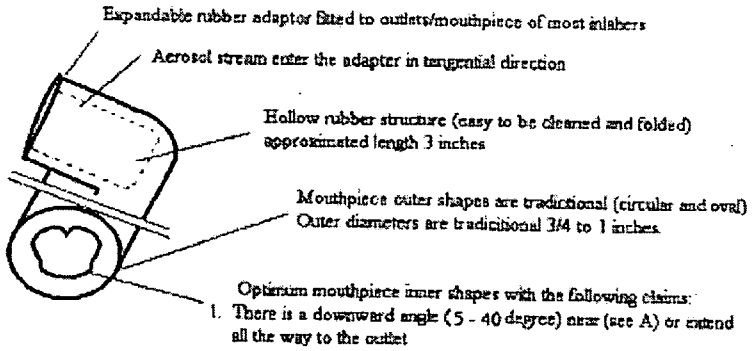
Expandable rubber adaptor fitted to outlets/mouthpiece of most inhalers
Aerosol stream enter the adapter in tangential direction
Hollow rubber structure (easy to be cleaned and folded) approximated length 3 inches
Mouthpiece outer shapes are traditional (circular and oval) Outer diameters are traditional 3/4 to 1 inches
Optimum mouthpiece inner shapes with the following claims:
1. There is a downward angle (5 - 40 degree) near (see A) or extend all the way to the outlet


2
3
A
I II
B
I III

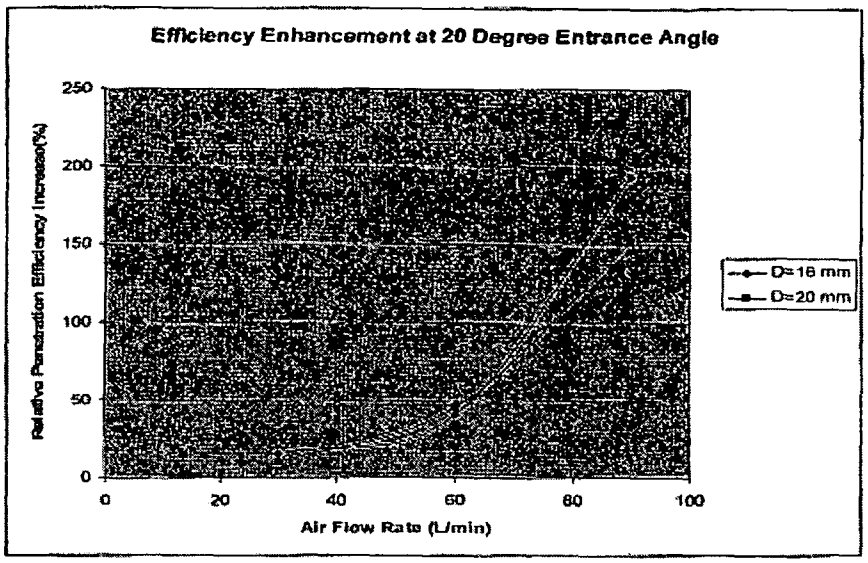
Efficiency Enhancement at 20 Degree Entrance Angle
Relative Penetration Efficiency Increase(%)
250
200
150
100
50
0
0
20
40
60
80
100
Air Flow Rate (L/min)
D=16 mm
D=20 mm

FIG. 23

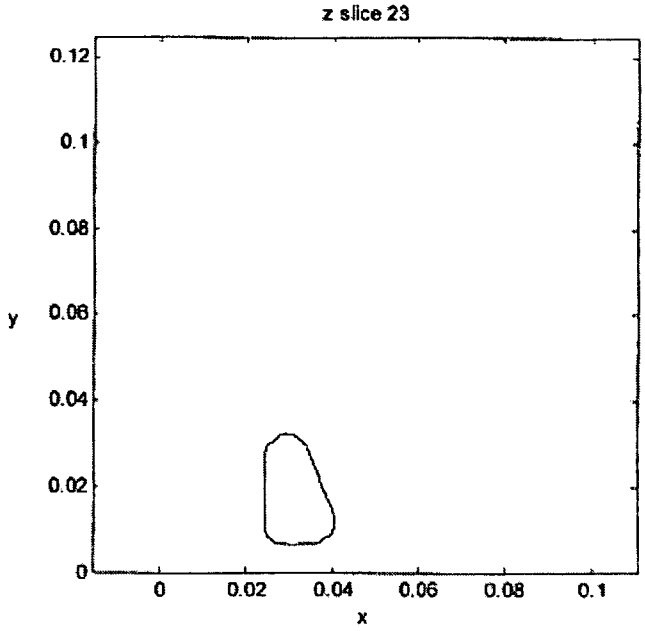
z slice 23
0.12
0.1
0.08
0.06
0.04
0.02
0
y
0
0.02
0.04
0.06
0.08
0.1
x

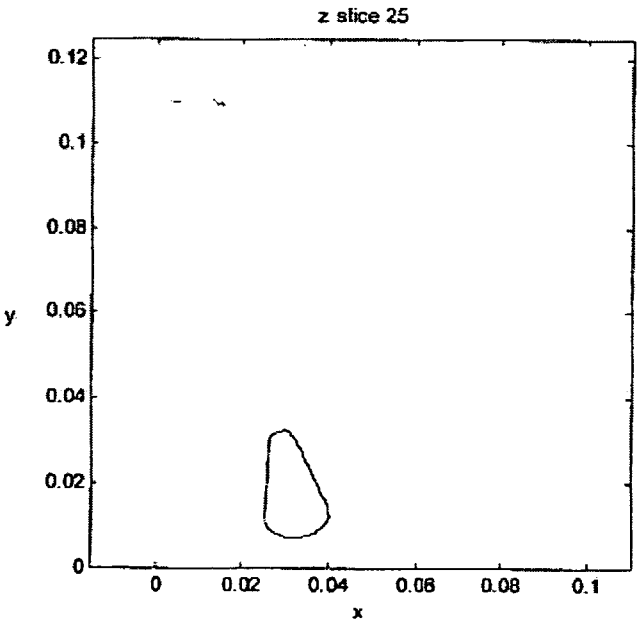
z slice 25
0.12
0.1
0.08
0.06
0.04
0.02
0
y
0
0.02
0.04
0.06
0.08
0.1
x

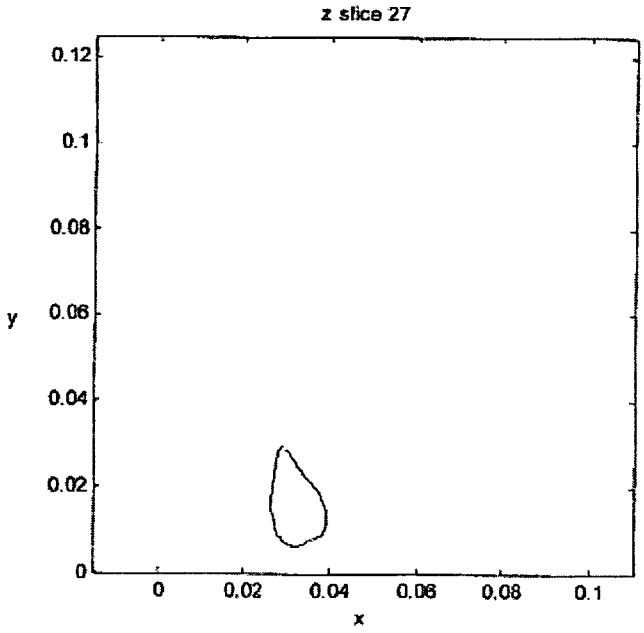
z slice 27
0.12
0.1
0.08
0.06
0.04
0.02
0
y
0
0.02
0.04
0.06
0.08
0.1
x

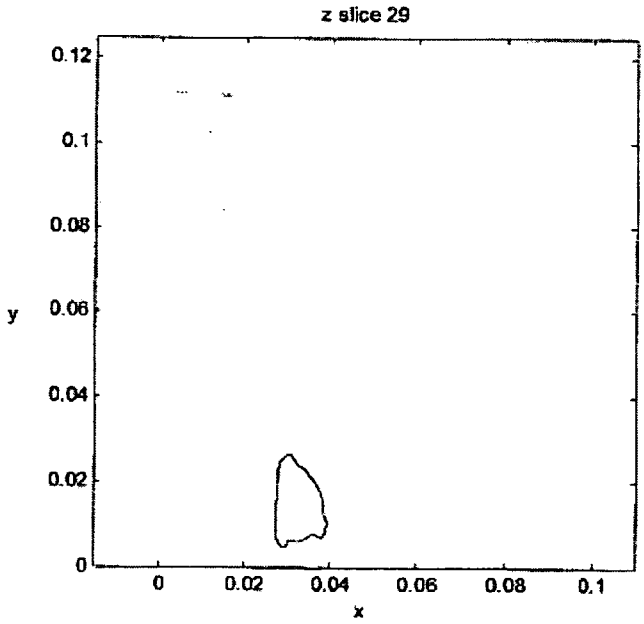
z slice 29
0.12
0.1
0.08
0.06
0.04
0.02
0
y
0
0.02
0.04
0.06
0.08
0.1
x

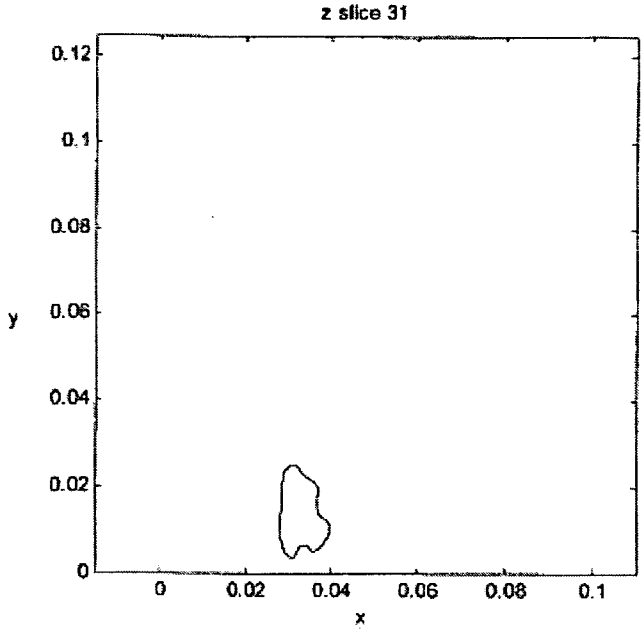
z slice 31
0.12
0.1
0.08
0.06
0.04
0.02
0
y
0
0.02
0.04
0.06
0.08
0.1
x

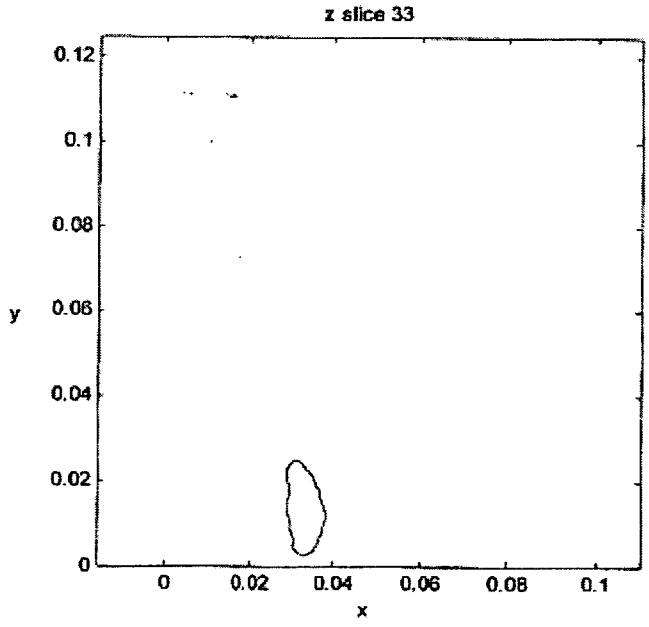
z slice 33
0.12
0.1
0.08
0.06
0.04
0.02
0
y
0
0.02
0.04
0.06
0.08
0.1
x

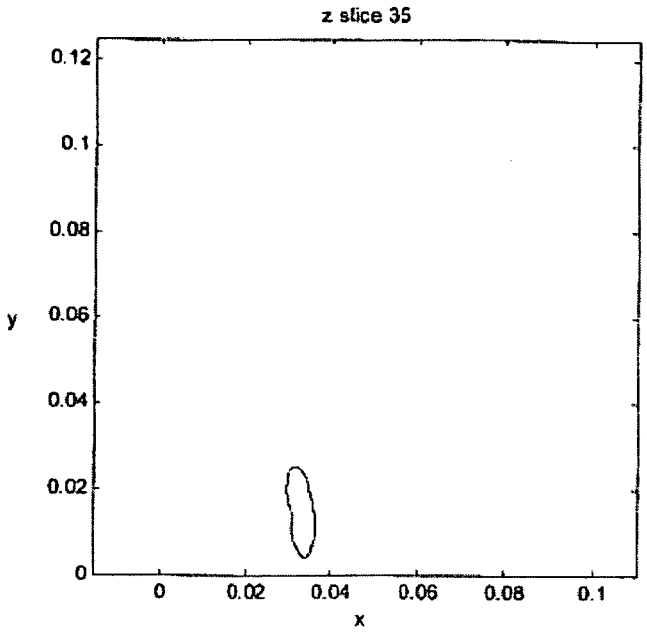
z slice 35
0.12
0.1
0.08
0.06
0.04
0.02
0
y
0
0.02
0.04
0.06
0.08
0.1
x

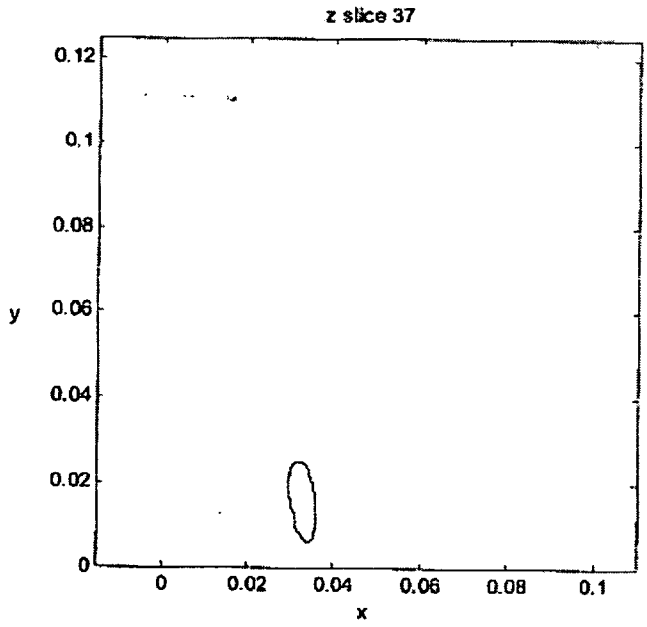
z slice 37
0.12
0.1
0.08
0.06
0.04
0.02
0
y
0
0.02
0.04
0.06
0.08
0.1
x

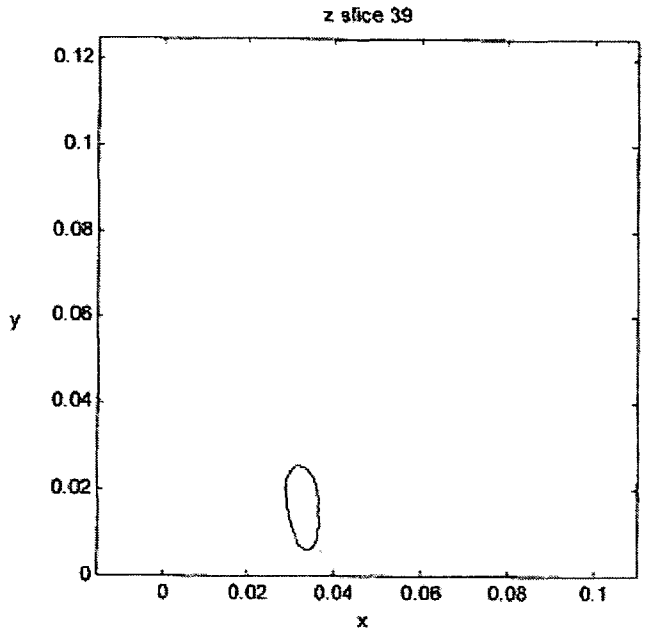
z slice 39
0.12
0.1
0.08
0.06
0.04
0.02
0
y
0
0.02
0.04
0.06
0.08
0.1
x

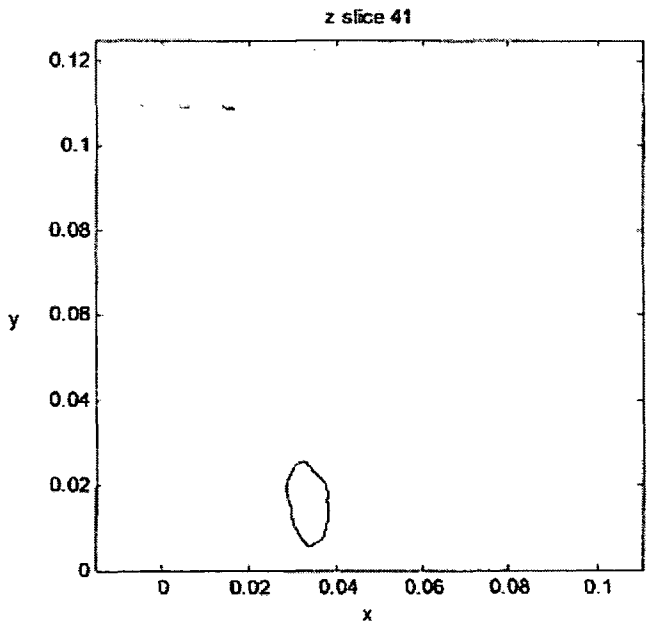
z slice 41
0.12
0.1
0.08
0.06
0.04
0.02
0
y
0
0.02
0.04
0.06
0.08
0.1
x

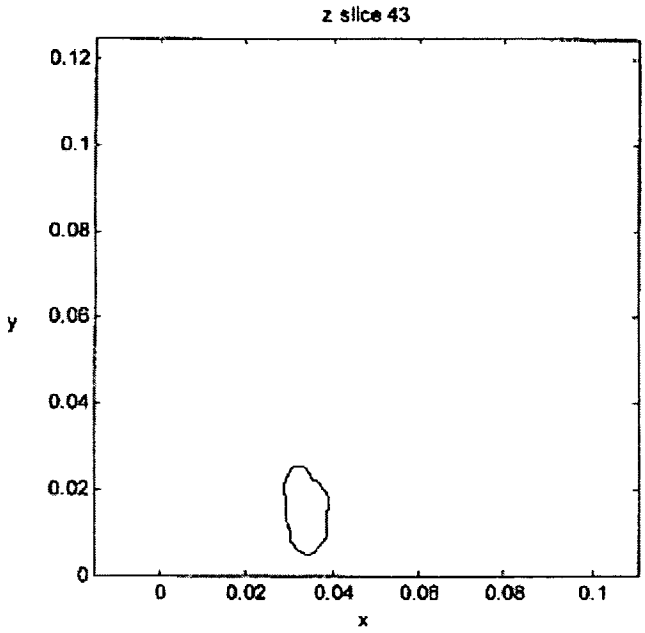
z slice 43
0.12
0.1
0.08
0.06
0.04
0.02
0
y
0
0.02
0.04
0.06
0.08
0.1
x

INTERNATIONAL SEARCH REPORT

International application No.
PCT/US 08/02989

A. CLASSIFICATION OF SUBJECT MATTER
IPC(8) - A61M 13/00 (2008.04)
USPC - 604/58
According to International Patent Classification (IPC) or to both national classification and IPC

B. FIELDS SEARCHED

Minimum documentation searched (classification system followed by classification symbols)
USPC 604/58

Documentation searched other than minimum documentation to the extent that such documents are included in the fields searched
All USPC; USPC 604/58, 128/200.14, 200.18, 203.12, 203.15; IPC A61M13/00

Electronic data base consulted during the international search (name of data base and, where practicable, search terms used)
PubWEST(USPT,PGPB,EPAB,JPAB); Google: @PD<20070305; inhaler; adapter; flow rate; design; medication

C. DOCUMENTS CONSIDERED TO BE RELEVANT

Category*	Citation of document, with indication, where appropriate, of the relevant passages	Relevant to claim No.
X	US 5,178,138 A (Walstrom, et. al.) 12 January 1993 (12.01.1993); Abstract; col 2, ln 38-64; col 5, ln 21 to col 7, ln 23; Fig 2-4, 8-11	1-3

☐ Further documents are listed in the continuation of Box C. ☐

* Special categories of cited documents:
"A" document defining the general state of the art which is not considered to be of particular relevance
"E" earlier application or patent but published on or after the international filing date
"L" document which may throw doubts on priority claim(s) or which is cited to establish the publication date of another citation or other special reason (as specified)
"O" document referring to an oral disclosure, use, exhibition or other means
"P" document published prior to the international filing date but later than the priority date claimed
"T" later document published after the international filing date or priority date and not in conflict with the application but cited to understand the principle or theory underlying the invention
"X" document of particular relevance; the claimed invention cannot be considered novel or cannot be considered to involve an inventive step when the document is taken alone
"Y" document of particular relevance; the claimed invention cannot be considered to involve an inventive step when the document is combined with one or more other such documents, such combination being obvious to a person skilled in the art
"&" document member of the same patent family

Date of the actual completion of the international search	Date of mailing of the international search report
15 October 2008 (15.10.2008)	31 OCT 2008
Name and mailing address of the ISA/US Mail Stop PCT, Attn: ISA/US, Commissioner for Patents P.O. Box 1450, Alexandria, Virginia 22313-1450 Facsimile No. 571-273-3201	Authorized officer: Lee W. Young PCT Helpdesk: 571-272-4300 PCT OSP: 571-272-7774

Form PCT/ISA/210 (second sheet) (April 2007)